# A DISTRIBUTED SEDIMENT DELIVERY RATIO CONCEPT FOR SEDIMENT YIELD MODELLING

**DAWIT BERHANE HAGOS**

**BSc Agric (Soil and Water Conservation), University of Asmara**

**Submitted in fulfilment of the requirement for the degree of**

**MSc IN HYDROLOGY**

**School of Bioresources Engineering and Environmental Hydrology**
**University of KwaZulu-Natal**
**Pietermaritzburg**
**South Africa**

**December 2004**

# DECLARATION

The research described in this dissertation was carried out within the School of Bioresources Engineering and Environmental Hydrology, University of KwaZulu-Natal, Pietermaritzburg, under the supervision of Professor S A Lorentz (School of Bioresources Engineering and Environmental Hydrology, University of KwaZulu-Natal).

I hereby certify that the research reported in this dissertation is my own original and unaided work except where specific acknowledgement is made.

Signed 

Dawit Berhane Hagos

Signed 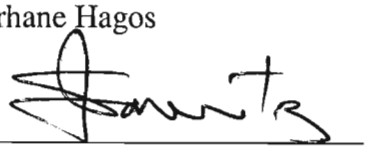

Simon A Lorentz

Associate Research Professor

(Supervisor)

# TABLE OF CONTENTS

# ABSTRACT

Identifying areas of the hillslope that are most sensitive to soil erosion and contribute significantly to sediment yield is a primary concern in environmental protection and conservation. Therefore the ability to predict the magnitude and variability of soil erosion and sediment yield is important to catchment managers in order to select the appropriate conservation practices that keep soil erosion and sediment yield within the tolerable limits.

A number of models have been developed for simulating soil erosion and sediment yield from a catchment. However, none of them are universally applicable and most of them require extensive data which are extremely costly, time consuming and sometimes not available except in research catchments. Hence it was concluded that the combined use of an empirically based soil loss model, RUSLE, Geographic Information Systems (GIS) techniques, and a Sediment Delivery Ratio (*SDR*) concept would be a candidate modelling tool, which would be a compromise between the advantages of simplicity, data availability, the complex spatial variability of hydrological and geomorphological characteristics of a catchment and the economic limitation of field data measurements in sediment yield studies.

Such a modelling tool was developed in this research and was able to identify sediment source areas and predict annual sediment yield from catchments. Data from the Henley catchment, South Africa have been used for demonstrating the potential use of the model in soil erosion and sediment yield studies. Arcview GIS grid functions were used to define the flow direction, accumulation, pathways, and velocity in a catchment as a function of topography and land use and to describe spatially variable input and output information. In addition the Arcview GIS grid function was used to discretise the catchment into hydrologically homogeneous grid cells to capture the catchment heterogeneity. The gross soil erosion in each cell was calculated using the soil loss model RUSLE while a distributed topography based *SDR* parameter was used to determine the mass of eroded sediment that would be transported to the nearest stream and ultimately to the catchment outlet.

The average annual soil loss and sediment yield values were 26 t. $ha^{-1}.yr^{-1}$ and 1.6 t. $ha^{-1}.yr^{-1}$ respectively. High soil erosion and sediment yield rates are evident in the residential and agricultural areas, which are characterised by degradation due to overgrazing and traditional and peri-urban settlements with mixed crops. The average annual *SDR* value was 0.19 for the Henley catchment and large *SDR* values are associated with areas adjacent to the channel system. This can be explained by recognizing that the *SDR* is significantly influenced by characteristics of the drainage system.

Comparison of event based simulations of sediment yields to those estimated from measurements demonstrated that the proposed model predictions ranged between 13 % and 60 % of the measured estimates, consistently over predicting. This is because the *SDR* component of the model is developed as a mean annual parameter, assuming that over a long period a stream system must intimately transport all the sediments delivered to it. Hence the channel network sediment delivery parameters would have to be considered at short temporal scales. Comparing the results of the model prediction against other sediment modelling techniques in South Africa demonstrated the usefulness of the model as an effective catchment management tool. The model has advantages over these other techniques since it includes a distributed grid based component, which enables the identification of sediment source areas in the catchment. The sensitivity analysis shows that the model was highly sensitive to parameters derived from topography and land use of the catchment.

Future research with the model should include further testing and analysis of its components on different catchments. The topography based *SDR* concept which is a key component in sediment routing for prediction of either long term average sediment yield or isolated storm event simulation from a catchment warrants specific attention. Effort in future should focus on identifying parameters which affect the sediment delivery within a catchment. This may be achieved by incorporating processes describing the movement of sediments in the channel network of the catchment.

# ACKNOWLEDGMENTS

The author wishes to express his sincere appreciation for the assistance given by the following:

**Professor S A Lorentz**, Associate Research Professor, School of Bioresources Engineering and Environmental Hydrology, University of KwaZulu-Natal for his encouragement, support, and supervision of this research. His sacrifice to the work in addition to his friendly and interactive approach is never to be forgotten;

**Mr A van Zyl**, Institute for Soil, Climate and Water (ISCW) Pretoria, for his co-supervision;

**Professor J C Smithers,** Professor of Agricultural Engineering and Head of the School of Bioresources Engineering and Environmental Hydrology, University of KwaZulu-Natal for his motivation, advice and making possible this research through his School;

**Dr T Zewotir**, School of Mathematics, Statistics and Information Technology, University of KwaZulu-Natal, for his advice in statistical analysis;

**Dr F Ahmed**, School of Applied Environmental Sciences, University of KwaZulu-Natal, for his support in GIS analysis;

**Mr M Horan,** GIS programmer, School of Bioresources Engineering and Environmental Hydrology, University of KwaZulu-Natal for his patient assistance in setting, extracting and advice in using the GIS;

**Mr O Idowu,** PhD student, School of Bioresources Engineering and Environmental Hydrology, University of KwaZulu-Natal for his assistance in editing my dissertation;

**Mrs S Kunz** and **Ms S Maney**, secretarial staff, School of Bioresources Engineering and Environmental Hydrology, University of KwaZulu-Natal, for their continuous support in providing the School services;

The World Bank in agreement with the Human Resource Development (HRD) of the University of Asmara, Eritrea funded the research and this support is gratefully acknowledged;

The research in this dissertation also emanated from a project funded by Water Research Commission (WRC) in contact with the School of Bioresources Engineering and Environmental Hydrology, University of KwaZulu-Natal;

**Nardos W. Selassie**, my wife, for her unending patience, encouragement and for always being there and believing in me during my study while away from her;

Colleagues **Solomon Gebremariam**, **Yonas Beyene**, **Mehari Sium**, **Mesfin Hagos** and all others, for their being at hand to help in different ways; and

Finally, my heartfelt thanks to **God** who helps me in every aspect of my life.

**TO MY PARENTS, FOR ALWAYS GIVING ME THE BEST OPPORTUNITIES THEY COULD.**

# LIST OF FIGURES

# LIST OF TABLES

# LIST OF APPENDICES

# LIST OF ABBREVIATIONS AND DEFINITIONS

**Abbreviations**

| | |
|---|---|
| ACRU | Agricultural Catchment Research Unit |
| ANSWERS | Arial Non-point Source Watershed Response Simulation |
| CALSITE | CALibrated SImulation Transported Erosion |
| CBD | Commercial Business District |
| CDF | Cumulative frequency Distribution Function |
| CREAMS | Chemicals, Runoff, and Erosion from Agricultural Management |
| DEM | Digital Elevation Model |
| ESRI | Environmental Systems Research Institute |
| EUROSEM | EUROpean Soil Erosion Model |
| GIS | Geographic Information Systems |
| INR | Institute of Natural Resources |
| ISCW | Institute for Soil, Climate and Water |
| KYERMO | Kentucky Erosion Model |
| LUT | Look-Up Table |
| MAP | Mean Annual Precipitation |
| MUSLE | Modified Universal Soil Loss Equation |
| RUNOFF | Runoff Model |
| RUSLE | Revised Universal Soil Loss Equation |
| SCS | Soil Conservation Service |
| SDR | Sediment Delivery Ratio |
| $SDR_i$ | Sediment Delivery Ratio of a grid cell |
| SIRI | Soil and Irrigation Research Institute |
| TIN | Triangular Irregular Network |
| UK | United Kingdom |
| USDA-SCS | United States Department of Agriculture Soil Conservation Service |
| USDA-SCS-TR-55 | United States Department of Agriculture Soil Conservation Service Technical Report No 55 |
| USLE | Universal Soil Loss Equation |

| | |
|---|---|
| WEPP | Water Erosion Prediction Project |

**Definitions**

| | |
|---|---|
| Erosion | defined as the detachment or entrainment of soil particles from a hillslope, thus distinguishing it from deposition or sedimentation and sediment transport (Khanbilvardi *et al.*, 1983; Onstad, 1984; Nearing *et al.*, 1994; Hudson, 1995; Morgan, 1995; Vijay *et al.,* 1996). |
| Sediment yield | defined as the amount of eroded material that passes a designed point at the outlet of a plot, field, channel, or catchment in a specified period of time (Khanbilvardi *et al.*, 1983; Onstad, 1984; Nearing *et al.*, 1994; Hudson, 1995; Morgan, 1995; Vijay *et al.,* 1996). |

# 1. INTRODUCTION

Annually, soil erosion exacts an enormous toll on catchments, both at the point of soil removal where erosion destroys agricultural potential, and at the point of deposition, where it limits the capacity of reservoirs and channels. This has been of concern to hydrologists, agricultural engineers and agronomists for several decades (Hadley and Mizuyama, 1993). The problem is not a new phenomenon, but is being taken more serious now than ever before (Lal, 1994; Morgan, 1995).

As is frequently cited by different researchers, quantities of between 15000-20000 million tonnes of soil is carried to the ocean each year from all the continents (Walling and Webb, 1996). Although, data are now available for an increasing number of the major rivers of the world, which in turn accounts for a substantial proportion of the land surface, uncertainties still exist regarding the sediment flux from smaller river basins draining to oceans. In addition, where data are available, uncertainties may exist because of lack of identification of the source of the information, short record lengths, differing periods of record, non-stationary river behaviour, and data reliability (Walling and Webb, 1996). Especially, the data reliability is recognised as a major problem since the measurement programmes employed in many areas of the world are inadequate for generating accurate assessments of sediment loads (Walling and Webb, 1996).

In the case of southern African, approximately 100-150 million tonnes of soil is carried to reservoirs each year (Howe, 1999). It is therefore, evident that erosion and sediment transport constitute a major problem facing development of water resources in southern Africa, which is predominantly semi-arid and consequently requires optimal management.

One of the main aims of catchment management plans is to develop cost effective practices and strategies for erosion and sedimentation control. These strategies are required to identify and reduce the loss of topsoil from the source area. This enables the reduction and maintenance of erosion from agricultural fields and hence the reduction of sediment delivery and prevention of the associated degradation of the water quality, reduction of the life span of downstream reservoirs and channels and flood problems (Kienzle *et al.*, 1997; Ouyang *et al.*, 1997).

Conservation practices rely on adequate prediction models which simulate the sediment yield consequences of perturbations in catchment land use. Such models are developed from an understanding of the erosion processes and underlying hydrological responses of catchments. The difficulty with such model development is that the dynamics of soil erosion and transport of sediments are relatively well studied at the point, laboratory or plot scale (Khanbilvardi *et al.*, 1983; Karvonen *et al.*, 1999), but catchment sediment yield modelling is less well developed. This is as a result of the complexity of the delivery processes at the catchment scale and the vast amounts of data required for simulating the variability of the parameters which describe these processes (Fefsgaard and Knudsen, 1996).

The sediment yield from a catchment at any instant in time is governed by the supply of the sediment available for transport and the capacity of the overland flow to transport the sediment to the catchment outlet (Nathalie, 1999). However, relatively little is understood about sequential processes regarding discontinuous erosion and transportation as sediment moves from source through the conveyance systems with intermittent periods of storage. Therefore, a difficulty associated with catchment sediment modelling is that the model has to describe spatially variable sources, sinks, temporary storage and transport processes, which are characterised by the catchment drainage network, which in turn is a function of the catchment topography (Dietrich *et al.*, 1999; Picouet *et al.*, 2001). This difficulty was highlighted by a review of the different environmental and geomorphological factors, the different forms and processes of soil erosion and sedimentation as currently understood and the various different catchment scale modelling approaches, which have been attempted. The difficulty is complicated as there is no standard method of prediction for soil erosion and sediment yield used by the developers of models (Elliot and Laflen, 1993; Owoputi and Stolte, 1995). The models are often developed with different purposes in mind or problems to solve and thus make use of different equations, parameters and assumptions.

Hence, in the light of the above, it was decided to combine a soil loss model, the Revised Universal Soil Loss Equation (RUSLE), a Geographic Information System (GIS) and a distributed grid based Sediment Delivery Ratio (*SDR*) concept for estimating the magnitude and describing the spatial variability of source erosion and sediment yield throughout the catchment.

More importantly, this technique allows for the determination of the effect of land use change on soil erosion and sediment yield of a catchment. In addition it allows easy definition of spatial subunits or grids of relatively uniform properties. Therefore with the aid of GIS, soil loss and sediment yield modelling can be performed on the individual subunits or grids. The identification of the spatially distributed source areas for sediment yield within the modelled catchment makes possible the implementation of special conservation efforts on these source areas. Further reasons for the value of this form of modelling are illustrated by examining the impacts of erosion and sedimentation.

## 1.1 Impacts of Erosion and Sedimentation

Erosion and sedimentation causes both environmental and economic impacts. Both are important, but, it is often only an economic impact that spurs action. Environmental impacts are difficult to assess at the initial stages. They tend to build slowly and not produce dramatic results for many years, by which time it may be too late to correct the problem (Goldman *et al.*, 1986). Some of the environmental and economic impacts are mentioned below.

### 1.1.1 Environmental impacts of erosion and sedimentation

Environmental impacts of erosion and sedimentation include the following:

- Eroded sediment contains nitrogen, phosphorous and other nutrients. When carried into water bodies, these nutrients trigger algal bloom that reduce water clarity, deplete oxygen, lead to fish kill, and create odours (Eck *et al.,* 1995; Gibson and Ford, 1998).
- Erosion of stream banks and adjacent areas destroys streamside vegetation that provides aquatic and wild life habitats (Goldman *et al.*, 1986).
- Turbidity from sediments reduces in-stream photosynthesis, which leads to a reduction in food supply and habitat (Eck *et al.,* 1995; Gibson and Ford, 1998).
- Suspended sediment abrades and coats aquatic organisms (Rekolainen *et al.*, 1998).
- Erosion removes the smaller and less dense constituents, *viz.* topsoil. These constituents, clay and fine silt particles and organic material, hold nutrients that plants require. The

remaining subsoil is often hard, rocky and infertile. Thus re-establishment of vegetation is difficult and the eroded soil produces less growth (Hudson, 1995).

### 1.1.2 Economic impacts of erosion and sedimentation

Some of the major economic impacts of erosion and sedimentation include:

- Excessive sediment accumulation results in significant loss of storage of reservoirs and channels and more frequent sediment removal is required (Walling and Webb, 1996).
- Erosion severely diminishes the ability of the soil to support plant growth. To restore this ability costs money, although restoration is not always undertaken (Goldman *et al.*, 1986).
- The associated water quality problems with reservoir siltation, such as eutrophication, require costly purification procedures (Mandavelle, 1997; Howe, 1999).
- Sediment deposition into streams increases the risk of flooding (Boardman *et al.*, 1990).

Therefore these impacts highlight the need for a simulation tool which can identify local erosion as well as the source of sediment yield that reaches downstream to water resource projects.

## 1.2 Aim and Motivation of the Research

During the past few decades, a number of different techniques or approaches have been attempted in predicting soil loss and sediment yield from a catchment. According to Wu *et al.* (1993), Wicks and Bathurst (1996) and Dietrich *et al.* (1999), of the different modelling approaches, physically based models are expected to provide the most reliable estimates of sediment yield. However, these models required the coordinated use of various submodels which describe the processes of particle detachment, transport and deposition. As a result, the input parameters for these models are extensive. The practical application of these models is still limited because of the difficulty in specifying model parameter values particularly in developing countries for which this research is intended and also because of the different scales of application that exist, for instance between catchment and field scale, where detailed process description may be inappropriate.

The solution is to employ a relatively simple tool for modelling soil loss and sediment yield i.e. to be able to maintain a balance between simplicity, the speed of obtaining results and the accuracy required for it to be effective. With this in mind, it is necessary to define a few requirements which need to be satisfied. These include the following:

- The model must provide a useful and efficient tool for predicting long term soil loss and sediment yield in developing regions where data are scarce or lacking;
- The model must be relatively easy to use, fast and cost-effective in the estimation of spatially distributed soil loss and sediment delivery, which is better for planning and management of water resources projects than the traditional method of long term data collection;
- The model needs to have a sediment delivery ratio function, which addresses the problem of sediment routing from the hillslopes to the catchment outlet and need to be applicable to catchments without suitable data for calibration;
- The model must be sufficiently accurate in approach in order to identify the spatial distribution of soil loss and sediment yield and make possible the implementation of special conservation effort at different areas in the catchment;
- The input data required by the model must be kept to a minimum and must be easily obtainable. This may enable the model to be transferable from one catchment to another; and
- Even though it is impossible to provide absolute values for sediment yield, the model must be able to provide values within a certain degree of confidence of the values being predicted.

Generally, the model presented in this research has been developed as the tool most likely to fulfil the requirements outlined above. A detailed description of the model is outlined in Chapter 4.

The aim of this research is to develop a modelling tool to estimate soil erosion and sediment yield in a catchment, based on the combined use of RUSLE, GIS and *SDR* concepts with the following specific objectives:

- To present a methodology that combines RUSLE, GIS and *SDR* concepts to estimate the magnitude and spatial distribution of soil erosion and sediment yield at a catchment scale. This was stimulated by recognizing the following:

  - The combined use of RUSLE, GIS and *SDR* would afford a ready means of catchment planning tool in developing regions where data are scarce and lacking;
  - The combined use of RUSLE, GIS and *SDR* is much faster and less expensive than the process based models for designing and planning of catchment management;
  - The combined use of RUSLE, GIS and *SDR* is sufficiently accurate technique to estimate sediment yield.

- To identify the main source of sediment delivered from upland slopes;
- To simulate the effects of land use change on soil erosion and sediment yield of a catchment;
- To demonstrate the use of this methodology by applying it to the Henley catchment, in the upper reaches of the Msunduzi River, consisting predominantly of informal traditional Zulu and peri-urban settlements interspersed with mixed crops, grassland and forestry and subjected to high mean annual sediment yield.

## 1.3 Structure of the Research

This research includes seven chapters. Chapter 2 discusses the different forms of soil erosion, local scale erosion and sediment transport processes and the equations which may be used in modelling and addressing the various approaches for modelling these processes.

Chapter 3 contains a review of a number of different approaches that have been attempted by researchers to upscale from the point and laboratory scales to the catchment scale modelling of soil loss and sediment yield. Owing to the complexity of the sediment delivery processes and the inherent upscaling difficulties, the models vary from empirical descriptions to attempts at physically based analysis are reviewed. The chapter places more emphasis on the deterministic sediment delivery ratio modelling approach (by giving an example of the CALSITE model which is a distributed delivery ratio based model) than the catchment specific sediment delivery ratio

models. In addition, this chapter discusses the effectiveness of coupling soil loss models with GIS for estimation of the magnitude and distribution of soil loss and sediment yield in a catchment.

Chapter 4 focuses on the development of a GIS distributed sediment delivery ratio model, which provides a useful and efficient tool for predicting long term soil erosion and sediment yield in developing regions where data are scarce and lacking. It also addresses the advantages of simplicity, and cost effectiveness in the estimation of spatially distributed soil erosion and sediment delivery over the traditional method of long term data collection on sediment yield. It argues that empirical sediment delivery ratio equations do not show the spatial variability of soil erosion and sediment yield. Hence the model developed in this research was motivated by its consideration of spatial variability of soil loss and sediment yield.

The spatial variation in source erosion and sediment yield is a function of the catchment topography (slope), land use, overland flow paths and velocity to the channel network and then to catchment outlet. These processes were considered important with regard to identifying areas of source erosion and modelling the potential of the eroded soil being transported to the catchment outlet. The model links the soil loss model RUSLE, GIS grid function and *SDR* to modelling the magnitude and spatial distribution of source erosion and sediment yield to the catchment outlet.

Chapter 5 describes the overview of the study area, the format and sources of the different data sets employed in the model. In Chapter 6, results and discussions of the model output, accompanied by verification of event basis sediment yields with observed measurements and comparison against other modelling techniques in South Africa are presented. In addition Chapter 6 presents the sensitivity of the model. Finally, Chapter 7 concludes the research with a review of the findings of the research and recommends ideas for future research.

# 2. PROCESSES AND FORMS OF SOIL LOSS AND SEDIMENT YIELD MODELLING

Modelling of soil erosion and sediment yield require an understanding of the different physical processes and forms of erosion and sedimentation that take place by running water. This is done before addressing the various approaches attempted for modelling theses processes which will be presented in Chapter 3. The different physical processes include soil particle detachment, transport and deposition and the different forms of soil erosion by water include interrill, rill, gully, and stream bank erosion. Modelling all these forms and physical processes would be a complex process. Hence describing the different forms and processes of soil erosion and sedimentation helps to identify which of these processes are most significant in contributing sediment in a catchment. This can be easily modelled with an empirically based soil loss model, RUSLE, which is shown to give some success in predicting sediment yield on a catchment scale by combining it with GIS technology and a sediment delivery ratio concept such as that presented in Chapter 4. Therefore this research is only concerned with modelling the effects of erosion and sediment transport through a catchment, by water and more specifically only the splash, sheet, rill erosion, and deposition and reintrainment processes.

## 2.1 Processes of Erosion and Sedimentation

Soil erosion and sedimentation are essentially a three part process, i.e. detachment, transport and deposition of soil particles by the erosive forces of raindrops and the overland flow of water (Novotny, 1980; Khanbilvardi *et al.*, 1983; Goldman *et al.*, 1986). Detachment and transport are basic processes occurring on source areas while transport and deposition are basic processes occurring on sink areas.

### 2.1.1 Soil particle detachment

Soil detachment rate is one of the most important components of the soil loss and sediment yield processes. Thus accurate prediction of detachment rates is fundamental to the development of any reliable soil loss and sediment yield models (Owoputi and Stolte, 1995).

Soil particle detachment is the dislodging of soil particles from the soil mass at a particular location on the soil surface by erosive forces of raindrops and by overland flow of water (Owoputi and Stolte, 1995). Owoputi and Stolte (1995) state that the controlling factors governing detachment are the shear stresses generated by overland flow and raindrops, and the reciprocal shear strength due to the cohesion of the soil particles and gravity. In order to detach and transport soil particles, the shear stresses generated by the overland flow and raindrop must exceed the shear stress of the soil gravity (Zhang *et al.*, 2002). The nature of the soil affects the critical shear stress for initiation of detachment of soil particles. The mechanism of soil detachment is a continuous process which ends for each dislodged particle when it either becomes incorporated into the flowing water or is simply moved from its original location (Cochrane and Flanagan, 1996).

Raindrop impact breaks the cohesive bonds between soil particles, thereby detaching particles from the soil mass and making them available for transport by surface water (Beuselinck *et al.*, 2002). Soil detachment by raindrop impact can be regarded as a measure of rainfall erosivity and soil erodibility. The rainfall parameters that are frequently used by many researchers in modelling of detachment by raindrop impact are rainfall intensity, momentum, kinetic energy, drop size, shape and velocity (Ghadiri and Payne, 1988). Soil parameters, which were found to be related to this aspect includes aggregate size and stability, bulk density, matric potential and shear strength (Francis and Cruse, 1983). Based on past research and the findings of Borah and Ashraf (1990), the rate of soil detachment due to raindrop impact might be expressed by Equations 2.1 and 2.2 given below.

$$E_r = a_r I^2 (1 - D_c)(1 - D_g)\left(1 - \frac{h+e}{3d_{50}}\right), \ if \ (h+e) < 3d_{50} \qquad 2.1$$

$$E_r = 0, \ if \ (h+e) \geq 3d_{50} \qquad 2.2$$

where $E_r$ = rate of soil detachment due to raindrop impact ($kg.s^{-1}$),

$a_r$ = raindrop detachment coefficient ($kg.s.m^{-2}$),

$I$ = rainfall intensity ($m.s^{-1}$),

$D_c$ = canopy cover density,

$D_g$ = ground cover density,

$h$ = water depth (m),

$e$ = thickness of the existing detached soil on the bed (m) and

$d_{50}$ = median raindrop diameter (m).

The detachment of soil particles by overland flow occurs when the shear stress applied by the overland flow is high enough to dislodge the soil particles from the soil mass. The amount of soil eroded depends on both the excess shear stress above the critical level for initiation of detachment, the extent to which the flow transport capacity exceeds the sediment load being supplied from upstream and the nature of the parent material (Nearing *et al.,* 1990). Models of erosion and sedimentation processes therefore have to distinguish between vulnerability to erosion of different soil surfaces, as in areas where mainly sheet flow occurs (interrill areas), areas where concentrated flow predominates (rill areas) and areas where gully erosion occurs. It is a reasonable assumption to identify the dominant erosion mechanism in the limited interrill regions as being rainfall detachment, with entrainment, or runoff detachment, dominating in rills (Rose *et al.,* 1990).

According to Wicks and Bathurst (1996), a common description of the soil erosion process involves detachment of soil particles by raindrop impact, transport of this material to rills by sheet flow, and further detachment and transport of soil particles by the rill flow. Most process based soil loss and sediment yield models assume a linear relationship for soil detachment in rills as a function of some hydraulic variables, often either shear stress (Nearing *et al.,* 1990), unit stream power (Zhang *et al.,* 2002), or stream power (Rose *et al.,* 1983; Hairsine and Rose, 1992). The parameter best suited to describe soil detachment for erosion prediction is still unclear.

### 2.1.2 Sediment transport

Most soil loss and sediment yield models rely upon the concept of transport capacity, which is defined as the maximum amount of sediment that a discharge can carry without net deposition occurring (Hairsine and Rose, 1992). Sediment transport capacity is very important in predicting

soil loss on hillslopes, but current understanding generally only allows for an estimate of transport capacity, to be within an order of magnitude of the correct value (Nearing *et al.,* 1990). Clearly, significant improvements in soil loss and sediment yield prediction technology will come as a result of improved sediment transport estimation techniques (Nearing *et al.,* 1990). Several transport capacity equations have been developed for transport of sediment in large channels and adapted for use in upland soil loss models. The choice of the best sediment transport capacity equation is subjective, and opinions vary as to the most appropriate equation to use (Nearing *et al.,* 1994). Apart from selecting an equation to use, it is important when modelling fundamental erosion and sedimentation processes, to understand what transport capacity involves and how it is represented in the model. Transport capacity is basically a balance between entrainment and deposition rate of the already detached sediment in the flow (Nearing *et al.,* 1994).

Nearing *et al.* (1990) stated that there are two explicit assumptions when using a sediment transport equation in describing soil loss and sediment yield. The first assumption is that the description of the entrainment process does not include a factor for cohesive soil forces, but considers only gravity forces of sediment, that must be overcome for the particle to be lifted into the flow. The implicit assumption, then, for erosion of cohesive soils is that cohesive forces are negligible, once the soil has been initially detached from the *in-situ* soil mass. The second assumption is the description of deposition as a continual process. Detachment refers to the process of removing *in-situ* soil particles from the bulk soil and net detachment refers to a balance between detachment, entrainment of previously detached particles, and deposition for the case when net movement of particles is from the soil surface into the flow. Some recent soil loss and sediment yield models have avoided the explicit use of existing sediment transport equations entirely (Nearing *et al.*, 1990). These models calculate simultaneously the processes of detachment by flow, entrainment by flow, detachment by rainfall, entrainment by rainfall and deposition of sediment. Foster *et al.* (1981) stated that if the potential accumulative sediment load along a defined flow path is less than the transport capacity of the flow, further detachment occurs either at a detachment rate controlled by the flow or at a rate that just fills the transport capacity. If the rate of detachment is greater than the transport capacity, the sediment is transported at the carrying capacity of flow.

The decisive factors governing transport capacity are fluid turbulence, the grain size and settling velocity of the transported particles (Owoputi and Stolte, 1995). In order to transport detached particles over a certain distance, the settling of the particles has to be counteracted by vertical, turbulent flow components within the fluid (Owoputi and Stolte, 1995).

A reliable estimation of the sediment transport capacity of surface flow is essential in developing sediment yield models which are designed to route sediment (Alonso *et al.,* 1981). Alonso *et al.* (1981), state that sediment transport capacity depends on many hydraulic and sediment related variables that affect the development of an equation where variables are expressed explicitly. Julien and Simons (1985) concluded that the slope length and gradient, unit discharge rate, which is a function of flow depth, flow velocity and rainfall intensity, and shear stress acting to detach soil, were the dominant geometric and flow variables for determining sediment transport capacity.

Several generalised formulas have been developed for computing sediment transport capacity. Many of the equations were developed for stream flows, and were later applied to shallow overland and channel flows. However, Alonso *et al.* (1981) evaluated nine sediment transport capacity formulas and concluded that the Yalin, 1963 equation provided reliable estimates of transport capacity for shallow overland and channel flow. The Yalin, 1963 (Equation 2.3), may be applied at any point on the hillslope to estimate the transport capacity ($T_c$) of the flow at the point, provided that estimates of hydraulic and sediment properties are available, and is expressed as:

$$\frac{T_c}{(SG)\,d\rho_w^{\,0.5}\tau_s^{\,0.5}} = 0.635\delta\left[1-\frac{1}{\gamma}\ln(1+\gamma)\right] \qquad 2.3$$

$$\gamma = 2.45(SG)^{-0.4}(Y_{cr})^{0.5}\delta \qquad 2.4$$

$$\delta = \frac{Y}{Y_{cr}} - 1 \quad (\text{when } Y<Y_{cr},\ \delta = 0) \qquad 2.5$$

$$Y = \frac{\frac{\tau_s}{\rho_w}}{(SG-1)gd} \qquad 2.6$$

where $T_c$ = sediment transport capacity ($kg.m^{-1}.s^{-1}$),

$SG$ = particle specific gravity (dimensionless),

$\rho_w$ = mass density of water ($kg.m^{-3}$),

$d$ = particle diameter (m),

$Y$ = dimensionless shear stress as defined above in Equation 2.6,

$Y_{cr}$ = dimensionless critical shear from shield diagram, a function of the *Re* (Reynolds's number) of the flow,

$g$ = acceleration of gravity ($m.s^{-2}$),

$\tau_s$ = shear stress acting to detach soil ($kg.m^{-1}.s^{-2}$),

$\gamma$ and $\delta$ = dimensionless parameters as defined above in Equations 2.4 and 2.5 respectively.

The Yalin, 1963 sediment transport equation or its modification has been used in many sediment yield models to estimate sediment transport capacity which is applied based on the assumption that sediment movement begins when the lifting force of the flow exceeds a derived critical lifting force. Models include the ANSWERS model (Beasley *et al.*, 1980), CREAMS model (Foster *et al.*, 1981), the upland model (Khanbilvardi *et al.*, 1983), KYERMO model (Hirschi and Barfield, 1988), RUNOFF model (Borah, 1989) and WEPP model (Nearing *et al.*, 1989) use this equation. Some of the common modifications made to the equation include sediment transport as a function of the distance along a complex slope and shear stress acting to detach the soil particles. When calibrated using the average of the hydraulic shear stresses at the end of a constant slope reference profile and at the end of the actual profile, the Yalin (1963) equation provides an accurate approximation (Nearing *et al.*, 1990).

### 2.1.3 Sediment deposition

Sediment is deposited when the sediment load exceeds the flow's total transport capacity or flow loses its capacity to transport coarser sized particles present in the sediment load (Hairsine and Rose, 1991). Bed load material is deposited immediately when transport capacity decreases below the sediment load, while suspended load responds more slowly to a reduced transport capacity (Owoputi and Stolte, 1995). The amount of sediment transported or deposited is the result of interactions between transport capacity of the flow and the amount of sediment entering,

and moving along the flow. Imbalances between sediment supply and transport capacity causes detachment and deposition. These processes are all interrelated and must satisfy locally the conservation principle of sediment mass (Borah and Ashraf, 1990).

For the sake of simplicity, Borah and Ashraf (1990) assumed, as for detachment, that sediment deposition is uniform over the overland and the channel beds. The mode of detachment and deposition depends on the carrying capacity of the flow, the sediment load and the amount of sediment present in the flow. If the capacity is higher than the sediment load, a detachment mode is assumed and the flow tends to pick up more materials from the bottom and if it is less, a deposition mode is assumed and the flow tends to deposit the excess material. Deposition may be described either as a separate process, as given in Equation 2.7 (Rose, 1985), or as a result of the difference between the actual sediment load and the transport of the flow as in (Equation 2.8) (Foster, 1982).

$$d_i = \alpha_i v_i c_i \qquad 2.7$$

where $d_i$ = mass rate of deposition per unit area of class, $i$, ($\alpha_i c_i$) is the sediment concentration adjacent to the bed (kg. $m^{-2}$),

$c_i$ = mean sediment concentration (mass of sediment per unit volume of solution) (kg. $m^{-3}$), and

$v_i$ = settling velocity representative of class $i$ (m. $s^{-1}$).

Note that the term $\alpha_i$ is a coefficient introduced to permit a non-uniform vertical distribution of sediment in the flow.

$$D_r = K_r(T_c - q_s) \qquad 2.8$$

where $D_r$ = rill detachment or deposition rate (kg.$s^{-1}$.$m^{-2}$),

$T_c$ = sediment transport capacity (kg.$s^{-1}$.$m^{-1}$),

$q_s$ = sediment load (kg. $s^{-1}$.$m^{-1}$), and

$K_r$ = a first order reaction rate coefficient for deposition ($m^{-1}$).

Deposition calculations are important for estimating the sediment delivery from a slope profile. Accurate deposition relationships are critical to providing accurate predictions of off-site sediment problems. Nearing *et al.* (1990) stated that much work has been done in the area of predicting deposition on complex slope profiles. Generally these studies recommend the following:

- If a single effective fall-velocity term is to be used to calculate net deposition, improved methods of calculating an effective fall velocity must be developed;
- Collections of reliable data are required for non-uniform slopes in the field and exact slope profile descriptions will be essential to interpreting the data. Also the rate of sediment delivery to the area of net deposition must be accurately measured as a function of time; and
- More basic, theoretical work needs to be performed to provide better estimates of transport and deposition rates for mixtures of particle size class.

Therefore the processes of soil erosion and sedimentation mentioned above are applicable in each of the forms of soil erosion and sedimentation depending on the factors such as topography, soils, vegetation cover and rainfall-runoff characteristics as detailed in Section 2.2 below.

## 2.2 Forms of Soil Erosion by Water

According to Kinnell (1993), Morgan (1995) and Schwab *et al.* (1995), soil erosion by water is divided into interrill erosion, rill erosion, gully erosion, and stream bank erosion. The details of these forms of soil erosion by water are given below.

### 2.2.1 Interrill erosion

Interrill erosion is sometimes referred to as sheet erosion (Morgan, 1995). The process is such that thin layers of soil are removed; one after the other, from the surface and the erosion is often not clearly evident when the soil surface is visually inspected (Owoputi and Stolte, 1995). In the

interrill areas, the mechanisms of raindrop and overland flow are jointly responsible for the detachment and transport of sediments (Kinnell, 1993).

Schwab *et al.* (1995) stated that in the interrill areas, soil detachment is mainly caused by raindrop impact while the flowing water accomplishes transport. However, these processes are very much interdependent. In the interrill erosion, the amount of soil detached by the raindrops is a function of the depth of overland flow with the flow depth being a measure of the erosive action of the overland flow (Hirschi and Barfield, 1988). The erosion caused by raindrops may also depend on the amount of sediment being transported per unit time by the overland flow. This implies that the erosive action of raindrops is not independent of the erosive action of overland flow. Similarly, the erosive action of overland flow, particularly its capability to transport sediments, is enhanced by raindrops (Kemper *et al.,* 1985).

Despite the inter-relationships between the erosive actions of raindrops and overland flow, the roles played by each of these erosive agents, either in the rill or interrill area, are very distinct (Hairsine and Rose, 1992). Most of the currently available equations for predicting soil detachment are either developed for overland flow or for raindrop impact; the inter-relationships between these erosive agents are not usually reflected (Hairsine and Rose, 1991; Schwab *et al.,* 1995).

### 2.2.2 Rill erosion

A rill is a small channel that is formed during a runoff event. It is different from a gully in that a rill is easily removed under normal tillage practice (Owoputi and Stolte, 1995). Different researchers give different definitions and significance of rill erosion. In the rill, the main causes of erosion is the shear forces from the overland flow or rill flow, which is a function of topography, soil properties and runoff rate, while the impact of raindrops on the detachment is commonly assumed not to be significant (Barfield *et al.,* 1983; Schwab *et al.,* 1995). In addition to its role in the detachment of soil particles, the rill flow is also the main transporting agent. Although many studies support the fact that raindrops do aid overland flow in transporting sediments, most of these studies were conducted in the interrill areas (Kinnell, 1993).

Some of the fundamental problems associated with the theory of rill erosion can be related to the prediction of the location and formation of rills, as well as their general behaviour during erosion events. This is so because of the complexities involved (Owoputi and Stolte, 1995). According to Moore *et al.* (1988), the development of rills is associated with the micro relief structures of the soil surface and the geometry of the slope, but the actual mechanisms responsible for rill development are generally unknown.

Many different equations have been developed by different researchers to describe the erosive action of raindrops and overland flow, either in the rill or interrill areas. However, these equations have various shortcomings, such as being empirically based, consequently requiring full understanding of all the physical processes involved in soil erosion. There is also a need to relate the impact of soil moisture and seepage interactions on soil characteristics and behaviour to soil erodibility (Owoputi and Stolte, 1995).

### 2.2.3 Gully erosion

A gully is defined as a steep sided channel, often with a steeply sloping and actively eroding head scarp caused by erosion due to the intermittent flow of water, usually during and immediately following heavy rains. As distinct from rills, gullies cannot be removed by tillage (Walling and Webb, 1996). Thus, gully erosion is an advanced stage of rill erosion.

The rate of gully erosion depends primarily on the runoff producing characteristics of the catchment above the gully, i.e. the drainage area, soil characteristics, the alignment, size and shape of the gully, and the slope of the channel (Schwab *et al.,* 1981). In addition, Morgan (1980) and Schwab *et al.* (1981) stated that a gully develops as a result of processes that may take place either simultaneously or during different periods of its development. These processes are waterfall erosion at the gully head, channel erosion caused by water flowing through the gully, raindrop splash on unprotected soil, alternate freezing and thawing of the exposed soil banks, and slides or mass movement of the soil in the gully.

According to Morgan (1995) and Walling and Webb (1996) when measuring and modelling sediment yield due to water erosion most attention has been given to interrill and rill erosion. However, field observation in the past few decades has indicated that, beside interrill and rill erosion, gully erosion is often a significant sediment source in a catchment.

Recent research has provided some insight into gully erosion processes and factors which might help in the modelling of some of these aspects or which, at least, draw attention to particular processes important for modelling gully erosion. In order to better simulate gully erosion subprocesses, more detailed monitoring and modelling of the development of gullies is needed. More precisely, there is a need to better predict the location, the total length and the cross-section (size and shape) of gullies. It has been recommended that existing concentrated flow soil loss and sediment yield models need to be refined to incorporate the effects of the resistance of various soil horizons to concentrated flow erosion, as well as other detaching mechanisms in gullies, such as soil fall, slumping and head cutting (Poesen *et al.,* 1998).

Models capable of representing these aspects of gully erosion are needed in order to more accurately predict the effects of environmental changes on soil losses, sediment sources and sediment volumes in upland areas. These processes operating in upland areas often contribute significantly to downstream flooding and sedimentation and need to be accounted for when evaluating the efficiency of gully erosion control measures (Morgan, 1995).

### 2.2.4 Stream bank erosion

Stream bank erosion consists of soil removal from stream banks or soil movement in the channel. Stream banks erode either by runoff flowing over the side of the stream bank or by scouring and undercutting below the water surface (Schwab *et al.*, 1981).

Sediment in streams is transported by suspension, by saltation, and by bed load movement (Moore *et al.*, 1988). Sediment loads may be estimated by resurveying reservoir bottoms and by sampling the flow of streams. According to Troeh *et al.* (1980) and Walling and Hadley (1980) variables that affecting sediment movement in streams include velocity of flow, turbulence,

particle size distribution, diameter, cohesiveness, specific gravity of transported material, channel roughness, abstraction to flow and availability of material for flow.

Although the actual area damaged by stream bank erosion is small compared to the area affected by other types of soil erosion by water, it is very important because bottomland soils damaged by this type of erosion are usually more productive than any other soils in the area, and because soil picked up by streams is carried completely away, with little or no chance for deposition close to the original site (Morgan and Davidson, 1986; Elliot and Laflen, 1993).

While the techniques defined above may provide an adequate description of the forms and local scale soil loss and sediment yield processes, their application at the catchment scale requires a vast amount of information to describe the morphology of the terrain and channel characteristics. It has also been debated whether the interacting processes that occur within a catchment can be represented by the physics included in these techniques. Therefore, a more empirical approach for these processes may be applicable for large spatial scale modelling of soil loss and sediment yield.

In the next chapter, the advantages, limitations, scale of simplicity, and effectiveness of the different modelling approaches are discussed in detail with special emphasise on the sediment delivery ratio modelling approach, by giving an example of the CALSITE model which is a distributed delivery ratio based model for estimating erosion and sediment yield. In addition, the contribution of GIS in modelling the spatial variability of erosion and sediment yield is reviewed.

# 3. CATCHMENT SCALE SOIL LOSS AND SEDIMENT YIELD MODELLING

Modelling soil loss and sediment yield is the process of mathematically describing the different processes and forms of soil erosion and sediment yield that are presented in Chapter 2. Sediment delivery at a catchment scale is compounded by a wide range of geomorphological and environmental factors affecting it, including the nature, extent and location of the sediment sources, relief and slope characteristics, the drainage pattern and channel conditions, vegetation cover and land use (Walling, 1983). However, the linkages between upslope soil loss and downstream sedimentation, including mechanisms of sediment delivery process are poorly understood (Richards, 1993). Sediment delivery modelling at the catchment scale is, therefore, limited by the complexity of the delivery processes and the vast amounts of input information required for simulating the variability of the parameters which describe the processes. Each modelling approach presented in this chapter is determined by its depth of the various physical processes try to describe. Hence reviewing of the different modelling approaches helps to identify which modelling approach is relatively accurate with minimum input data sets. It seems useful for soil loss and sediment yield models to be linked to GIS, in order to cope with the spatial variability inherent in modelling these processes.

Soil loss and sediment yield prediction models could be used for erosion control planning, water resources planning and design, and water quality modelling (Walling and Hadley, 1980). Some of these problems can be solved with simple models, while others may require more complex models. However, prediction requirements for each of these problems are largely determined by the duration of the event, size of area to be simulated and whether or not sediment sources are to be identified (Borah and Ashraf, 1990).

## 3.1 Importance of Modelling

Assessing soil erosion helps in identifying the area and extent of an erosion hazard. Such assessment is not, however, aimed at quantifying the soil erosion accurately instead, it provides estimation (Lal, 1994; Morgan, 1995). For that reason modelling becomes important. Attaining

the soil loss threshold is the objective of most conservation programmes. The loss threshold is defined as "being in equilibrium with the soil formation rate" (Scotney and McPhee, 1992; Wild, 1993; Hudson, 1995; Miller and Gardiner, 1998).

The first step that has to be made in any conservation programme is assessing the extent of soil erosion (Lal, 1994), which could be quantitative by the use of available technology to process the existing data, or qualitative by visual observation. Quantitative evaluations of soil erosion and sediment yield assessment that use different approaches are briefly discussed in Section 3.2, since these approaches may vary conceptually in the mechanism by which sediment delivery processes are generated. The importance of models is immense for various reasons. In general, models simulate the real phenomena by using a small dataset to provide knowledge about the larger phenomena for the purpose of prediction (Miller and Gardiner, 1998). Lal (1994) and Nearing *et al.* (1994) summarised the main reasons for modelling soil loss and sediment yield as follows:

- soil loss and sediment yield models can be used as predictive tools for assessing soil loss for conservation planning, project planning, soil erosion inventories, and for regulation;
- Physically based soil loss and sediment yield models can predict where and when erosion is occurring and thus would help the conservation planner target efforts to reduce erosion;
- Models can be used as tools to understand the complex erosion and sedimentation processes and their interactions; and
- Knowing the similarities and differences between models would be important for users in applying models and for researchers to setting research priorities.

Covering the whole subject of study of soil erosion and sediment yield is impractical. Therefore, it becomes necessary that a good representative site be selected and its results extrapolated (Young, 1994). The other advantage of models is related to recommendations that can be made. The ultimate goal of soil erosion and sediment yield assessment is to conserve soil in accordance with the nature and extent of the impact (Lal, 1994; Young, 1994; Hudson, 1995). As soil loss and sediment yield models require data inputs (which are factors that affect soil erosion and sediment yield) as separate quantitative parameters, each input is treated for its share in contributing to the overall soil loss and sediment yield. Consequently, a soil conservation

programme can give more consideration to factors that have a greater share of the cause of erosion (Lal, 1994).

## 3.2 Approaches to Modelling Soil Loss and Sediment Yield

Owing to the complexity of the sediment delivery processes presented in Chapter 2, the complexity of models developed to simulate soil loss and sediment yield from catchments, varies considerably. These models ranges from simple empirical (statistical) models and conceptual models to complex physically based models.

Most current modelling techniques compute the amount of sediment detached as well as the transport capacity of the overland flow, and then move the lesser of the two quantities downstream. Figure 3.1 illustrates, by means of an example flow chart, how the sediment detachment-transport-deposition process would operate in a model which calculates the sediment flux for a hillslope or channel segment. There is, however, only a limited theoretical understanding of these complex interactions, which is probably the main cause for the sometimes poor results obtained with soil loss and sediment yield models (Gerits *et al.*, 1990; De Roo and Offermans, 1995). Generally sediment yield models have been developed with different purposes or problems to solve and thus may require different relationships, parameters and assumptions. In order for a model to be used properly, a clear concept of the soil loss and sediment yield processes must be understood (Bingner, 1990).

### 3.2.1 Empirical models

Empirical models belong to "black-box" type relating sediment loss to either rainfall or runoff (Morgan, 1995). Most of these models are based on multiple regression analysis and usually predict the total load of suspended sediment carried during a given runoff producing rainfall event (Picouet *et al.*, 2001). According to Walling and Webb (1996), sediment yield models derived from statistical analyses have frequently been used to estimate sediment yield. These types of models usually relate sediment yield to one or more catchment characteristic or climatic factor, with little or no understanding of the processes involved in its transformation (Lal, 1994).

Because of their nature, they require relatively large quantities of data both on catchment characteristics and on sediment discharges. These models are generally applied to problems requiring sediment averages over long periods of time.

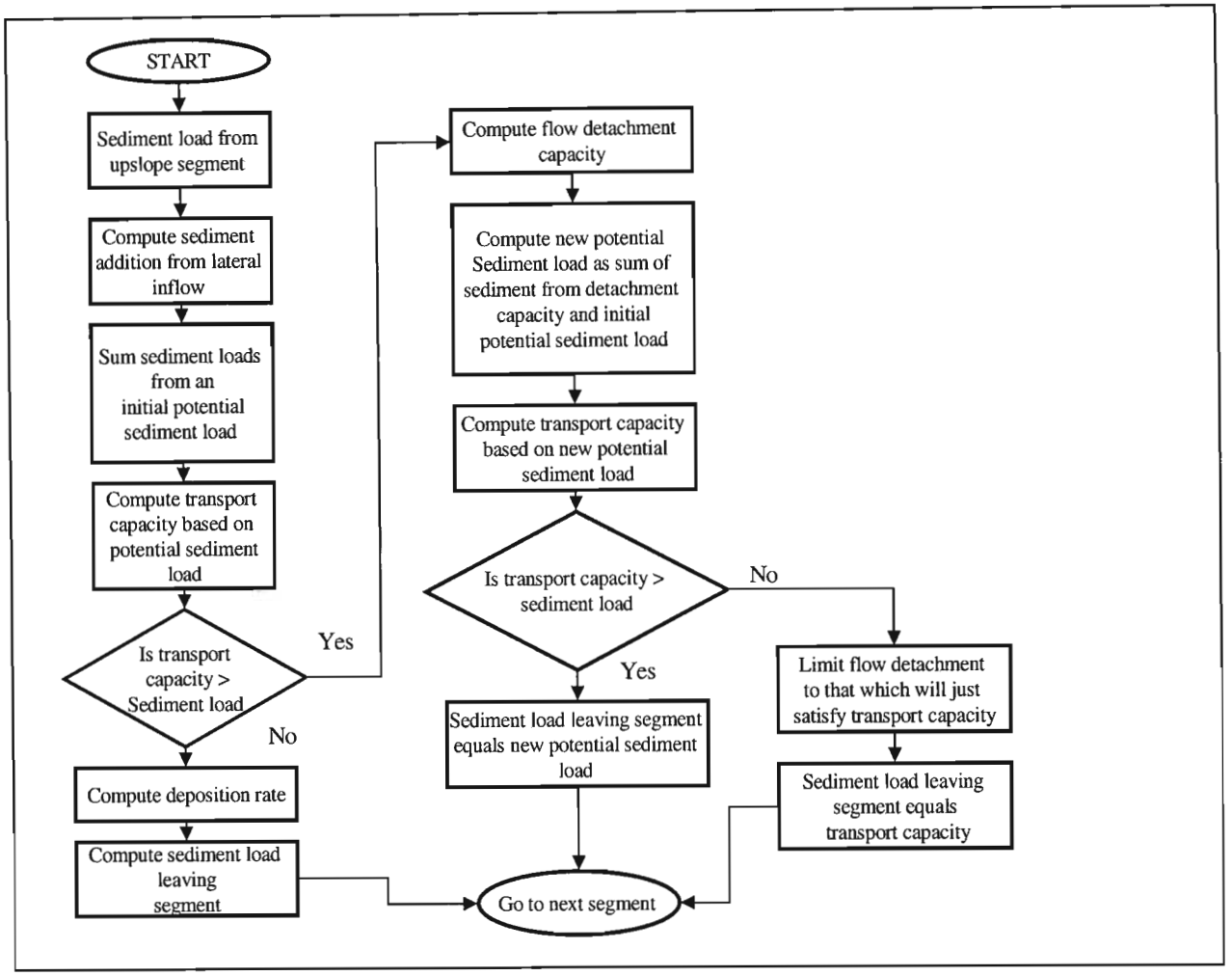


**Figure 3.1** Flow chart for detachment-transport-deposition computations within a segment of an overflow or channel element (after Foster *et al.*, 1981)

Refsgaard and Knudsen (1996) stated that the great majority of modelling systems used in practice today belong to the simple empirical or conceptual models and require a modest number of parameters to be calibrated for their operation. A severe drawback of these models is that their parameters are not directly related to the physical characteristics of the catchment (Picouet *et al.*, 2001). Accordingly, it may be expected that their applicability is limited to areas where they

have been measured for years and where no significant change in the catchment conditions have occurred (Walling and Webb, 1996; Kienzle *et al.*, 1997). Moreover, criticism of these empirical modelling approaches has arisen mainly because the observed relationship between water discharge and sediment concentration is essentially non-linear, time-dependent and varies from site to site (Muzik, 1996). In addition, theses models cannot give an indication of why soil loss takes place and cannot be extrapolated beyond their data range with confidence, either to more extreme events or to other geographical areas (Morgan, 1995).

At different time and space scales, these models exhibit hysteresis with different properties (Picouet *et al.*, 2001). Good examples of these types of models are those describing the relationships between sediment load and instantaneous water discharge from the drainage catchment or those that predict gully or stream bank erosion. The most common relationship is the rating curve, as given in Equation 3.1 that takes the form of a power function (Picouet *et al.*, 2001).

$$C = aQ^b \qquad 3.1$$

where $C$ = suspended sediment concentration (mg. $l^{-1}$),
$Q$ = water discharge ($m^3$. $s^{-1}$), and
$a$ and $b$ = empirically derived regression coefficients.

Another example of simple empirical models is the Rooseboom Sediment Yield Map of southern africa, which has been developed by Rooseboom *et al.* (1992). The model used results from 120 reservoir catchment surveys to determine the spatial variations of sediment yield production in southern africa and to form a database for the calibration of a revised sediment yield map. Rooseboom *et al.* (1992) established a relationship between the observed sediment yields and the various physical and geographic features of southern african catchments. The relationship includes sediment yield with sediment delivery potential of different regions, land use, average slope for defining sediment transport capacities and rainfall erosivity. This method is used for quick estimation of the annual average potential sediment yield from a catchment in southern africa as a function of its location and size. However, due to the high degree of variability in

sediment yields in the region and the simplicity of the technique, it should not be used rigidly (Rooseboom *et al.*, 1992).

### 3.2.2 Conceptual models

Conceptual models are the so-called "grey box" models, lying somewhere between physically based models and empirical models, and representing a partial representation of the hydrological sediment yield processes (Karvonen *et al.*, 1999). According to Muzik (1996) and Kienzle *et al.* (1997), the common feature of all conceptual models is that they ignore or simplify spatial variations of hydrological processes, and are characterised by spatially averaged inputs, outputs and parameter values i.e. they tend to be lumped models. Therefore the focus of conceptual models is to predict sediment yields based on spatially lumped forms of water and sediment continuity equations.

The advantage of conceptual models is their relative simplicity. Thus, conceptual models are often used in sediment yield estimation, but their usefulness has been limited by the inability to account for internal variations of hydrological systems and processes (Muzik, 1996). It might be argued that the spatial variability is broadly related to a catchment size and therefore a maximum catchment size could be established up to which in general, conceptual models could be safely applied (Picouet *et al.*, 2001). Such a generalisation, however, may be possible only in a regional context, since hydrology is the product of complex climate-catchment interactions, with local variations superimposed on considerable global variations of both climate and catchment characteristics (Moore and Clarke, 1983). Some of the limitations of conceptual lumped models which are given by different researchers are as follows:

- Conceptual models need sufficiently long meteorological and hydrological records for their calibration, which may not always be available at the location of concern (Muzik, 1996);
- The equations of lumped conceptual models can only be an approximate representation of the real world, and as a result they introduce some error arising from model structure (Beven, 1989);

- Spatial heterogeneities in system response may not be well represented by catchment average parameters (Ferro, 1997);
- The accuracy with which a model can be calibrated or validated is very dependent on errors in the observation of both input and output data (Hornberger *et al.*, 1985);
- There is a great danger of overestimation if an attempt has been made to simulate all hydrological processes thought to be relevant, and fit the relevant parameters by optimisation against an observed sediment record (Hornberger *et al.*, 1985);
- The calibrated parameters of such models may be expected to show a degree of independence, so that equally good results may be obtained with a different set of parameter values. This may be true even though a model has only a small number of parameters (Beven, 1989).

Different models have been developed using this modelling approach with different aims and purposes, in different regions of the world. A good example of this modelling approach is the *ACRU* agrohydrological model, a conceptually lumped model which developed by Schulze (1995). The *ACRU* sediment yield routine option (Lorentz and Schulze, 1995) uses the Modified Universal Soil Loss Equation, MUSLE (Williams, 1975), to estimate a daily sediment yield on a daily basis at a catchment or subcatchment scale. The MUSLE estimate of the sediment yield due to the interrill and rill erosion at the outlet of the catchment is calculated by the following expression:

$$Y_{sd} = \alpha_{sy} (Q_v \times q_p)^{\beta_{sy}} \times K \times LS \times C \times P \qquad 3.2$$

where $Y_{sd}$ = sediment yield from an individual event (tonnes),
$Q$ = stormflow volume for the event ($m^3$),
$q_p$ = peak discharge for the event ($m^3 . s^{-1}$),
$K$ = soil erodibility factor (tonne. h. $N^{-1}$. $ha^{-1}$),
$LS$ = slope length and gradient factor (dimensionless),
$C$ = cover and management factor (dimensionless),
$P$ = support practice factor (dimensionless), and
$\alpha_{sy}$ *and* $\beta_{sy}$ = local specific MUSLE coefficients.

There are various options in the *ACRU* sediment yield modelling by MUSLE to estimate the soil erodibility factor (*K*), slope length and gradient factor (*LS*), cover and management factor (*C*) and support practice factor (*P*), depending on the level of information available. These options in the *ACRU* model were adopted from information contained in the Universal Soil Loss Equation (USLE) (Wischmeier and Smith, 1978), the Revised Universal Soil Loss Equation (RUSLE) (Renard *et al.*, 1991) as well as experimental observations from modelling experiences in southern Africa conducted by local experts (e.g: Lorentz and Schulze, 1995). For general application of the *ACRU* model, the RUSLE parameters for soil erodibility, slope steepness, vegetation cover and management practice may be averaged for each subcatchment by overlaying the respective GIS grid coverage with the subcatchment boundaries (Lorentz and Schulze, 1995).

In recent years, significant advances in the knowledge of mechanics of soil erosion processes, and increasing availability of data and software for processing spatial information is changing the manner in which the hydrological system is assessed (Quimpo, 1993). As a result, greater emphasis is now being placed on developing physically based or white box models which are described below.

### 3.2.3 Physically based models

Physically based models belong to the group of "white box" models, in which the behaviour of the hydrological system is described in terms of mathematical relationships which outline the interactions and linkages of the various components of spatially and temporally varying catchment hydrological processes (Kienzle *et al.*, 1997). According to Wicks and Bathurst (1996) and Dietrich *et al.* (1999), physically based soil loss and sediment yield models describe the detachment, transport and deposition processes with equations derived from mechanics and hydraulic sciences. These models theoretically overcome many of the deficiencies stated earlier through their use of parameters which have a physical interpretation and through their representation of spatial variability in the parameter values.

The problems encountered when physically based models are used, include the large number of parameters and physical properties necessary to describe the phenomena (such as soil erodibility,

hillslopes and channel slope). The calibration of parameters is always a source of concern, especially when they cannot be related to physical characteristics of the study area. The second difficulty has to do with the application of such models to large catchments because of the complexity and multiplicity of the equation describing the processes involved. Finally these models often require catchment scale rainfall intensity data, which are often unknown because of the high spatial variability (Picouet *et al.,* 2001). In the light of this limitation, it is imperative to carefully consider the degree of resolution at which a physically based model is useful for a particular catchment (Karvonen *et al.,* 1999). Nevertheless, a large number of process based models have become available, but many are still in various stages of testing and development.

As a result of the spatial complexity involved in most physically based models, some degree of lumping is required. The user must decide on the scale at which the lumping of parameters will take place. The scale of lumping can vary widely, from distances measured in centimetres to areas of subcatchment size (Refsgaard and Knudsen, 1996). The choice of scale of distributed elements in models is generally depend out on the purpose of simulation, the level of accuracy required and the knowledge, scale and experience of the modeller, as well as the availability of financial resources, time and technology (Wicks and Bathurst, 1996). As mentioned above, physically based models require a vast amount of data, and are computationally very demanding and intensive when compared to empirical and conceptual models. The computational aspects of physically based modelling are becoming less of a problem nowadays when combined with a GIS in which sophisticated graphic capabilities are used to visualise spatial prediction to the point where results can be convincing (Grayson *et al.*, 1993).

Hence, in light of the above modelling approaches, a technique i.e. able to maintain a balance between simplicity, the speed of obtaining results and accuracy for designing and planning of catchment management is, needed. This can be achieved using sediment delivery ratio models. The inclusion, of sediment delivery ratio models in a GIS interface highlights their ability in the identification and estimation of the spatial distribution of soil erosion and sediment yield and thereafter the implementation of specific conservation efforts. The following section discusses the concept behind this modelling approach and its merits linking GIS environment.

### 3.2.4 Delivery ratio models

The delivery ratio method of predicting sediment yield is well known and is used regularly in many countries (Walling, 1983). Novotny (1980) and Ferro (1997) defined the sediment delivery ratio as the fraction of gross soil erosion by water that is delivered to a particular point in the drainage system, and it is sometimes referred to as the transmission coefficient. Mathematically it is expressed as follows:

$$SDR = \frac{SY}{SE} \qquad 3.3$$

where $SDR$ = sediment delivery ratio, with a value ranging from 0 to 1,
$SY$ = sediment delivered, and
$SE$ = soil erosion over the catchment.

According to Khanbilvardi *et al.* (1983) and Ferro (1997), a reduction in the erosion rate is observed within the catchment when comparisons are made between erosion measured on hillslopes and at the catchment outlet and this is because a wide range of environmental and geomorphological factors affect the sediment delivery ratio. These factors could be sediment source and texture, proximity to mainstream, channel density (bifurcation ratio), catchment area and slope, length of the channels, land use or land cover and rainfall-runoff factors.

The failure to produce a generally applicable prediction equation is mainly due to the complexity of the sediment delivery processes and their interaction with catchment characteristics, and partly owing to a lack of definitive assessments of the dependent variables (such as, soil erosion and sediment yield )(Ferro, 1997). Assessments that have been undertaken are themselves primarily based on a comparison of measured with simulated sediment yield with an estimate of gross erosion. In addition, the lack of a generally applicable predictive technique shows that there is no simple relationship between gross erosion and sediment yield. These problems relate in particular to the temporal and spatial lumping inherent in the concept (Walling, 1983). Since sediment is produced from different source areas distributed throughout a catchment, sediment delivery

processes have to be modelled by a spatially distributed criterion (Novotny, 1980). For modelling the spatial disaggregating of the sediment delivery processes, the catchment has to be discretised into morphological units (Ferro, 1997), i.e. to areas of having clearly defined length and steepness.

Sediment transport on the catchment hillslope is a physical process distinct from transport within the channel networks. Therefore, hillslope and channel sediment delivery processes have to be considered and modelled separately (Atkison, 1995). The sediment delivery effects in the channel system can be neglected for small catchments in which well developed floodplains do not usually exist. Under this hypothesis, Ferro and Minacapilli (1995) suggested that taking into account the intra-catchment variability of the sediment delivery processes by calculating the sediment delivery ratio of each morphological unit into which the catchment is divided, can reduce the error.

It seems clear that a more detailed representation of the various algorithms inherent in sediment delivery require a good understanding of the processes and linkage between source area erosion and downstream sediment yield. A simple sediment delivery ratio must be replaced by a model which takes cognisance of, the various processes involved in the movement of sediment from the source area through the catchment system to the outlet, and which can take account of spatial variability within the system and the various time constants involved (Walling, 1983).

In the past few decades, several studies have been attempted by different researchers to produce empirical prediction equations for the delivery ratio, stimulated by the recognition that a reliable assessment of the sediment delivery ratio would afford a ready means of estimating the sediment yield of a catchment. Table 3.1 gives some examples of the proposed relationships developed between sediment delivery ratio and catchment characteristics. Although several such equations for calculating sediment delivery ratios exist and are all attractive because of their simplicity, none of them are universally applicable. This is mainly due to the complexity of the sediment delivery processes and their interactions with the catchment characteristics. These problems relate in particular to the temporal and spatial lumping inherent in the concept and to its "blackbox" nature (Walling, 1983).

In the light of the above problems it was necessary to develop a distributed sediment delivery ratio model that would account for the spatial distribution of both hydrological and geomorphological characteristics of a catchment. A good example of such a distributed sediment delivery ratio model is the CALibrated SImulation of Transported Erosion Model (CALSITE), developed by Bradbury *et al.* (1993).

**Table 3.1** Examples of proposed relationships between sediment delivery ratios and catchment characteristics (after Lorentz and Howe, 1995)

| Authors | Region | Equation |
|---|---|---|
| Maner (1958)* | Kansas, U.S.A. | $\log DR = 2.962 + 0.869 \log R - 0.854 \log L$ |
| Roehl (1962)* | South East U.S.A. | $\log DR = 4.5 - 0.23 \log A - 0.510 \times \text{colog } R/L - 2.786 \log BR$ |
| Williams and Berndt (1972)* | Brushy Creek, Texas, U.S.A. | $DR = 0.627\ SLP^{0.403}$ |
| Mutchler and Bowie (1976)* | Pigeon Roost Creek, Mississippi, U.S.A. | $DR = 0.488 - 0.006A + 0.010RO$ |
| Williams (1977)* | Texas, U.S.A. | $DR = 1.366 \times 10^{-11} A^{-0.100} R/L^{0.363} CN^{5.444}$ |
| Mou and Meng (1980)* | Dali River Basin, Shaanxi, China | $DR = 1.29 + 1.37 \ln Rc - 0.025 \ln A$ |
| Hession and Shanholtz (1988) | Virginia, U.S.A. | $DR_i = 10(R/L_{fi})$ |
| Tim, Mostaghimi, and Shanholtz (1992) | Virginia, U.S.A. | $DR_i = \exp(-KS_{fi}L_{fi})$ |
| CALCITE, Bradbury *et al.* (1993) | Wallingford, UK | $DI_p = \min [F^{0.5}. Pa^{0.7}.SLP_{\%}^{1.67}]$ |

DR = sediment delivery ratio; BR = Bifurcation Ratio; $S_{fi}$ = slope function for grid cell i;
R = basin relief; Rc = gully density; L = basin length;
$DR_i$ = Delivery Ratio of a grid cell Pa = total annual rainfall CN = S.C.S. curve number;
A = basin area; RO = annual runoff; R/L= relief/length ratio;
K = land cover co-efficient; SLP = % slope of main stem channel; i = grid cell reference number;
$L_{fi}$ = length of flow path between grid cell i and channel outlet; Note: Units vary between equations.
F = the number of upstream flow paths which cross a given cell; * After Walling (1983)

The CALSITE model uses a combination of the Universal Soil Loss Equation (USLE) and a delivery ratio function to determine the annual sediment yield from a catchment. The model is implemented on a raster based IDRISI GIS to enable the combined analysis of different types of spatial data. The contribution to annual sediment yield made by each of the grid cells within the catchment is termed "transported erosion" (*TE*) and is computed by Equation 3.4.

$$TE = SE \cdot f(DI_p) \cdot k \qquad 3.4$$

where $SE$ = source erosion (t. grid cell$^{-1}$. yr $^{-1}$),
$DI_p$ = delivery index for a given grid cell,
$f(DI_p)$ = calibrated delivery ratio, and
$k$ = scaling constant.

The source erosion in this model is calculated on a cell by cell basis using a formula based on the USLE. A simple physically based delivery index equation was chosen for the 1993 version of CALSITE and this could be derived solely from the elevation image, without requiring any runoff information. A delivery index value ranging from 0 to 100 was produced for each cell, based on Equation 3.5.

$$DI_p = \min X_f \qquad 3.5$$

where $\min X_f$ = minimum sediment concentration transporting capacity along the flow path from each source cell within the catchment to defined stream channel.

The sediment transporting capacity is a function of water discharge and slope. The likely scale of the annual water discharge crossing a cell can be related to the number of cells contributing runoff from upstream and the amount of rain falling on the catchment. In that case, Equation 3.5 on a per cell basis then becomes:

$$DI_p = \min \left[ F^{0.5} \cdot P_a^{0.7} \cdot S_{\%}^{1.67} \right] \quad 3.6$$

where $F$ = the number of upstream flowpaths which cross a given cell,

$P_a$ = total annual rainfall (mm), and

$S_{\%}$ = slope (%) of cell.

The delivery index values for each source cell are converted to delivery ratio ($DR_p$) values in the range 0 to 1 by using of a delivery look-up table (*LUT*). The values in the delivery *LUT* are S-shaped and characterised by a lower threshold value below which $DR_p = 0$ and an upper saturation value above which $DR_p = 1$. In order to obtain the calibrated delivery ratio value, the threshold and saturation levels for the delivery *LUT* function are set by default to those values which minimise the variance between observed and predicted sediment yields.

Even though the model is promising for estimating and identifying the spatial distribution of source erosion and sediment yield, it still requires actual data for its calibration. These are not always available especially in regions where lack of information on sediment yield data is evident. Therefore, a distributed sediment delivery ratio model that is implemented in a raster Arcview GIS, which is developed only from morphological and land use characteristics of a catchment as described in Chapter 4, is more applicable when compared to the long term sediment yield data collection required for model calibration.

## 3.3 GIS Modelling of Soil Loss and Sediment Yield

In recent years, considerable effort has been devoted to utilising GIS in erosion and sediment yield studies to extract inputs like soils, land use, topography and rainfall erosivity for comprehensive simulation models and to spatially displayed model outputs (Mankin *et al.*, 2002). Many of the initial researches were devoted to linking single event grid models with raster based GIS (Boardman and Favis-Mortlock, 1998). More recently, an input interface is being developed to automatically sub-divide a catchment into grid or subcatchment and then extract model input data from map layers and the associated databases. Soils, land use, climate and topographic data

are collected and written to appropriate model input files. The output interface allows the user to display output information (Zhang *et al.*, 1990; Mankin *et al.*, 2002).

Linkage between GIS and soil loss models depends on both the GIS and the model itself. GIS and grid cell based models can easily be combined because of the capacity of GIS to analyse raster data (Mankin *et al.*, 2002). It is easy to interface empirical models such as the RUSLE with GIS because of the simplicity of the equation (Ferro *et al.*, 1998), whereas physically based models require detailed data inputs to make multiple layers (Mankin *et al.*, 2002).

The main reasons for using a GIS is that hydrological, geomorphological and soil erosion processes vary spatially, so that the cell sizes should be selected that allow spatial variations to be taken into account. Also, the data for the large number of cells required is enormous and cannot easily be entered by hand, but can be obtained by using a GIS (Hession and Shanholtz, 1988). Further advantages of using a GIS are the possibilities of rapidly producing modified input maps with different land use patterns or conservation measures to simulate alternative scenarios, the ability to use a very large catchment with many pixels, so that the catchment can be simulated with more details and the facility to display the results as maps (Vijay and Fiorentino, 1996). Other advantages of incorporating soil loss and sediment yield models in GIS are data accuracy, data integrity and multiple attributes capability.

Many process based soil loss and sediment yield models have been developed, such as ANSWERS (Beasley *et al.*, 1980), WEPP (Nearing *et al.*, 1989) and EUROSEM (Morgan *et al.*, 1992). Although some of these models use spatial variables that are generated with a GIS, only few are, however, really integrated in a raster GIS (Boardman and Favis-Mortlock, 1998).

This chapter has provided an insight to the main modelling approaches that have been attempted to simulate soil erosion and sediment yield from catchments. It should be noted that there is no specific "universally" accepted modelling approach. Each catchment needs then to be considered uniquely with its own characteristics and an approach adopted accordingly.

It can generally be concluded that relatively simple but valid prediction models *viz.* sediment delivery ratio models can be highly beneficial for most management purposes in regions with limited hydrological information, mainly because of their simplicity, cost effectiveness and efficiency for predicting long term water erosion and sediment yield. However, these models are still in their pioneering stage of development in incorporating the spatial distribution of soil erosion and sediment yield estimation. Therefore further work may yet yield promising results by placing these models in a GIS environment in which sophisticated graphic capabilities are used to visualise spatial predictions to the point where the results can be convincing of the above mentioned fundamentals.

Finally, all the approaches discussed in this chapter were used to aid the combined use of RUSLE, GIS and distributed sediment delivery ratio (*SDR*) concept in modelling soil loss and sediment yield from a catchment. The abilities of the proposed model are highlighted in the identification and estimation of the spatial distribution of soil erosion and sediment yield and thereafter the implementation of a specific conservation effort.

In the chapter which follows, an attempt has been made to develop a technique which accounts for the combined use of RUSLE, GIS and distributed *SDR* concept.

# 4. THE MODEL: COMBINING THE RUSLE, GIS AND DISTRIBUTED SEDIMENT DELIVERY RATIO CONCEPTS

## 4.1 Concepts and Theory

The erosion and sediment delivery processes described in the previous chapters serve to highlight the problem of using empirical and lumped soil loss and sediment yield models in estimating erosion and sediment yield. In addition data requirements for physically based models are often excessive. It has been accepted that soil loss and sediment yield models should be able to predict the spatial variation in sediment source areas and reflect the effects of routing such source area erosion on the final distribution of sediment yield in the catchment. It was concluded that in order to improve the source area sediment yield modelling, it would be necessary to improve the integration of indicated catchment source area erosion (on site erosion) to the final sediment yield at the outlet of the catchment with the concept of distributed sediment delivery ratio. Better use should be made of the state of the art spatial data management and processing technique development in GIS in regard to developing a more spatial sediment yield model. This should be a model which accounts for the spatial heterogeneity of rainfall, soil, catchment morphology and land use and their effects on spatial patterns of soil erosion and sediment yield in a catchment. Such variability has promoted the use of data intensive distributed models for the estimation of catchment erosion and sediment yield *viz.* by discretising a catchment into sub-areas (grid cells) each having approximately homogeneous characteristics (Young *et al.*, 1987; Wicks and Bathurst, 1996).

In this research, a comprehensive methodology that integrates the Revised Universal Soil Loss Equation (RUSLE), Geographic Information System (GIS) techniques, and a Sediment Delivery Ratio (*SDR*) concept for estimating water erosion and sediment delivery at the catchment scale is presented. The RUSLE (Renard *et al.*, 1991) was used to determine the source erosion. The *SDR* was used to route sediment from source areas to the nearest stream reach. The spatial pattern of source erosion and sediment yield was obtained by integrating RUSLE, *SDR*, and a raster Arcview GIS.

A schematic conceptual diagram (Figure 4.1) shows the integration of all the major procedures in developing the model for estimating the spatially distributed source erosion, *SDR* and sediment yield using GIS.

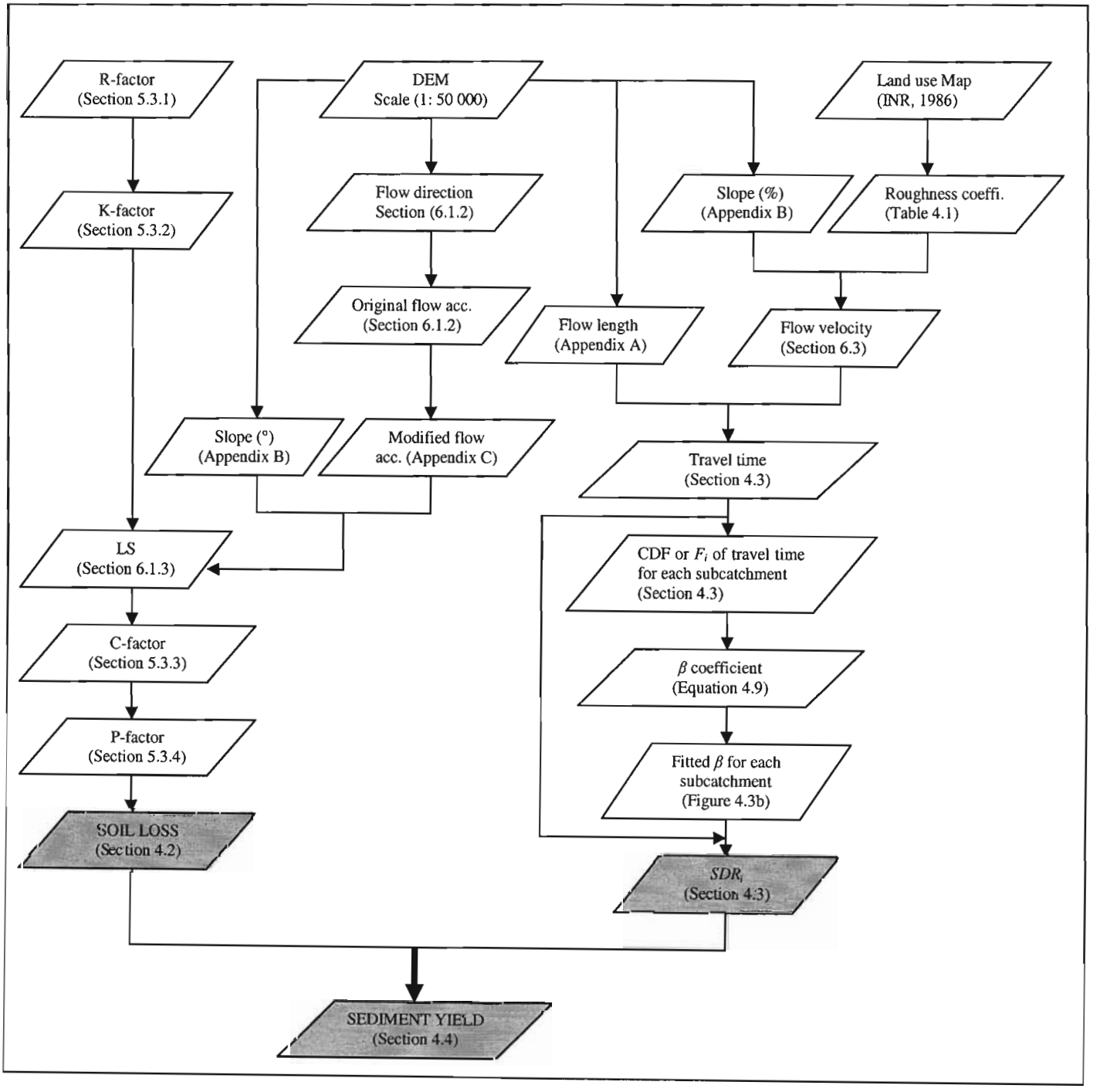


**Figure 4.1** Flow chart illustrating the various calculations and paths available in the model developed in this research

The model developed in this research differs from the modelling approaches presented in Chapter 3 in that the coefficient values used in various equations of the model especially the *SDR* component was determined using standard procedures and without any calibration. This is done because the model is developed under the premise of applying it to ungauged catchments where there is a lack of sediment yield data for calibration.

The model can be broken down into three components:

- Calculation of source erosion;
- Calculation of the sediment delivery ratio; and
- Calculation of sediment yield.

The output of the proposed model is in the form of digital images of the soil erosion, sediment delivery ratio and sediment yield, along with tabulated results shows the accuracy of sediment yield estimates against actual measurements and other modelling techniques in South Africa.

## 4.2 Calculation of Source Erosion

The term source erosion is defined as the soil erosion occurring at the place of origin within the catchment. At this stage no transporting activities have occurred on the sediments that have been generated. The calculation of source erosion in the model was done with the use of the RUSLE.

The RUSLE model is designed to predict the long term average soil losses from specific field-size areas in specified cropping and management systems. RUSLE combines the erosion factors covering interrill and rill erosion over a catchment into one equation. RUSLE comprises of five submodels/model components on rainfall characteristics, soil properties, topography, ground surface conditions, and erosion conservation measures, each of which is represented by empirical algorithms. There is ample evidence in the literature, that the RUSLE yields a good estimate of the amount of detached soil (source erosion) from interrill and rill areas at the cell size which presumes homogeneity (Renard *et al.*, 1997). Source erosion is thus computed within the individual cells using the RUSLE which has been enhanced over the last 10 years of research

(Renard *et al.*, 1997). RUSLE has been widely accepted and enjoys wide use, is simple and easy to parameterise, and requires fewer data and time to run than most models dealing with rill and interrill erosion (Jones *et al.*, 1996).

RUSLE, a functional model derived from the analysis of intensive soil erosion data, has seen wide application in long term soil erosion prediction (Renard *et al.*, 1997). Most efforts linking RUSLE and GIS have been carried out within raster GIS. Raster models are cell based representations of map features, which offer analytical capabilities for continuous data and allow fast processing of map layer overlay operations (ESRI, 1996). In a raster GIS, the mean annual gross soil erosion is calculated at a cell level as the product of the five RUSLE factors as follows:

$$A_i = R_i \; K_i \; L \, S_i \; C_i \; P_i \qquad 4.1$$

where

| | | |
|---|---|---|
| $i$ | = | i-th cell |
| $A_i$ | = | computed soil loss per unit area (t. ha $^{-1}$.yr $^{-1}$), |
| $R_i$ | = | the rainfall and runoff factor, equal to the sum of the annual or seasonal energy intensity (EI) interaction factor for all storms (MJ. ha $^{-1}$ .mm. h $^{-1}$.yr $^{-1}$), |
| $K_i$ | = | soil erodibility factor (t. h. MJ $^{-1}$.mm $^{-1}$), |
| $LS_i$ | = | the length and steepness factor (dimensionless) |
| $C_i$ | = | the cover and management factor (dimensionless), and |
| $P_i$ | = | the support practice factor (dimensionless). |

As mentioned earlier in Chapter 2, numerous variables and interactions influence interrill and rill erosion. The RUSLE groups these variables under five major erosion factors (*R*, *K*, *LS*, *C*, and *P*), the product of which, for a particular set of conditions, represents the average annual soil erosion (Renard *et al.*, 1991). Each of these factors has certain variables applicable to different conditions. Various researchers have contributed to determining these variables for each of these factors applicable to the model (e.g: Wischmeier and Smith, 1978; Renard *et al.*, 1991; 1997).

### 4.2.1 The rainfall-runoff erosivity factor (*R*)

The rainfall-runoff erosivity factor, *R*, is defined as the long term average annual erosivity of rain at a specific locality (Renard, *et al.*, 1991). The most commonly used parameter to represent the *R*-factor is the rainfall erosivity, $EI_{30}$, which is determined from the product of storm kinetic energy, E, expressed in $J.m^{-2}$, and the maximum 30 minute storm intensity, $I_{30}$, expressed in $mm.h^{-1}$ (Smithen and Schulze, 1982). $EI_{30}$ has been accepted as reliable indicator of rainfall erosivity (McPhee and Smithen, 1984).

Smithen and Schulze (1982) suggested that the *R*-factor is a climatic parameter which can only be determined from local data. To represent the *R*-factor for an event, an approach initially developed by these researchers, using data from autographic rainfall records was modified by Kienzle *et al.* (1997) and used as a first step. This modified approach recognises that the estimated average annual erosion potential is significantly different when using average annual rainfall erosivity applied to average annual crop cover factors compared to using average monthly rainfall erosivity applied to average monthly crop cover factors and then summing the average monthly erosion potentials to derive an estimate of the average annual soil erosion potential. According to Kienzle *et al.* (1997) using an average monthly $EI_{30}$ analysis generates more accurate erosion potential estimates since high summer rainfall erosivity associated with convective rainfall can then be applied to appropriate crop cover factors representing denser rain season vegetation with greater protection against soil losses. Low winter rainfall erosivity values can similarly be applied to poorer dry season cover protection indicators. Therefore this average monthly $EI_{30}$ erosivity value has been found to be suitable for input into the RUSLE's *R*-factor in the calculation of source erosion in this research.

### 4.2.2 The soil erodibility factor (*K*)

In soil loss and sediment yield studies, soil physical properties are usually represented by a soil erodibility factor, *K*, which is defined as the rate of soil loss per rainfall erosion index unit as measured on a standard plot (Renard *et al.*, 1991). The standard plot is 22.1 m long and has a 9 % slope and is continuously in a clean tilled fallow condition with tillage performed up and downslope (Renard *et al.*, 1991).

Physical properties of soil affect the infiltration capacity and the extent to which soil particles can be dispersed and transported (Schwab *et al.,* 1995). The most common soil characteristics that are important in determining soil erodibility are texture, organic matter content, structure, permeability, aggregate stability, shear strength and infiltration capacity (Goldman *et al.,* 1986). Therefore, the *K*-factor can be determined in various ways depending on the level of information available for the soil properties mentioned above. Often however, all the information concerning the soil properties may not be available for all types of soils. To avoid this problem, alternative techniques have been derived for different regions.

In South Africa, spatial soil information is fairly limited. The only national data set available with soils information are the land type maps of the Soil and Irrigation Research Institute (SIRI), now known as Institute for Soil, Climate and Water (ISCW) of the Agricultural Research Council Development. MacVicar *et al.* (1974) define a land type as a class of land over which macroclimate, terrain form and soil pattern each display a marked degree of uniformity. This uniformity is such that there would be little advantage in defining, on a countrywide basis, smaller more uniform landscape entities for the purpose of agricultural potential determination. These land type maps were thus generated for agricultural purposes rather than for hydrological purposes; however they have been used with some degree of success in hydrological research (Schulze *et al.,* 1991) and sediment yield studies (Lorentz and Schulze, 1995). This information and assumptions have been found suitable as input to determine the RUSLE's *K*-factor in the calculation of source erosion because there is no data for the above mentioned soil properties in the study area.

### 4.2.3 The length and steepness factor (*LS*)

The length and steepness factor, *LS*, is defined as the ratio of soil loss per unit area on a site to the corresponding loss from the unit plot of 22.1 m long at a 9 % slope (Wichmeier and Smith, 1978; Renard *et al.*, 1997). The slope length is defined as the distance from the point of origin of overland flow to the point where either the slope gradient decreases sufficiently for deposition to take place, or runoff enters a well defined natural or artificial constructed channel (Lorentz and Schulze, 1995). More questions and concerns have been expressed over the slope length than any

other of the RUSLE factors particularly in applying it to real landscapes as part of GIS. One reason is that the choice of a slope length involves judgement, and different users choose different slope length for similar situations. Hence, more emphasis is given to the *LS*-factor because it is a measure of the sediment transport capacity of overland flow (Moore and Wilson, 1992).

Various approaches have been used by different researchers to calculate the *LS*-factor for the RUSLE in different conditions. Examples include Renard *et al.* (1991); Mc Cool *et al.* (1993); Lorentz and Schulze (1995) and Desmet and Govers (1996). In the case of uniform slope conditions the combined *LS*-factor of a given segment of land can be calculated by applying Equation 4.2 (Wischmeier and Smith, 1978; Renard *et al.*, 1997).

$$LS = (\lambda / 22.1)^{m} (0.065 + 0.045 \sin\ s + 0.0065 \sin\ s^{2}) \qquad 4.2$$

where $LS$ = the combined length and steepness factor,

$\lambda$ = slope length in (m),

$s$ = slope gradient (%) and

$m$ = length exponent specified as 0.5 for slopes of 5 % or more, 0.4 for slopes between 3.5 and 4.5 %, 0.3 if slope is between 1 to 3 %, and 0.2 if slope is less than 1 % (Wischmeier and Smith, 1978).

In complex topographic conditions the RUSLE applies Equation 4.3 of Foster and Wischmeier (1974).

$$LS = \frac{S_j \left( \lambda_j^{\,m+1} - \lambda_{j-1}^{m+1} \right)}{(\lambda_j - \lambda_{j-1})(22.13)} \qquad 4.3$$

where $L$ = slope length factor for the $j^{th}$ segment,

$S_j$ = slope factor for the $j^{th}$ segment,

$\lambda_j$ = distance from the lowest boundary of the $j^{th}$ segment to the upslope field boundary, and

$m$ = length exponent of the USLE-*LS* factor.

Later, Desmet and Govers (1996) modified Equation 4.3, to produce Equations 4.4a and 4.4b:

$$L_{i,j} = \frac{U_{i,j-out}^{m+1} - U_{i,j-in}^{m+1}}{\left(U_{i,j-out} - U_{i,j-in}\right) \cdot (22.13)^m} \qquad 4.4a$$

where $L_{i,j}$ = the slope length factor of the cell with coordinates ($i$, $j$),

$U_{i,j-out}$ = upslope contributing area per unit contour width at the outlet of the grid cell with coordinates ($i$, $j$), ($m^2$)

$U_{i,j-in}$ = upslope contributing area per unit contour width at the inlet of a grid cell with coordinates ($i$, $j$), ($m^2 .m^{-1}$) and

$m$ = the slope length exponent of the RUSLE *S*-factor.

$$S = -1.5 + \frac{17}{1 + e^{2.3 - 6.1 \sin\theta}} \qquad 4.4b$$

where $\theta$ = the slope angle of the grid cell (°).

In this research, to incorporate the impact of flow convergence, the hillslope length factor was replaced by the upslope contributing area of Desmet and Govers (1996). The advantage of the above modification is that it works on the basis of flow accumulation. Mitasova *et al.* (1996) further simplified the formula to derive the *LS*-factor at a point on a hillslope. Their formula is used in this research, and is given by the GIS executable equation as follows:

$$LS(r) = (m+1)\left[\frac{A(r)}{a_o}\right]^m \left[\frac{\sin\theta}{b_o}\right]^n \qquad 4.5$$

where $LS$ = the combined length and steepness factor at a given point $r$ with coordinates x and y,

| | | |
|---|---|---|
| $A\,(r)$ | = | upslope contributing area per unit contour width (m), which is perpendicular to the flow direction (aspect), |
| $\theta$ | = | the slope (°), |
| $m$ and $n$ | = | parameters set as 0.6 and 1.3 respectively. These constant values are taken because their results conform with slope length if slope length is less than 100 m and gradient is less than 14° (Moore and Wilson, 1992), |
| $a_o$ | = | 22.1 m is the slope length of the standard plot, and |
| $b_o$ | = | 0.09 = 9 % is the slope of the standard USLE gradient. |

The advantage of replacing the slope length by upslope area (length upslope based *LS* versus area based *LS*) is that the upslope area better reflects the impact of concentrated flow on increased erosion (Mitasova and Mitas, 1999).

The above modified Equation 4.5 can be properly applied only to areas experiencing net erosion. Depositional areas should be excluded from the study area because the model assumes that transport capacity exceeds detachment capacity everywhere and that erosion and sediment transport are detachment limited.

### 4.2.4 The cover and management factor (*C*)

The cover and management factor, *C*, is defined as the ratio of soil loss from land under specified crop or mulch conditions to the corresponding loss from tilled bare soil (Goldman *et al.*, 1986). Cover, including plant canopy and materials like mulches, plant residues, or dense growing plants in direct contact with the soil surface, is the most important phenomenon in erosion because it represents conditions that can most easily be managed to reduce erosion (Renard *et al.*, 1994). Thus the cover and management factor reduces the soil loss estimate according to the effectiveness of the cover by preventing detachment and transport of soil particles (Goldman *et al.*, 1986). Also the range of *C*-factor is much greater than that of any other RUSLE factor.

The cover and management factor is possibly the most important factor in the RUSLE equation as a result of its considerable range, the difficulties in its estimation as well as its variation during

the year (Lorentz and Schulze, 1995). Therefore, the accurate determination of the cover and management factor requires careful evaluation. One of the major improvements in the accuracy of this factor within the RUSLE (Renard *et al.,* 1997) model is the use of subfactors. These subfactors include:

- Prior land use, PLU;
- Canopy cover, CC;
- Surface vegetation or mulch cover, SC;
- Surface roughness, SR; and
- Soil moisture, SM.

Values for soil cover can vary from near zero for a very well protected soil to greater than one for a finely tilled ridged surface that produces much runoff and leaves the soil highly susceptible to erosion (Lal, 1994). Values for this factor are a weighted average of soil loss ratios that represent the soil loss for a given condition at a given time to that of the standard plot (Renard *et al.,* 1994). Thus, soil loss ratios vary during the year as soil and cover conditions change. There are different options in determining the *C*-factor depending on the level of information available. Lorentz and Schulze (1995) suggested the following:

- Cover and management factor when only the SCS curve number is known;
- Cover and management factor when limited vegetation information is available; and
- Cover and management factor when comprehensive vegetation information is available.

Undertaking the measurement of the subfactors as outlined in the RUSLE (Renard *et al.,* 1997) guideline is data demanding and time consuming. For this reason, in the present research the information for the *C*-factor is taken from the work of Kienzle *et al.* (1997) on the Mgeni catchment which used an annual variation in canopy cover, mulch cover, litter mass and root mass of the top 100 mm to develop the RUSLE cover factor for the cover class. The cover factors are then incorporated into a GIS coverage, resulting in a set of monthly *C*-factors for each individual grid cell representing the land cover influence on soil loss.

### 4.2.5 Support practice factor (*P*)

The support practice factor, *P*, is defined as the ratio of soil loss with a specific support practice to the loss with the up and down slope tillage (Goldman *et al.,* 1986; Lorentz and Schulze, 1995). The support practice factor is the most uncertain factor both in the USLE and the RUSLE because different studies show that there is a variation in the outcome of the *P*-factor for similar practices (Renard *et al.,* 1994; Hudson, 1995; Renard *et al.,* 1996). However, the *P*-factor in the RUSLE considers more variables than it does in the USLE (Renard *et al.,* 1994; 1996; Miller and Gardiner, 1998). After evaluating extensive data to assess the effect of contouring on soil erosion, factors such as slope, ridge height, row grade, and climatic erosivity are identified as decisive parameters to consider. Strip cropping consideration in the RUSLE includes sediment movement both to the strips and through the strips (Miller and Gardiner, 1998). Moreover, Lorentz and Schulze (1995) stated that the support practice factor affects erosion by modifying the flow pattern, grade and direction of subsurface flow and by reducing the runoff amounts and rates. There are options for calculating the support practice factor depending on the level of information available.

In this research, the support practice factor, *P*, is taken from the work of Kienzle *et al.* (1997) on the study of the Mgeni catchment and was determined by combining land cover and slope information and assessing a set of rules for farming practices across the range of agricultural land uses in the catchment. The support practice factor is then incorporated into a GIS coverage results as a *P*-factor for each individual grid cell, representing the support practice factor influence on soil erosion.

## 4.3 Calculation of the Distributed Sediment Delivery Ratio

When considering catchment scale processes, part of the soil eroded in an overland surface is deposited within the catchment before reaching its outlet. For this reason a concept known as the sediment delivery ratio has been defined as the fraction of gross soil loss (interrill, rill, gully, and stream bank erosion) which is delivered to the outlet of the catchment (Ferro and Minacapilli, 1995; Ferro, 1997; Kothyari and Jain, 1997; Ferro *et al.*, 1998; Jain and Kothyari, 2000). There is

currently no universally applicable prediction technique that may be used to estimate a sediment delivery ratio in the manner that the RUSLE is used for determination of source erosion. Several different equations (cf. Table 3.1) resulting from various studies have been developed for proposed relationships between sediment delivery ratios and catchment and climatic characteristics; however none are generally applicable (Walling, 1983; Lorentz and Howe, 1995).

The sediment delivery ratio is a spatially lumped concept. However, in reality, sediments are produced from different sources distributed throughout the catchment. Each catchment is characterised by its local processes (sediment detachment, transport, deposition) which emphasises the need to use the spatially distributed approach for modelling this phenomenon (Ferro and Minacapilli, 1995; Ferro, 1997; Kothyari and Jain, 1997; Ferro *et al.*, 1998; Jain and Kothyari, 2000). Such a distributed approach allows for within-catchment variability of the sediment delivery ratio and in particular, takes into account the following circumstances:

- Low slope downstream areas have low sediment delivery ratios (Boyce, 1975);
- Much of the predicted sediment yield is often produced in a small percentage of the total catchment area (Beven, 1989; Ferro and Minacapilli, 1995); and
- Steep fallow areas near main channels contribute to both erosion and sediment yield while steep row cropped fields remote from the channel network are characterised by local erosion but may contribute little to the sediment yield (Ferro and Minacapilli, 1995).

Ferro and Minacapilli (1995) hypothesised that the subcatchment sediment delivery ratio, (*SDR*) in a GIS grid cell network is a measurement of the probability that the eroded particles arrive from all grid cells into the nearest stream reach. The sediment delivery ratio of each grid cell ($SDR_i$) is a strong function of the travel time ($t_i$) of overland flow of the discharge from each grid cell in a subcatchment. The travel time is also strongly dependent on the topographic and land use characteristics of an area and therefore its relationship with sediment delivery ratio (*SDR*) is justified. In their study Ferro and Minacapilli (1995) assumed that the probability of the eroded particles arriving from each grid cell into the nearest stream reach is proportional to the probability of non-exceedence of the travel time, $t_i$ of each grid cell. Therefore, in order to specify the mathematical shape of the relationship between $SDR_i$ and travel time the empirical cumulative

frequency distribution function (CDF) of the variable (travel time) of each grid cell is required. The CDF comprises the number of occurrences greater than and equal to the given category of (travel times), $t_i$, divided by the total frequency of the category (travel time) of each grid cell in a subcatchment.

Based on the above hypothesis a relationship between the cumulative frequency of travel times and the travel time has been developed by Ferro and Minacapilli (1995) and later used by Ferro (1997); Jain and Kothyari (2000); Ferro and Porto (2000) and Fernandez *et al.*(2003) on different catchments. Ferro and Minacapilli (1995) found that the relationship between the logarithm of the empirical cumulative frequency of travel time $F_i$, $lnF_i$, and travel time ($t_i$) is linear for a given subcatchment. Therefore mathematically this argument can be explained by introducing a constant parameter $\beta$ for a given subcatchment as follows:

$$\ln(F_i) = \beta t_i \qquad 4.6$$

Thus Equation 4.6 can be rewritten as:

$$F_i = e^{-\beta t_i} \qquad 4.7$$

where $F_i$ = CDF of the travel time ($t_i$) of each grid cell to the nearest stream in a subcatchment, (ranges from 0 to 1),

$\beta$ = catchment specific parameter considered as a constant for a given subcatchment which depends on the topographic factor slope and landuse, and

$t_i$ = travel time (h) of overland flow from the i-th overland grid to the nearest channel grid down the drainage path.

For a given i-th grid, the $SDR_i$ (a measure of the probability that the eroded particles from each grid cell arrive into the nearest stream reach) is assumed equal to the empirical cumulative frequency $F_i$ of non-exceedence of the travel time $t_i$, (Ferro and Minacapilli, 1995). According to this concept the relationship (Equation 4.8) is deduced from Equation 4.7 which can be used for

calculating the catchment sediment delivery ratio (*SDR*) for each cell *i* that defines the fraction of sediment that actually reaches a continuous stream system from a specific cell,

$$SDR_i = e^{-\beta t_i} \qquad 4.8$$

where $SDR_i$ = the fraction of sediment from i-th cell that actually reaches a continuous stream system,

$\beta$ = catchment specific parameter considered as a constant for a given subcatchment which depends on the topographic factor slope and landuse, and

$t_i$ = travel time (h) of overland flow from the i-th overland grid to the nearest channel grid down the drainage path.

The exponential function in Equation 4.8 describes the decreasing rate of sediment delivery from cell *i* as the travel time increases. The catchment specific parameter ($\beta$) which is determined on a subcatchment basis shows the trapping efficiency of the overland cells and stream network for the eroded particles in a subcatchment. The simple characteristics of the model are shown in Figure 4.2. This can be explained in a specific subcatchment, in which the sediment delivery ratio and travel times are inversely related i.e. the furthest cell, (in terms of travel time); to the nearest stream reach has the smallest sediment delivery ratio (*SDR*). This represents the increasing opportunity for sediment deposition along the travel path.

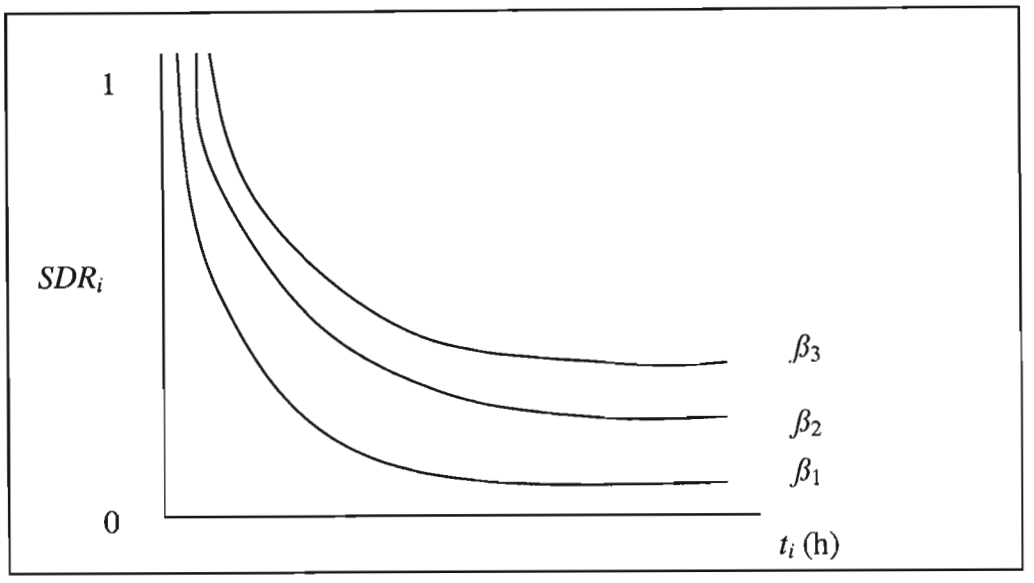


**Figure 4.2** Schematic relationship of sediment delivery ratio ($SDR_i$), travel time ($t_i$) and the subcatchment specific parameter $\beta$ (where $\beta_1 > \beta_2 > \beta_3$) for typical subcatchments *1*, *2* and *3*

### 4.3.1 A morphological estimate criterion of the subcatchment specific parameter ($\beta$)

The subcatchment specific parameter ($\beta$) is a coefficient assumed constant for a given subcatchment because it was found that the relationship between $F_i$, $lnF_i$, and travel time ($t_i$) is linear in a given subcatchment (Ferro and Minacapilli, 1995). The subcatchment specific parameter $\beta$, which depends primarily on catchment morphological data, can be estimated with different approaches. In this research, the subcatchment specific parameter $\beta$ is derived only from the topographic parameter, slope and land use as they influence travel time of discharge from each grid cell in a subcatchment as follows:

***Step one***

Discretise an arbitrary subcatchment into grid cells which presume homogeneity in terms of topography and roughness characteristic (land use) in a GIS environment (Figure 4.3a).

***Step two***

Calculate the travel times (Figure 4.3a) from each grid cell to the nearest stream reach in a subcatchment as a function of topography (slope $m.m^{-1}$) and roughness characteristics of each grid cell as demonstrated in Section 4.3.2. Therefore, the subcatchment specific parameter ($\beta$) can be deduced from Equation 4.6 as follows:

$$\beta = \frac{-\ln F_i}{t_i} \qquad 4.9$$

where $t_i$ = the travel time (h) of flow from each grid cell to the nearest stream of a specific subcatchment, and

$F_i$ = CDF of the travel time ($t_i$) of each grid cell to the nearest stream in a subcatchment which ranges from 0 to 1.

***Step three***

The subcatchment specific parameters $\beta$ for each subcatchment were determined by a regression that fits the relationship between $lnF_i$, and travel time ($t_i$) of each grid cell in a given subcatchment (Figure 4.3b). Once the fitted value $\beta$, has been obtained for all grid cells in a given subcatchment, the individual cell sediment delivery ratios, $SDR_i$ can be calculated from Equation 4.8 for each subcatchment in the study area.

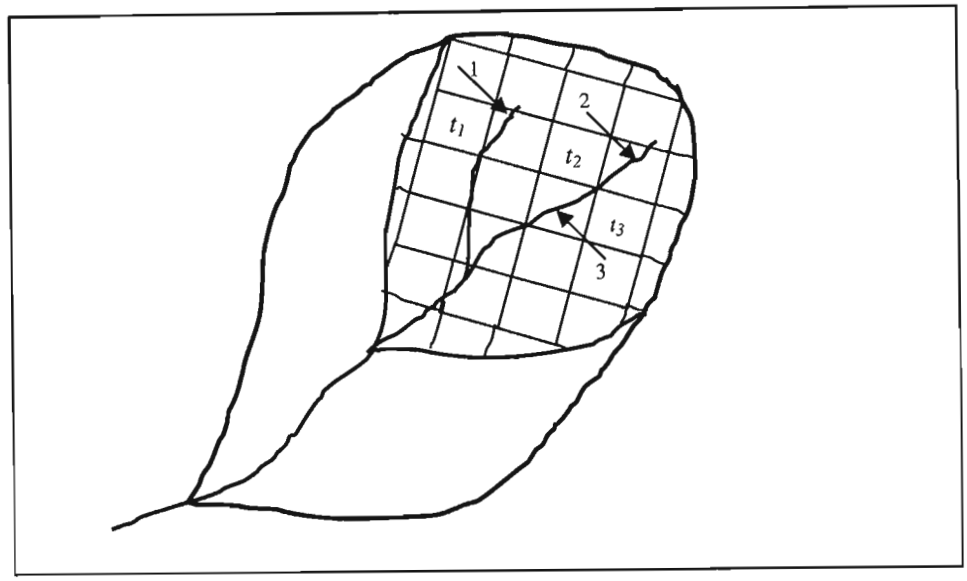


**Figure 4.3a** A schematic of the travel pathways of eroded particles from three typical cells into the nearest stream reach as a function of travel time $t_i$ in a given subcatchment

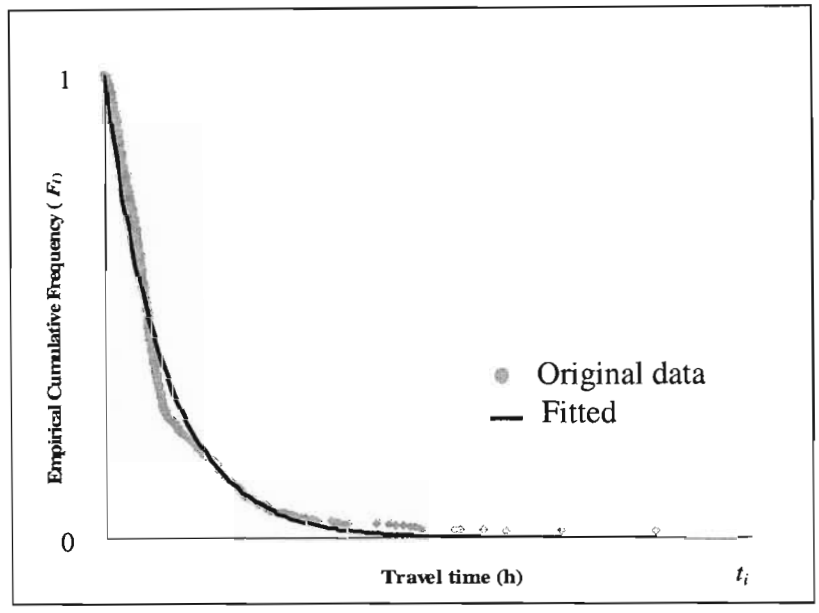


**Figure 4.3b** A graph showing the Cumulative Frequency Distribution of travel times, ($F_i$) and the fitted curve (Equation 4.9) yielding the parameter, $\beta$ for a given subcatchment

Hence the sediment delivery ratio of the model developed in this research was derived from readily available morphological and land use data only. This differs from the CALSITE approach

that was developed by Bradbury *et al.* (1993), which requires actual sediment yield data for calibration in its development of the sediment delivery ratio component of the model.

### 4.3.2 Calculation of travel time

The travel time for runoff water from one point to another in a catchment can be estimated if one knows the flow distance and velocity along the flow path (USDA-SCS, 1975; Bao *et al.*, 1997). In grid based GIS analysis, the direction of flow from one cell to the neighbouring cell is determined by using an eight direction pour point algorithm (ESRI, 1994; 1996). This algorithm chooses the direction of steepest descent among the eight permitted choices. Once the pour point algorithm identifies the flow direction in each cell, a cell to cell flow length is determined to the nearest stream channel (Maidment, 1994). If the flow path from cell $i$ to the nearest channel cell traverses $N$ cells and the flow length of the i-th cell is $l_i$ (which can be equal to the length of a square side or to a diagonal, depending on the direction of flow in the i-th cell) with the velocity of flow in cell $i$ being $v_i$, then the travel time $t_i$ from cell $i$ to the nearest channel can be calculated by adding the travel time for each of the $N$ cells located along the flow path (Jain and Kothyari, 2000). This is given by Equation 4.10 below, which is used in this research.

$$t_i = \sum_{i=1}^{N} \frac{l_i}{v_i} \qquad 4.10$$

where $l_i$ = length of segment $i$ in the flow path (m) and is equal to the length of the side or diagonal of a grid cell depending on the flow direction in the grid cell, and

$v_i$ = flow velocity for a given cell ($m.s^{-1}$).

#### *4.3.2.1 Calculation of flow length*

Flow length is defined as the distance from any point in the catchment to the nearest stream. This distance is measured along the flow direction, not "as the crow flies". In this research, the flow length, or distance to the nearest stream channel, is calculated using a syntax algorithm written in

Arcview avenue script (Appendix A) Moglen (2004) which represents the accumulated flow length from upslope cells draining down to each downslope cell.

#### *4.3.2.2 Calculation of overland flow velocity*

For the present research, the method for the determination of the overland flow velocity proposed by the USDA-SCS is chosen due to its simplicity and availability of the information required (USDA-SCS, 1975). The flow velocity is considered to be a function of the land surface slope and the land cover characteristics as follows:

$$v_i = \alpha_i S_i^b \qquad 4.11$$

where $v_i$ = overland flow velocity from cell $i$,

$b$ = a numerical constant normally set to 0.5 (SCS, 1975; Ferro and Minacapilli, 1995),

$S_i$ = the slope of the i-th cell ($m.m^{-1}$) (calculated by slope surface option in hydrology extension of Arcview (ESRI, 1996)), and

$\alpha_i$ = a coefficient related to land use, (given in Table 4.1).

## 4.4 Calculation of Sediment Yield

Once the source erosion ($A_i$) and sediment delivery ratio ($SDR_i$) have been determined within each grid cell, the final sediment yield ($Y_i$) of the i-th cell of the subcatchment is estimated using Equation 4.12.

$$Y_i = A_i \cdot SDR_i \cdot a_i \qquad 4.12$$

where $Y_i$ = sediment yield from each grid cell $i$ ($t.ha.^{-1}\ yr^{-1}$),

$A_i$ = the average annual soil loss per unit area within the cell ($t.ha^{-1}.yr^{-1}$),

$a_i$ = area of the i-th cell (ha) and

$SDR_i$ = the fraction of $A_i$ that ultimately reaches the nearest channel.

**Table 4.1** Surface roughness characteristics adopted from Table 3.20 of Haan *et al.* (1994)

| Surface | $\alpha_i$ (m.s$^{-1}$) |
|---|---|
| *Overland flow* | |
| Forest | 0.76 |
| Contour strip cropped | 1.56 |
| Short grass | 2.13 |
| Straight row cultivation | 2.62 |
| Paved | 6.19 |
| *Shallow concentrated flow* | |
| Alluvial fans | 3.08 |
| Grassed waterways | 4.91 |
| Small upland gullies | 6.19 |

Since the $SDR_i$ of a cell is hypothesised as a function of travel time to the nearest channel, it implies that the gross soil erosion ($A_i$) in that cell multiplied by the $SDR_i$ value of the cell becomes the sediment yield contribution of that cell to the nearest stream channel (Jain and Kothyari, 2000). This hypothesis is accurate at the event scale only if the catchment is small because there is no well developed stream network for temporary storage of sediments. Otherwise it is applicable at the mean annual scale in large catchments, according to Playfair's law (Boyce, 1975) which states that over a long time, a stream must essentially transport all sediment delivered to it.

Subcatchment estimation of sediment yields are necessary to show the importance of the distributed sediment delivery ratio concept that switch from empirical sediment delivery ratio (Table 3.1) to distributed mode of sediment delivery modelling. This is because distributed mode accounts the drainage system, topography and land use of each subcatchment which highly affect the sediment delivery process. In addition this distributed mode allows for the identification of the spatially varying sediment transport capacity and ultimately the sediment yield from each subcatchment.

Apart from the *LS* factor which is derived from the Digital Elevation Model (DEM) with the new concept of upslope area Equation 4.5, the relevant data sets: rainfall erosivity (*R*-factor), soil erodibility (*K*-factor), cover and management (*C*-factor), support practice (*P*-factor), land type and land use map for this research are obtained in digital format (raster image) from the work of Kienzle *et al.* (1997) in the Mgeni catchment and Howe (1999) in the Henley catchment. The detailed descriptions of these data are given in the next chapter. Figure 4.1 illustrates how these input data sets are used to produce images which are used for the calculation of source erosion, sediment delivery ratio and sediment yield in the model.

# 5. HENLEY CATCHMENT AND INPUT DATA SETS

## 5.1 Overview

The Henley catchment covers an area of approximately 178 $km^2$. It is located in south western portion (29° 35'-29° 49'S; 30° 02'-30° 18'E) of the Mgeni catchment in the KwaZulu-Natal province, South Africa (Figure 5.1). The mean annual precipitation (MAP) within the catchment ranges from 800 mm to 1136 mm in accordance with the elevation which varies from 937 to 1601 m. The mean annual runoff coefficient is approximately 21.4 % (Kienzle *et al.*, 1997). The Henley catchment comprises the headwaters of the Msunduzi River. The Msunduzi River is the largest river flowing through the city of Pietermaritzburg, some 15 km downstream of the Henley weir.

The land use in the catchment consists predominantly of informal traditional Zulu and peri-urban settlements interspersed with mixed crops, grassland and forestry. The grassland is heavily grazed and the traditional and peri-urban settlements with mixed crops were identified as potential non-point sources of sediment yield.

Geologically, the catchment consists of unconsolidated coastal sediment and sands; Ecca shales, Dyamictite and Natal Group sandstone are found further upstream. Intrusions of dolerites dykes and sills are found near Pietermaritzburg.

The catchment was selected to verify a comprehensive methodology that integrates the Revised Universal Soil Loss Equation (RUSLE) a soil loss model, Geographic Information System (GIS) techniques and distributed Sediment Delivery Ratio (*SDR*) concept for soil loss and sediment yield modelling because of its high average annual sediment yield, estimated at 42 t. $km^{-2}$ from a survey of the Henley dam (Rooseboom *et al.*, 1992).

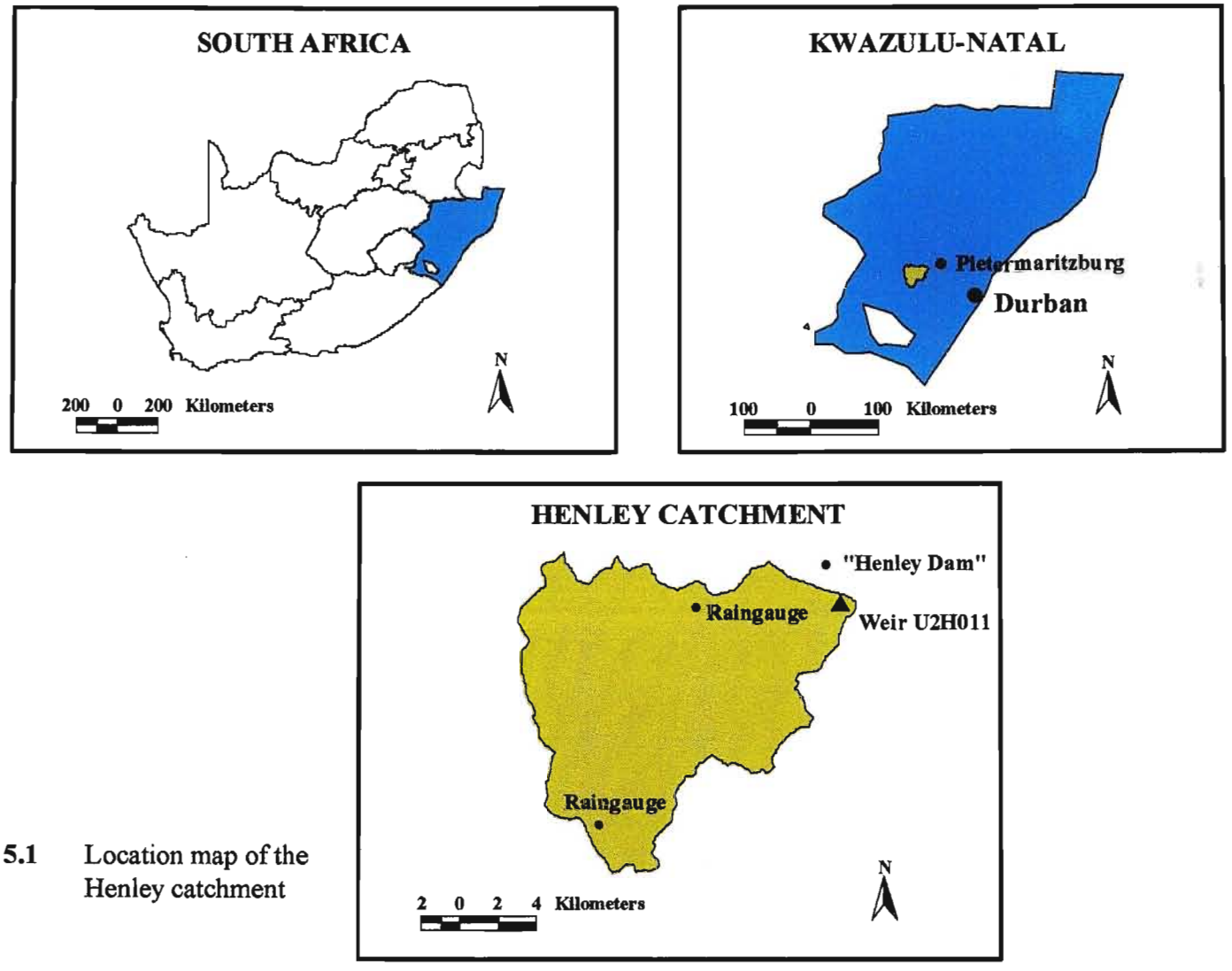


**Figure 5.1** Location map of the Henley catchment

## 5.2 Topography and Catchment Discretisation

Drainage networks describing the process of gravity acting on slopes, the associated channel links and catchments are fundamental concepts in hydrology which describe the transport of water and associated material out of a local region (O'Callaghan and Mark, 1984). The catchment was discretised into a DEM of 50 m × 50 m resolution grid cells which were presumed to exhibit homogenous properties. The DEM, treated to remove pits and flat areas in order to maintain continuity of flow to the nearest stream channel. However, these areas are real landscape that should be handled in a hydrologically meaningful way during drainage analysis (Martz and Garbecht, 1998). Therefore, consideration of depressions and flat areas may have improved the accuracy of the sediment yield analysis as the catchment has about 5.8 $km^2$ of these areas. The DEM was developed by line digitisation at 20 m contour intervals and spot heights from a 1: 50 000 scale topographical map. It was fitted to a triangular irregular network (TIN) in ARC/INFO (version 7.0.3) before establishing a regular elevation grid by Kienzle and Lorentz (1993). This DEM was used as a primary data set for subsequent calculations on slope, slope length, flow direction, flow accumulation and flow length.

In this research, the eight pour point algorithm of Jenson and Domingue (1988) was used to delineate the stream network and subcatchments from a raster DEM in ARC/INFO (version 7.0.3) hydrological grid functions. This algorithm was processed on this DEM to extract the topographic structure, and identifies the grid cell, out of the eight surrounding cells, towards which water will flow by gravity. Figure 5.3 illustrates an application of the ARC/INFO's GIS grid eight direction pour point algorithm with regards to deriving a drainage network given a DEM for a catchment. The flow accumulation, which denotes the accumulated upslope contributing area for a given cell was calculated by summing the cell areas of all upslope cells draining to it.

Nine subcatchments were identified for the Henley catchment (Figure 5.5). The delineated channel system (Figure 5.5) shows areas where flow concentrates in the catchment as a function of topography as derived from the DEM and the GIS techniques described above. The delineated channel system is checked against the topographic map to ensure that it adequately reflect reality.

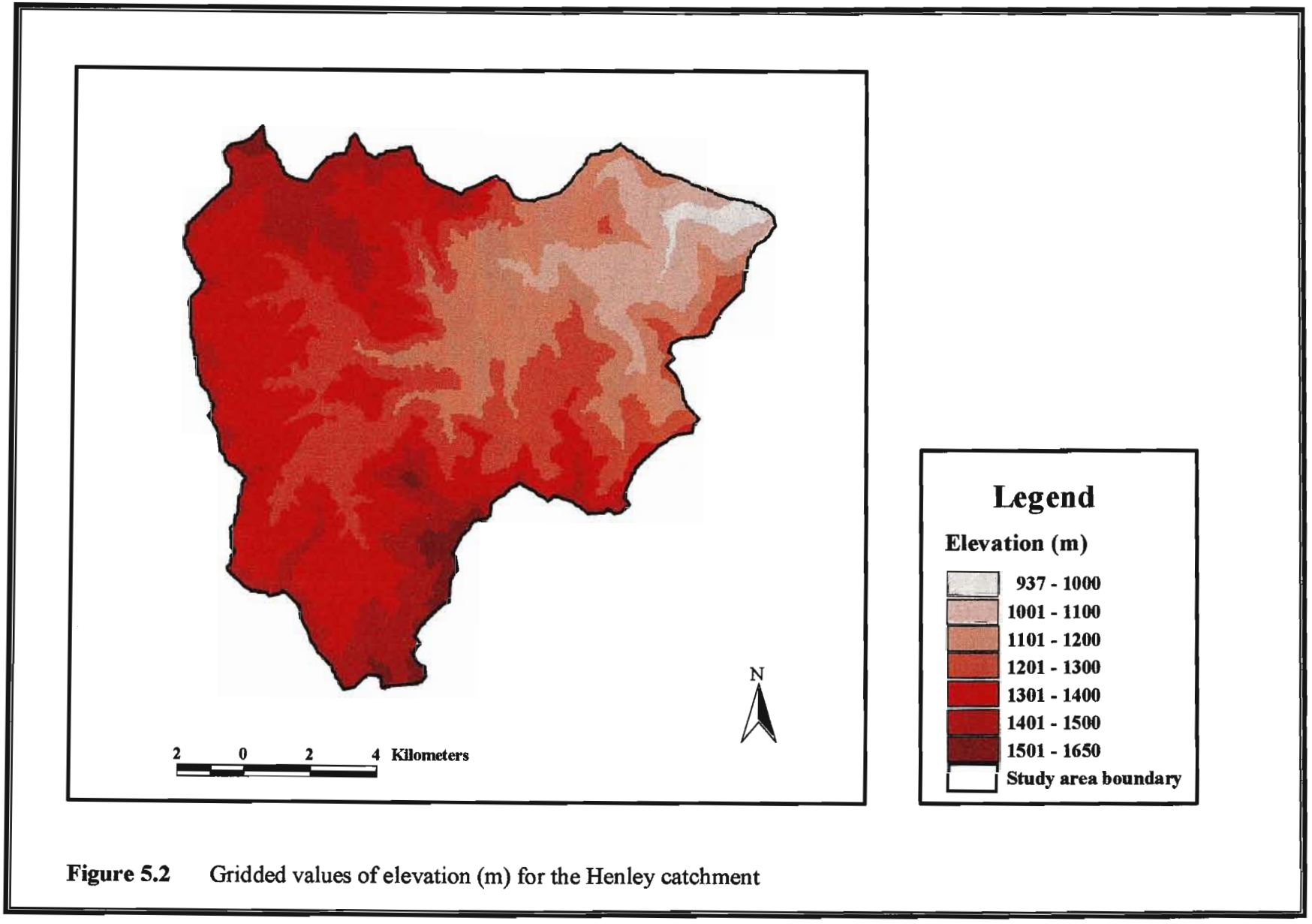


**Figure 5.2** Gridded values of elevation (m) for the Henley catchment

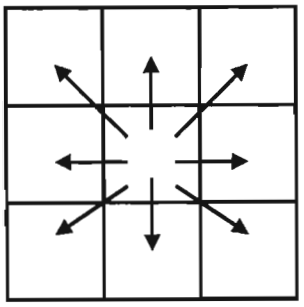

(a)

| | | | | | |
|---|---|---|---|---|---|
| 78 | 72 | 69 | 71 | 58 | 49 |
| 74 | 67 | 56 | 49 | 46 | 58 |
| 69 | 53 | 44 | 37 | 38 | 48 |
| 64 | 58 | 55 | 22 | 31 | 24 |
| 68 | 61 | 47 | 21 | 16 | 19 |
| 74 | 53 | 34 | 12 | 11 | 12 |

(b)

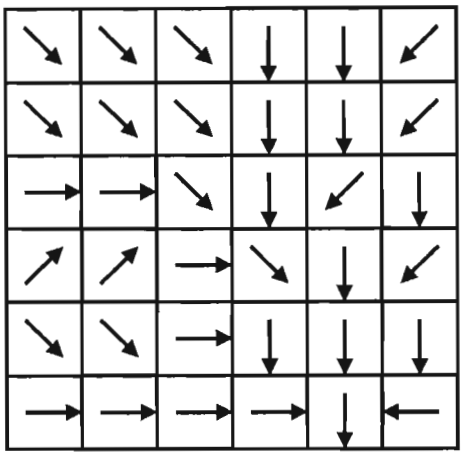

(c)

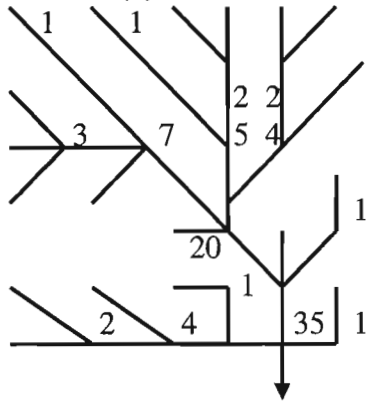


(d)

**Figure 5.3** ARC/INFO GIS grid techniques used in this research: (a) the eight direction pour point model, (b) a digital elevation grid required as input, (c) the corresponding grid of flow directions, and (d) the resulting equivalent flow accumulation network (after Maidment, 1993)

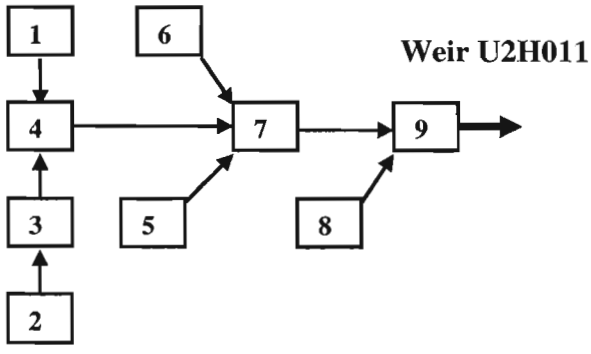


**Figure 5.4** Henley study area subcatchment configuration to weir U2H011

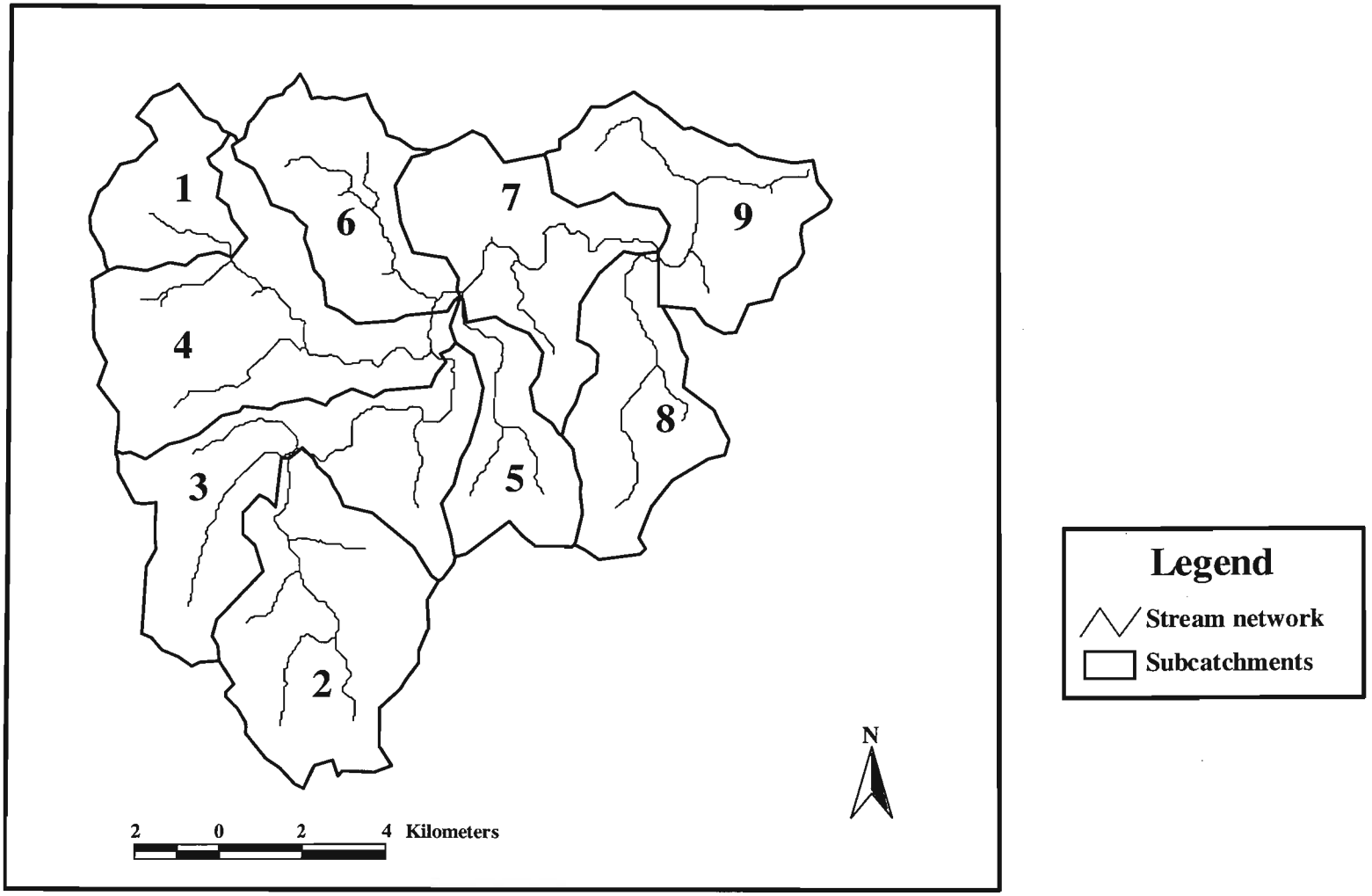


**Figure 5.5** Stream network and subcatchments for the Henley catchment

## 5.3 Input Data Sets

Owing to the complexity of the variables involved in soil loss and sediment yield studies, and since they interact in a wide spatial domain, simplicity of data management becomes very important.

According to Renard *et al.* (1997), the RUSLE model yields a good estimate of the amount of detached soil from rill and interrill at the cell basis. They suggested that for computational purposes, a complex catchment must be divided into hydrologically homogenous subunits (grid cells). They, furthermore, suggested that applying the model to complex catchment by using overall averages of all the RUSLE parameters would be incorrect.

Based on the above facts, it is preferable to use a raster GIS approach for modelling complex catchments, as the raster approach allows for uniform delineation of the catchment into regular grid cell size. Each of these grid cells will be equal in size, and will model the same area on the earth's surface, for each of the RUSLE parameters in the model. Therefore, a grid system is an ideal environment for spatial analysis where a number of different features have to be combined as is the case in the calculation of soil erosion and the identification of sediment source areas (Kienzle and Lorentz, 1993). The discretisation of a catchment into many small cells (grids) makes the application of field scale models, such as RUSLE an attractive option. RUSLE, (Renard *et al.,* 1991) requires the same input parameters as the well known USLE, *viz.* parameters for rainfall erosivity (*R*-factor), soil erodibility (*K*-factor), slope length and gradient (*LS*-factor), cover and management (*C*-factor) and conservation practices (*P*-factor). However, many significant erosion and deposition mechanisms have been incorporated into the revised parameters.

It is known that the RUSLE soil loss model refers to a unit plot size. The RUSLE plot size is arbitrarily defined as 22.1 m long and a uniform lengthwise slope of 9 % in a continuously clean tilled fallow condition, with tillage performed up and downslope (Renard *et al.,* 1997). Ideally, therefore, the grid cell size, used in modelling should be of similar size to the standard plots in order to use this equation as close to its original specifications as possible.

However, this is not possible, as the cell size used for modelling needs to be determined from the scale at which the data sets were captured. In this research, the data sets for elevation were captured at a scale of 1: 50 000. According to Bradbury (1995), the cell size should therefore not be smaller than 50 m resolution grid because it may cause discrepancy from the original data values of the data set.

Not all the data sets were, however, captured at this scale. With the exception of the elevation data, all the RUSLE parameters were captured at a larger scale. The elevation data set consisting of sampled points derived from modelling techniques (interpolating techniques) are not absolute data. If the elevation data were re-sampled, the original data would be affected. For example, if the data from a 50 m resolution is re-sampled to a 30 m resolution grid, the cell sizes would all have to be re-analysed depending on the techniques chosen for re-sampling. If the cubic re-sampling technique is used, the new 30 m resolution cell value would be generated from an average of the nearest sixteen neighbouring cells, thus changing the original data values of the data set may cause missing of some physical features (Donald, 1997).

The other data sets, rainfall erosivity, soil erodibility, cover and management and support practice parameters were captured at a larger scale. It can therefore be assumed that re-sampling these data sets on a smaller scale would not have an extreme effect on the accuracy of the data sets. For example, the rainfall erosivity data have been captured at a 250 m grid. If the data set is re-sampled to a 50 m resolution grid, the original grid will be replaced with sixteen grids of 50 m resolution, each with the same value for rainfall erosivity as the original cell from the 250 m resolution grid.

In this research, the cover and management factor $C$ and practice factor $P$ are estimated according to Wischmeier and Smith (1978), while the soil erodibility factor $K$ and slope-length factors $LS$ are calculated by the new approaches of Renard *et al.* (1991) and upslope area method of Desmet and Govers (1996) respectively. The rainfall erosivity factor $R$, is determined by correlating average monthly $EI_{30}$ to average monthly rainfall at recording stations by applying an inverse distance weighted interpolation algorithm to the altitude of the catchment by Kienzle *et al.* (1997). The format and sources of information for each of the RUSLE factors are given below.

### 5.3.1 Derivation of rainfall-runoff erosivity factor (*R*)

It should be recalled from Chapter 4 that the most commonly used parameter to represent the rainfall-runoff erosivity factor *R* in the RUSLE is rainfall erosivity ($EI_{30}$). McPhee and Smithen (1984) suggested that rainfall erosivity was a reliable indicator for *R*-factor. Smithen and Schulze (1982) also reported that following stringent statistical tests of results from experimental plots, $EI_{30}$ could be widely recognised as being sufficiently accurate for soil erosion modelling.

In the past few decades many attempts have been made by different researchers in southern Africa. This includes the long term average annual $EI_{30}$ values produced by Smithen and Schulze (1982) for southern Africa from 55 years of data from 403 stations across the country. These values were joined by lines of equal rainfall erosivity to form an iso-erodent map for southern Africa. This map provides a means for obtaining an *R*-factor value, for use in the RUSLE, anywhere in southern Africa.

However, in this research, the average monthly $EI_{30}$ erosivity values that were determined by correlating average monthly $EI_{30}$ to average monthly rainfall at recording rainfall stations at various altitudes from the coast to the highest recording station in the Mgeni catchment, as described by Kienzle *et al.* (1997) was used. From the correlation of monthly $EI_{30}$ and monthly rainfall at each station, a typical relationship was derived associating $EI_{30}$ to the elevation and Mean Annual Precipitation (MAP). The relationships were used with the 250 m elevation grid and the median monthly rainfall coverage to produce coverage of median monthly $EI_{30}$ values for use in RUSLE, in the Mgeni catchment. This coverage is later used as input image for the proposed model in this research. Figure 5.6 shows the annual $EI_{30}$ 50 m grid values for the Henley catchment clipped from the original 250 m grid map of the Mgeni catchment of Kienzle *et al.* (1997).

### 5.3.2 Derivation of soil erodibility factor (*K*)

In this research, the soil erodibility factor, *K*, was used from the original work of Kienzle *et al.* (1997) on the Mgeni catchment. This factor was derived from the values of the land type survey

which are documented in a land type map for each region at a 1: 250 000 scale and memoirs of each map, containing tabulated land type information. Land types are presented on the map in colour with a unique code. Figure 5.7 is a representation taken from the Institute for Soil, Climate and Water (ISCW) maps of the land types and the various codes for each land type of the Henley catchment. There are six land types represented in the Henley catchment.

A description of the field methods used and the interpretation of the land type memoirs occurring in each of the Soil and Irrigation Research Institute (SIRI) Memoirs (1989) are briefly described using Table 5.1 as an example. In each of the tables a heading referring to the terrain unit can be determined. This terrain unit is defined as any part of the land surface with homogeneous form and slope (SIRI, 1989), and is divided into five classes which represent a crest, scarp, midslope, footslope and valley bottom.

For example, in land type Ab38, only terrain units 1, 3 and 5 occur. These can be identified in the sketch of the terrain type. The percentages of each terrain unit, area, slope, slope length, and slope shape are presented in each table. Thus, land type Ab38 is composed of 10 % of unit 1, 85 % of unit 3 and 5 % of unit 5. Unit 1 has a slope of 12-20 %, unit 3 a slope of 6-40 % and unit 5 a slope of 4-20 %. The slope length and shape can be read off in a similar manner from the table.

The soil series and soil depths are also defined according to the terrain units. These are also represented as averaged values for the entire land type under the total column. Information on the soil texture, clay content, and the nature of material which is limiting soil depth is also presented. For example in Land type Ab38, terrain unit 1 consists of 80 % Farningham Hu17, Balmoral Hu18, Hutton Hu16, 10 % of Saintfaiths GS19, Robmore Gs18, and 10 % rock. Terrain unit 3 is composed of a similar soil series. However, terrain unit 5 is composed of 30 % of Farningham Hu17, Balmoral Hu18, Hutton Hu16, 15 % of Saintfaiths GS19, Robmore Gs18, 50 % of Koedoesvlei Oa37 and 5 % rock. In total for the land type the composition is, 77.5 % of Farningham Hu17, Balmoral Hu18, Hutton Hu16, 10.3 % of Saintfaiths GS19, Robmore Gs18, 2.5 % of Koedoesvlei Oa37 and 9.8 % rock.

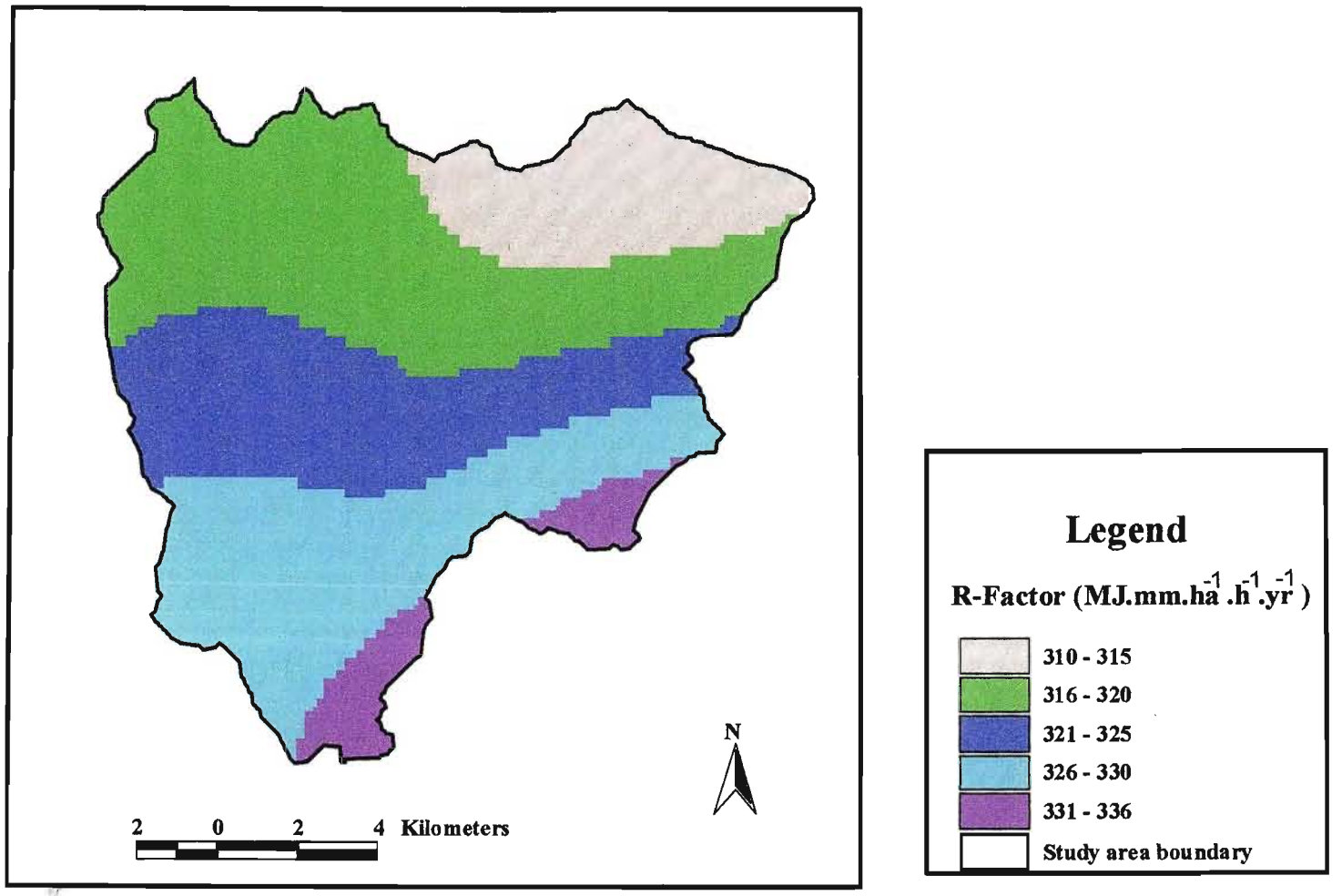


**Figure 5.6** Gridded values of rainfall-runoff erosivity (MJ.mm.ha$^{-1}$.h$^{-1}$.yr$^{-1}$) for the Henley catchment

The textural classes of each of the soil series are also represented. For example; Koedoesvlei Oa37 is classified as me/coSaClLm-Cl, which is medium to coarse sandy, clay loam tending to clay. The clay percentage of each soil type is also available from the SIRI Memories. For example, Koedoesvlei Oa37 has 30-45 % clay content. Based on these two variables, *viz.* textural class and clay percentage, a percentage of sand, silt and clay for each soil series can be determined. These can then be used as input into the erodibility hazard rating information derived for each soil type by Smithers and Schulze (1995) and then the *K*-values suggested for each of these classes by Crosby *et al* (1983), can be used to determine suitable erodibility factor (*K*) for use in the USLE and RUSLE.

The methodology used was to list the percentage of each soil series occurring and their respective percentage occurring in each land type, obtained from the SIRI land type maps. These lists of soils, which may consist of two or more soil series, were represented by a single percentage value. It was assumed that there was equal representation of each of the soil series. For example, land type Ab10 consists of Robmore Gs18, Sainftaiths Gs19 and Hutton Farningham Hu17, all combined to constitute 27 % of the land type. These three soil series were therefore represented as making up a composition of 9 % each.

A mean value was derived for each of the erodibility classes (Table 5.2) defined by Crosby *et al.* (1983) and listed next to each soil series according to their erodibility class. These erodibility values were then multiplied by the fraction of each individual soil series occurring within the land type. The result was a value representing the contribution of that soil series to the total *K*-value for the land type. These contributing *K*-values were then summarised to give a *K*-value for that land type.

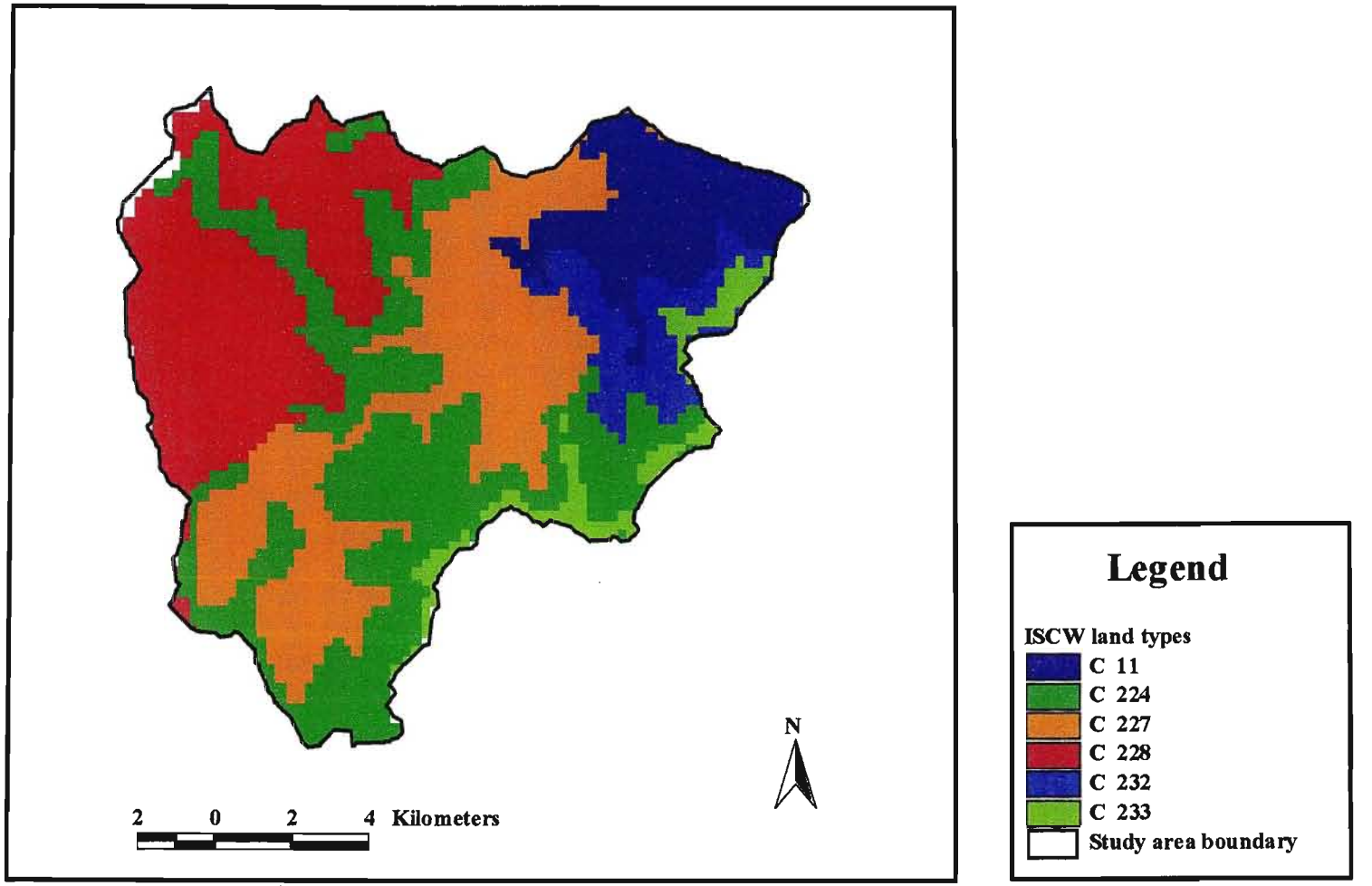


**Figure 5.7** Gridded values of land type for the Henley catchment (after ISCW, 1993)

**Table 5.1** Land type Ab38 from SIRI Memoirs number 12 (1989)

Land type : Ab38
Climate Zone : 9725
Area : 5300ha
Estimated area unavailable for agriculture: 20ha

Occurrence (maps)

Inventory by: JL Schoeman
Modal profiles
None

| | 2430 Pilgrim's Rest (5120ha) | | | | 2530 Barberton (180ha) | |
|---|---|---|---|---|---|---|
| Terrain unit | 1 | 3 | 5 | Total | Clay content (%) | Texture / Depth limiting material |
| % of land type | 10 | 85 | 5 | | | |
| Area (ha) | 530 | 4505 | 265 | | | |
| Slope (%) | 12-20 | 6-40 | 4-20 | | | |
| Slope length (m) | 100-300 | 250-800 | 10-50 | | | |
| Slope shape | Y | Y | X | | | |
| MBO (ha) | 477 | 4055 | 253 | S > 12% | 2544 | |
| | | | | S < 12% | 2239 | |
| MB2 – MB4 (ha) | 53 | 451 | 13 | | 517 | |

| Soil series/land classes | Depth (mm) | MB | % | ha | % | ha | % | ha | ha | % | A | E | B21 Horizon | | Class | |
|---|---|---|---|---|---|---|---|---|---|---|---|---|---|---|---|---|
| Farningham Hu17, Balmoral Hu18, Hutton Hu16 | 500-1200 | 0 | 80 | 424 | 80 | 3604 | 30 | 80 | 4108 | 77.5 | 30-55 | | 30-60 | B | coSaClLm-Cl | so |
| Saintfaiths GS19, Robmore Gs18 | 400-600 | 0 | 10 | 53 | 10 | 451 | 15 | 40 | 543 | 10.3 | 30-45 | | | A | coSaClLm-Cl | lc |
| Koedoesvlei Oa37 | > 1200 | 0 | | | | | 50 | 133 | 133 | 2.5 | 30-45 | | 30-50 | B | me/coSaClLm-Cl | |
| Rock | | 4 | 10 | 53 | 10 | 451 | 5 | 13 | 517 | 9.8 | | | | | | |

**Terrain type : C4**

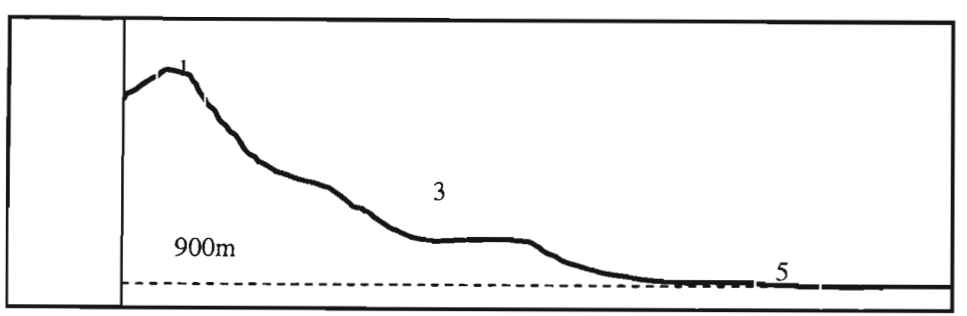


For an explanation of this table, consult LAND TYPE INVENTORY (table of contents)
Geology: Unnamed potassic granite and granodiorite (Archaeosoic)

**Table 5.2** Erodibility factor values for various soil erodibility classes (Crosby *et al.*, 1983)

| Soil erodibility Classes | Soil *K* Factor |
|---|---|
| Very High | > 0.70 |
| High | 0.50-0.70 |
| Moderate | 0.25-0.50 |
| Low | 0.13-0.25 |
| Very Low | < 0.13 |

Based on the above concept, the relevant soil information for this research was obtained from the land type maps of the former SIRI, now ISCW, as percentages of areas covered by a certain soil type on a specific terrain unit within the soil associations termed land types (Figure 5.7). In order to translate land type information into soil properties required to calculate the RUSLE *K*-factor, the terrain units of the study area were spatially defined by combining slope and surface curvature information according to the ISCW's definition of terrain units. The soil erodibility grid (Figure 5.8) shows the 250 m grid map of Kienzle *et al.* (1997), derived the *K*-values for a 50 m grid for the Henley catchment clipped from the original Mgeni. This was done first by obtaining a detailed description of the spatial distribution of the different soils' physical and hydraulic properties within the catchment. Thereafter it was established by overlaying the terrain unit coverage of the Henley catchment, derived according to the definition of the terrain units set out by the ISCW, with the corresponding ISCW land type coverage (Figure 5.7) and associated database. The soil erodibility factor was calculated for each grid cell using this information and the RUSLE algorithms (Renard *et al.*, 1991). Values from this soil erodibility grid (Figure 5.8) are used in this research to calculate the source soil erosion.

### 5.3.3 Cover and management factor (*C*)

The cover and management factor, *C*, is regarded as the most important factor in developing soil loss and sediment yield models (Crosby *et al.*, 1983). The values for this factor were taken from the work of Kienzle *et al.* (1997) on Mgeni catchment. How they were derived is presented in the following paragraphs.

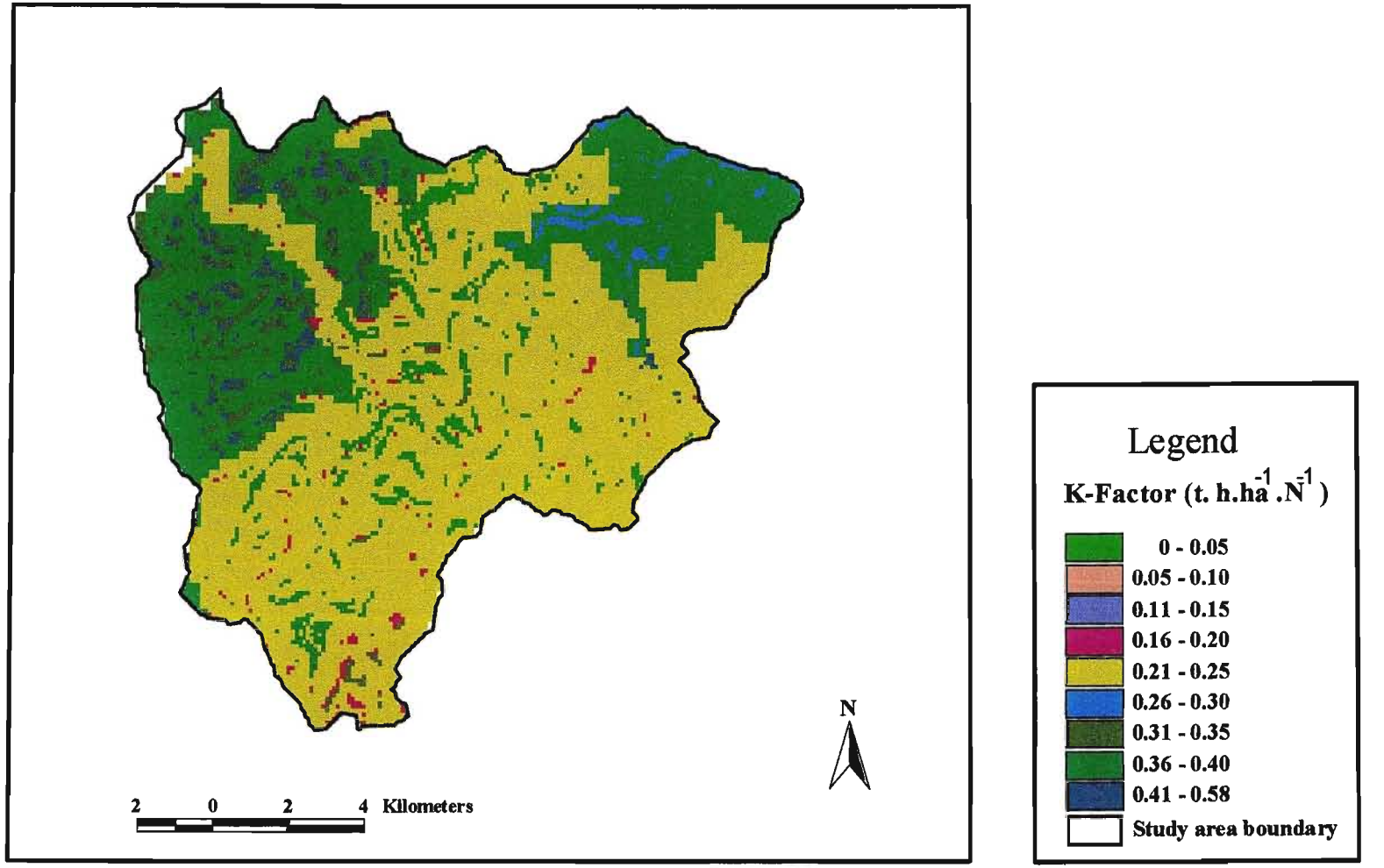


**Figure 5.8** Gridded values of soil erodibility (t. h. ha $^{-1}$.N$^{-1}$) for the Henley catchment

For undisturbed land, a methodology by Crosby *et al.* (1983) proposed that the quantitative evaluation of *C*-factors could be derived directly from Wischmeier and Smith (1978) using basic information on canopy and basal cover percentage. The derivation of the *C*-factor using this methodology was further proposed by Lorentz and Schulze (1995) who suggested using the Wischmeier and Smith (1978) tables to determine *C*-factor values for uncultivated land, where limited information on land cover was available.

Tables 5.3 and 5.4 are the Wischmeier and Smith (1978) tables referred to in the above concept and information from the table was used to calculate the *C*-factor values for permanent pasture, veld, woodland and undisturbed forest land. From these tables, it is evident that information regarding the canopy and ground cover of a region is necessary to determine *C*-values for that particular region. In addition, the knowledge and expert opinion of the local condition of the study area are important in order to generate the *C*-values for a land cover in that region.

A raster land cover map based on a 1986 SPOT satellite image with a grid size of 250 m was produced for the Mgeni catchment by the Institute of Natural Resources (INR) (Bromley, 1989). This map was verified using aerial photography, topographical maps and ground truthing. The Henley land cover map (Figure 5.9) was clipped out from this map and re-sampled to a 50 m grid size. Twelve values were calculated, one for each month of the year, for each of the twelve land uses identified in the Henley catchment. These cover factor grids are a function of the annual variation in canopy cover and root mass of the top 100 mm of the soil (Howe, 1999). Figure 5.10 illustrates the annually averaged *C*-factor grid for the Henley catchment.

**Table 5.3** *C*-factor values for undisturbed forest land (after Wischmeier and Smith, 1978)

| % of area covered by canopy of trees and undergrowth | % of area covered by duff at least 5 cm deep | Factor $C^1$ |
|---|---|---|
| 100-75 | 100-90 | 0.0001-0.001 |
| 70-45 | 85-75 | 0.002-0.004 |
| 40-20 | 70-40 | 0.003-0.009 |

1 The ranges in listed *C*-values are caused by the ranges in the specified forest litter and canopy covers and by variations in effective canopy heights.

**Table 5.4** *C*-factor values for permanent pasture, veld and woodland [1] (after Wischmeier and Smith, 1978)

| Vegetation canopy | | Cover that contacts the soil surface | | | | | | |
|---|---|---|---|---|---|---|---|---|
| Type and height [2] | % cover [3] | | % Ground cover | | | | | |
| | | Type [4] | 0 | 20 | 40 | 60 | 80 | 95+ |
| No appreciable canopy cover | | G | 0.45 | 0.20 | 0.10 | 0.042 | 0.013 | 0.003 |
| | | W | 0.45 | 0.24 | 0.15 | 0.091 | 0.043 | 0.011 |
| Tall weeds or short brush with average drop fall height of 0.5m | 25 | G | 0.36 | 0.17 | 0.09 | 0.038 | 0.013 | 0.003 |
| | | W | 0.36 | 0.20 | 0.13 | 0.083 | 0.041 | 0.011 |
| | 50 | G | 0.26 | 0.13 | 0.07 | 0.035 | 0.012 | 0.003 |
| | | W | 0.26 | 0.16 | 0.11 | 0.076 | 0.039 | 0.011 |
| | 75 | G | 0.17 | 0.10 | 0.06 | 0.032 | 0.011 | 0.003 |
| | | W | 0.17 | 0.12 | 0.09 | 0.068 | 0.038 | 0.011 |
| Appreciable brush or bushes, with average drop fall height of 2m | 25 | G | 0.40 | 0.18 | 0.09 | 0.040 | 0.013 | 0.003 |
| | | W | 0.40 | 0.22 | 0.14 | 0.087 | 0.042 | 0.011 |
| | 50 | G | 0.34 | 0.16 | 0.08 | 0.038 | 0.012 | 0.003 |
| | | W | 0.34 | 0.19 | 0.13 | 0.082 | 0.041 | 0.011 |
| | 75 | G | 0.28 | 0.14 | 0.08 | 0.036 | 0.012 | 0.003 |
| | | W | 0.28 | 0.17 | 0.12 | 0.078 | 0.040 | 0.011 |
| Trees, but no appreciable low brush. Average drop fall height of 4m. | 25 | G | 0.42 | 0.19 | 0.10 | 0.041 | 0.013 | 0.003 |
| | | W | 0.42 | 0.23 | 0.14 | 0.089 | 0.042 | 0.011 |
| | 50 | G | 0.39 | 0.18 | 0.09 | 0.040 | 0.013 | 0.003 |
| | | W | 0.39 | 0.21 | 0.14 | 0.087 | 0.042 | 0.011 |
| | 75 | G | 0.36 | 0.17 | 0.09 | 0.039 | 0.012 | 0.003 |
| | | W | 0.36 | 0.20 | 0.13 | 0.084 | 0.041 | 0.011 |

1 The listed *C*-values assume that the vegetation and mulch are randomly distributed over the entire area.

2 Canopy height is measured as the average fall height of water drops falling from the canopy to the ground. Canopy effect is inversely proportional to drop fall height and is negligible if fall height exceeds 10meters.

3 Portion of total area surface that would be hidden from view by canopy in a vertical projection (a birds eye view).

4 G: cover at surface is grass, grass like plants, decaying compacted duff, or litter at least 50mm deep.

5 W: cover at surface is mostly broadleaf herbaceous plants (as weeds with little lateral root network near the surface) or undecayed residues or both.

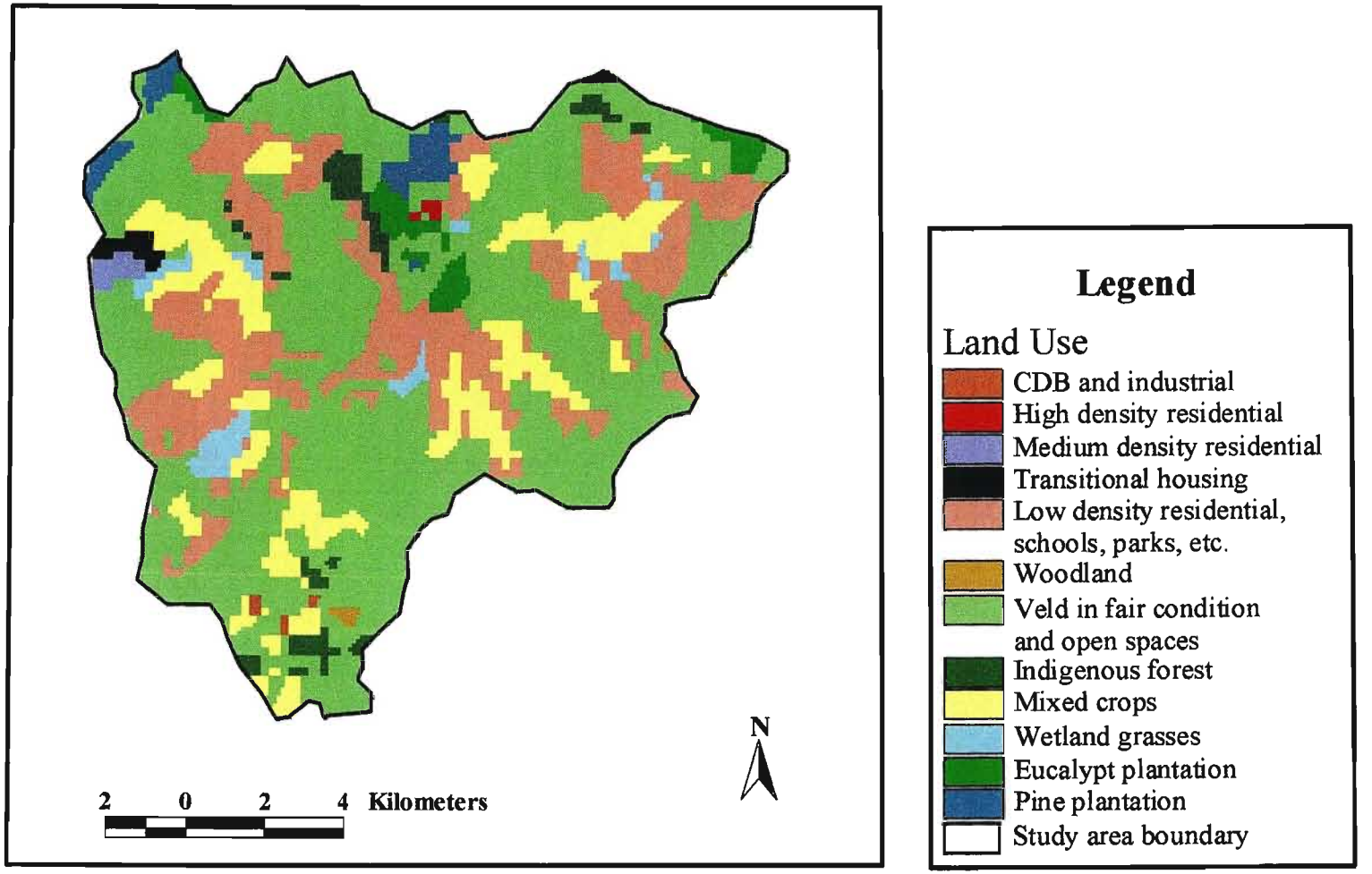


**Figure 5.9** Gridded land use for the Henley catchment (INR, 1986)

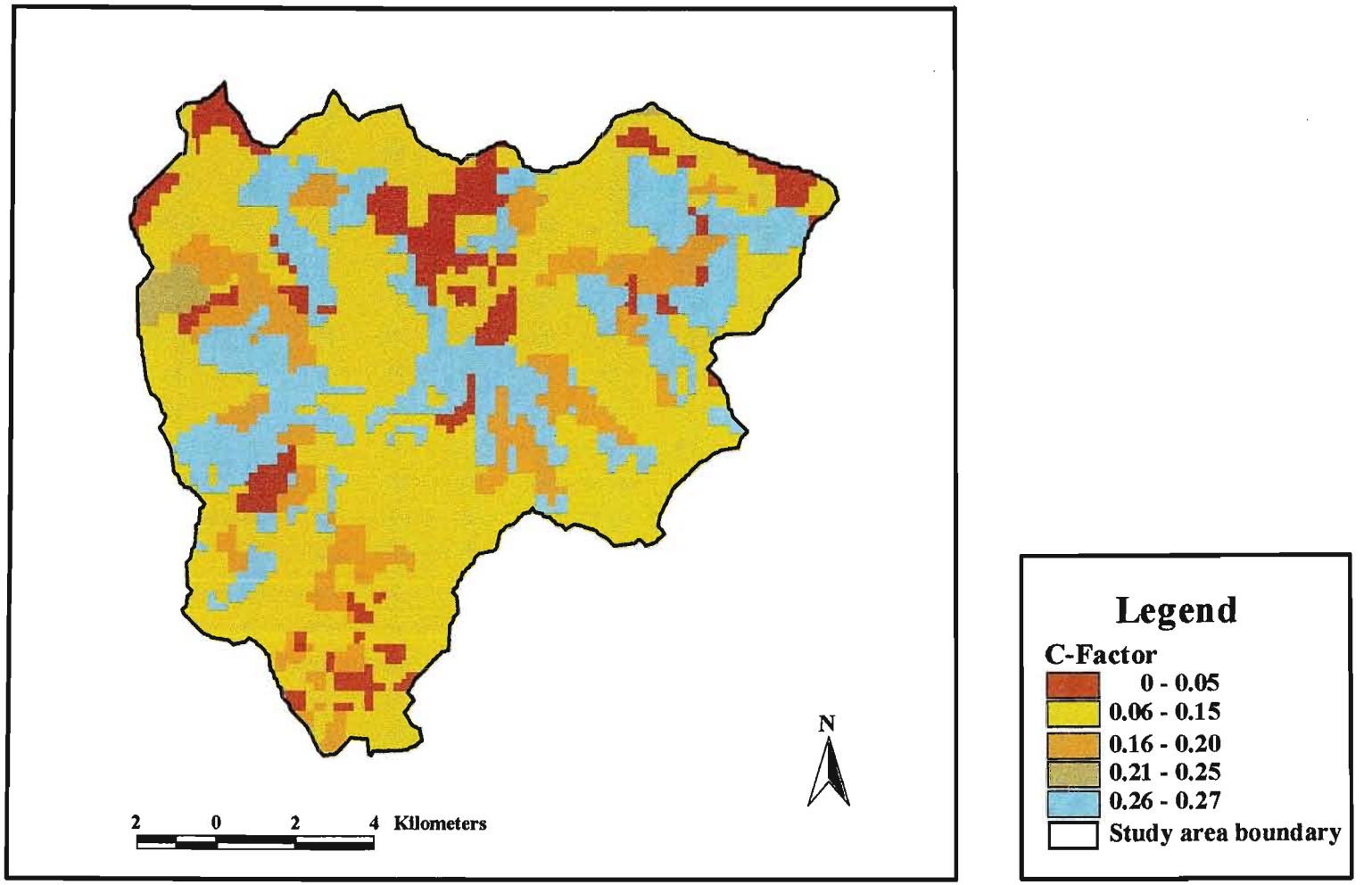


**Figure 5.10** Gridded values of annually averaged cover and management factor for the Henley catchment

### 5.3.4 Support practice factor (*P*)

The support practice factor, *P*, is the ratio of soil loss with a specific support practice to the soil loss with the up and downslope tillage. This factor principally affects erosion by modifying the flow pattern, grade and direction of surface runoff and by reducing the runoff amount and rate (Lorentz and Schulze, 1995). Therefore, care should be taken to determine this factor.

In this research the values of this factor were taken from the original work of Kienzle *et al.* (1997) on the Mgeni catchment. It was determined by combining slope and land cover for contour tilled and contour banks with grassed waterways using estimated values given by Wischmeier and Smith (1978) (Table 5.5). For uncultivated lands, the values for *P*-factor were generally assumed to be equal to unity.

**Table 5.5** *P*-factor values for contour tilled lands and lands with contour banks (after Wischmeier and Smith, 1978)

| Land slope (%) | Contour tilled | Contour banks with grassed waterways |
|---|---|---|
| 1-2 | 0.60 | 0.12 |
| 3-8 | 0.50 | 0.10 |
| 9-12 | 0.60 | 0.12 |
| 13-16 | 0.70 | 0.14 |
| 17-20 | 0.80 | 0.16 |
| 21-25 | 0.90 | 0.18 |

These values of the *P*-factor were then incorporated into a GIS environment to produce a *P*-factor grid (Figure 5.11) which is taken from the original work of Kienzle *et al.* (1997) in the Mgeni study. Finally, values from this grid are used in the calculation of potential soil erosion for the present research.

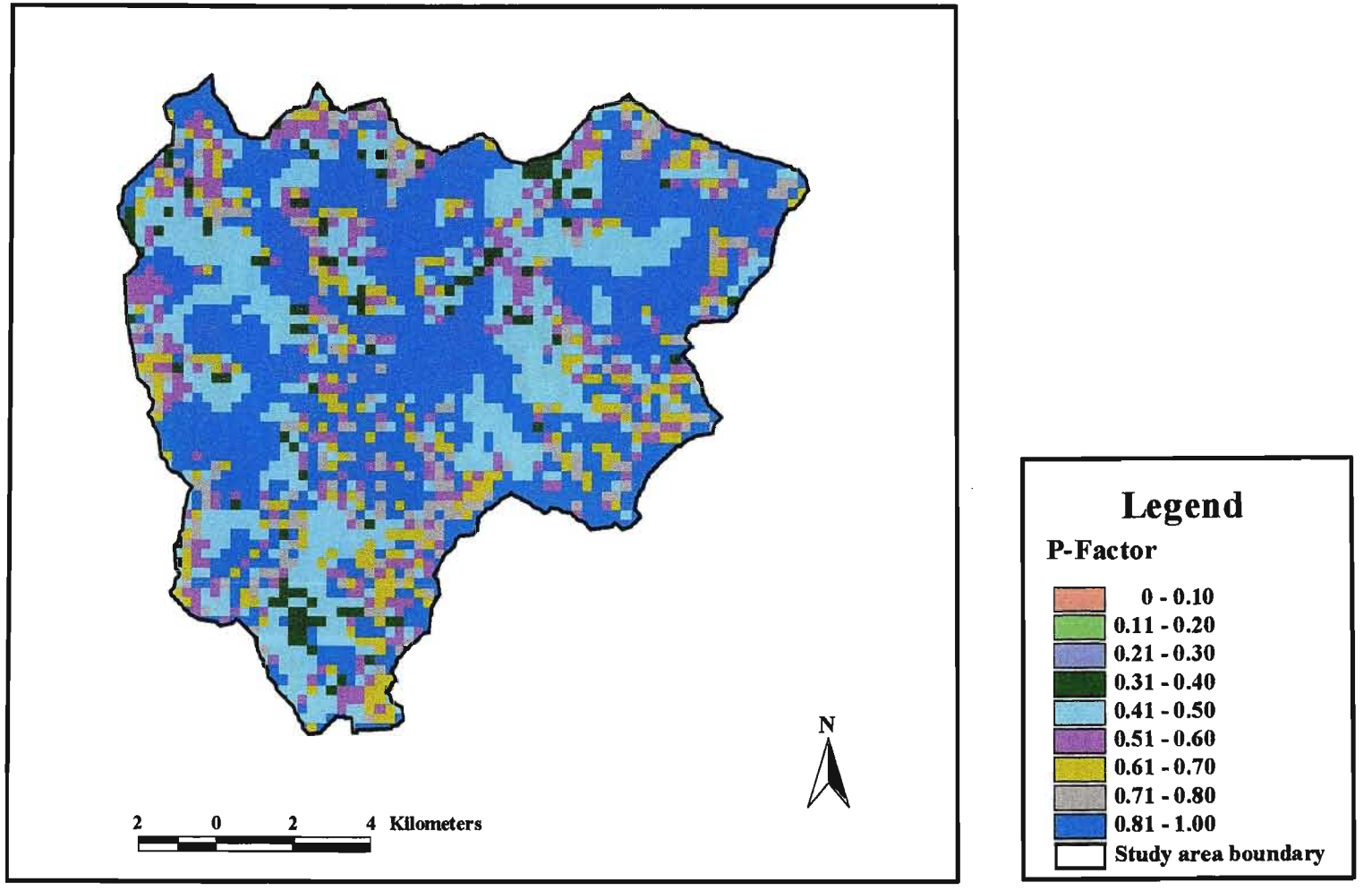


**Figure 5.11** Gridded values of support practice factor for the Henley catchment

# 6. RESULTS AND DISCUSSIONS

Soil loss and sediment yield models applied to a Geographic Information System (GIS) are a powerful land use management tool, but the quality of the result matches the quality of the input data used (Svorin, 2003). When these models are applied to a GIS and used at a catchment scale, some assumptions, made while developing the models, regarding climate, land use, and slope are easily broken. In this research, the importance of the selection of methods to generate input data especially the slope length (*LS*) factor incorporated into a GIS is examined. The modelling results are verified using a quantitative comparison with measured data at the catchment outlet and against other modelling techniques such as mean annual sediment yield modelled by *ACRU* in the Mgeni catchment and mean annual sediment yield reported by Rooseboom *et al.* (1992) for this region. The results are presented according to the methods followed to generate input data. The generated input data are presented first and the final results combining all the factors are presented thereafter.

## 6.1 Topographic Factors

### 6.1.1 Slope steepness factor

The slope map (Figure 6.1), which is an indication of steepness, accounts for the effect of slope angle on soil erosion and sediment yield rates. Generally, higher slope angle values have greater erosion and sediment yield rates. Nowadays, the slope steepness factor is derived from DEMs. Calculation of the slope steepness factor from a DEM is relatively simple, but care must be taken when selecting an algorithm. Today, different GIS packages use different methods of slope angle calculation and give varying results. In this research, the nearest neighbouring method, (employed by ARC/INFO grid (ESRI, 1996) (Appendix B)), is used because this algorithm calculates an average slope across the centre cell using at least four of the surrounding eight cells. The slope steepness which was derived from the DEM for the Henley catchment ranges from 0 % (0°) to about 77 % (38°) (Table 6.1). The mean slope of the catchment is about 14.7 % (8.4°) and the standard deviation is 10 % (5.5°).

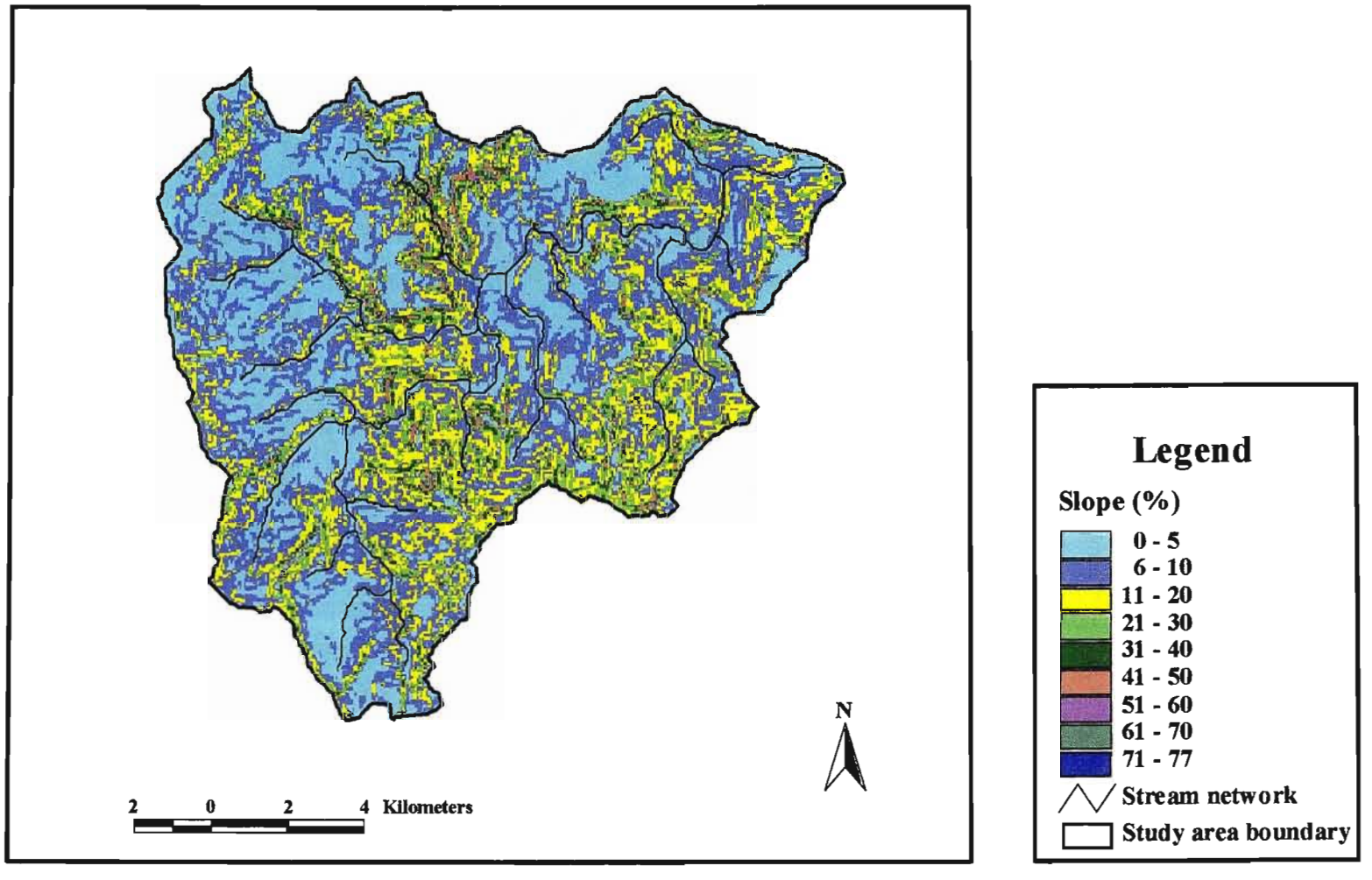


**Figure 6.1** Gridded values of slope (%) for the Henley catchment

**Table 6.1** Slope classes with their areal coverage for the Henley catchment

| Slope in per cent | | Slope in degrees | |
|---|---|---|---|
| Classes | % of areal coverage | Class | % of areal coverage |
| 0-5 | 30.4 | 0-5 | 22.8 |
| 6-10 | 26.2 | 6-10 | 32.1 |
| 11-20 | 18.0 | 11-15 | 27.1 |
| 21-30 | 11.9 | 16-20 | 10.0 |
| 31- 40 | 8.6 | 21-25 | 4.8 |
| 41-50 | 3.3 | 26-30 | 2.1 |
| 51-60 | 1.2 | 31-35 | 0.8 |
| 61-77 | 0.4 | 36-38 | 0.30 |

### 6.1.2 Flow accumulation

The first step in determining flow accumulation is identifying the direction of flow from one pixel to the nearest neighbour(s) (ESRI, 1996). This is based on the principle that water flows from one grid cell to the next following the steepest descent as calculated by Equation 6.1 (ESRI, 1996). The flow direction values for the Henley catchment are presented in Figure 6.2. The steepest descent is the result of elevation comparison of a 3 by 3 matrix of cells whereby the 8 cells surrounding a particular cell releases flow. The cell slopes are calculated from:

$$Slope = \left( \frac{drop\ in\ Z}{S} \right) \cdot 100 \qquad 6.1$$

where $Z$ = elevation (m) of the grid cell and

$S$ = distance (m) taken between the centres of neighbouring cells.

Flow accumulation then uses flow direction as input for its derivation and is given as a number of cells that drain into an output grid cell (ESRI, 1996). Since this output is the network of cells over which water flows, the number of cells that flow into this "channel" is high.

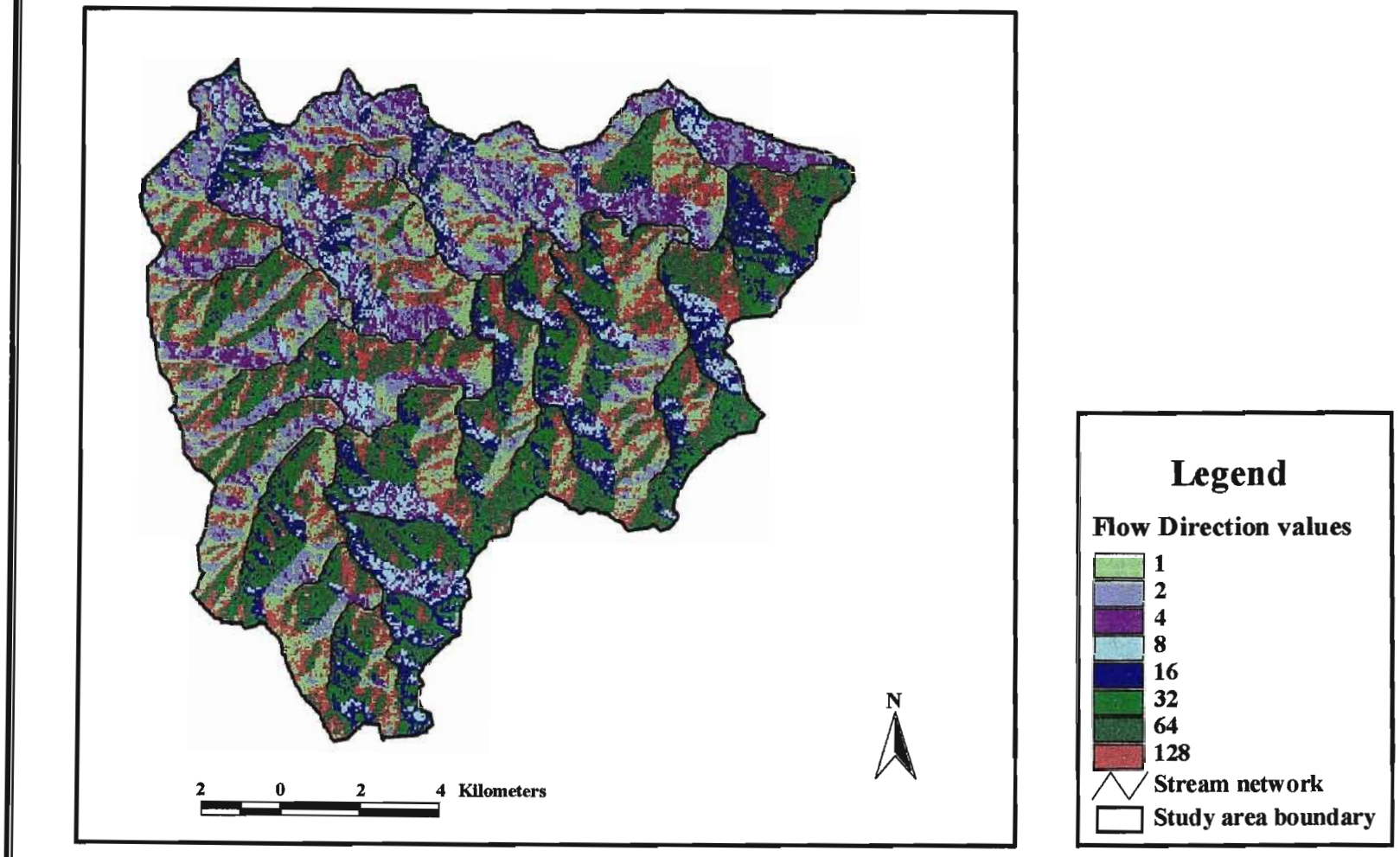


**Figure 6.2** Gridded values of flow direction for the Henley catchment

This value should therefore be modified since RUSLE is only suitable for estimating erosion due to interrill and rill processes (Engel, 2003; Mitasova, 2004). Therefore, a slope length limit should be imposed to appropriately represent the interrill and rill erosion processes in soil loss modelling (McCool *et al.*, 1993). In this research, the upper boundary on the slope length from which flow can be concentrated is taken as 150 m due to the undulating nature of the landscape. Since the grid cell width (resolution) is 50 m, this translates to an accumulation of a maximum of 3 grid cells whereas the minimum is 1 cell where flow will be initiated. The original flow accumulation (Figure 6.3) was used as input to calculate the modified flow accumulation (Figure 6.4) which is calculated based on (Appendix C) has a mean value and standard deviation of 1.05 and 0.26 respectively. Almost all of the flow accumulation (99 %) has values ranging from 1 to 2, i.e. 50 m to 100 m (Table 6.2).

**Table 6.2** Modified flow accumulation classes with their areal coverage for the Henley catchment

| Accumulated number of cells | Area ($km^2$) | % of areal coverage |
|---|---|---|
| 1-2 | 175.7 | 99 |
| 2-3 | 2.3 | 1 |

### 6.1.3 Slope length (*LS*) calculation

It should be recalled from Chapter 4 that the slope length calculation is often the most problematic of the soil loss model using RUSLE parameters. Combining the slope and the flow accumulation within the Arcview GIS using Equation 4.5 yields the *LS* factor surface map (Figure 6.5) with values ranging from 0 to 23. The mean value is 2.24 whereas the standard deviation is 1.99. The variation of the grid cell *LS* values is therefore low. The majority of the catchment area (79.6 %) falls below the mean value. In general, the *LS* value might appear high, which is to be expected because of the low resolution of the DEM that tends to miss physical barriers within the specified grids and which reduces runoff (Hickey *et al.*, 1994). Since the *LS*-factor is the product of the slope length (flow accumulation) and slope steepness, its value is directly proportional.

**Table 6.3** Combined *LS* values with their areal coverage for the Henley catchment

| Classes | % of areal coverage |
|---|---|
| 0-5 | 95.8 |
| 6-10 | 3.5 |
| 11-15 | 0.5 |
| 16-20 | 0.16 |
| 21-25 | 0.04 |

## 6.2 Calculation of Flow Length

Flow length has been defined in Chapter 4 as the distance from any point in the catchment to the nearest stream channel. This distance is measured along the flow direction, not "as the crow flies". In this research, the flow length or distance to the nearest stream was calculated from the DEM by writing syntax in Arcview avenue script (Appendix A) which gives the accumulated flow length downstream of each cell as shown in Figure 6.6. These values rang from 0 to 11.5 km. The mean value is 3.2 km whereas the standard deviation is 2 km, which indicates that the variation of the grid cells in their value of this factor is high. Table 6.4 shows the flow length or distance with their respective areal coverage in the catchment.

**Table 6.4** Flow length or distance classes with their areal coverage for the Henley catchment

| Flow length classes (km) | Area ($km^2$) | % of areal coverage |
|---|---|---|
| 0-2 | 29.5 | 16.6 |
| 2-4 | 85.6 | 48.1 |
| 4-6 | 32.2 | 18.1 |
| 6-8 | 18.7 | 10.5 |
| 8-10 | 10.5 | 5.2 |
| 10-11.5 | 1.4 | 1.5 |

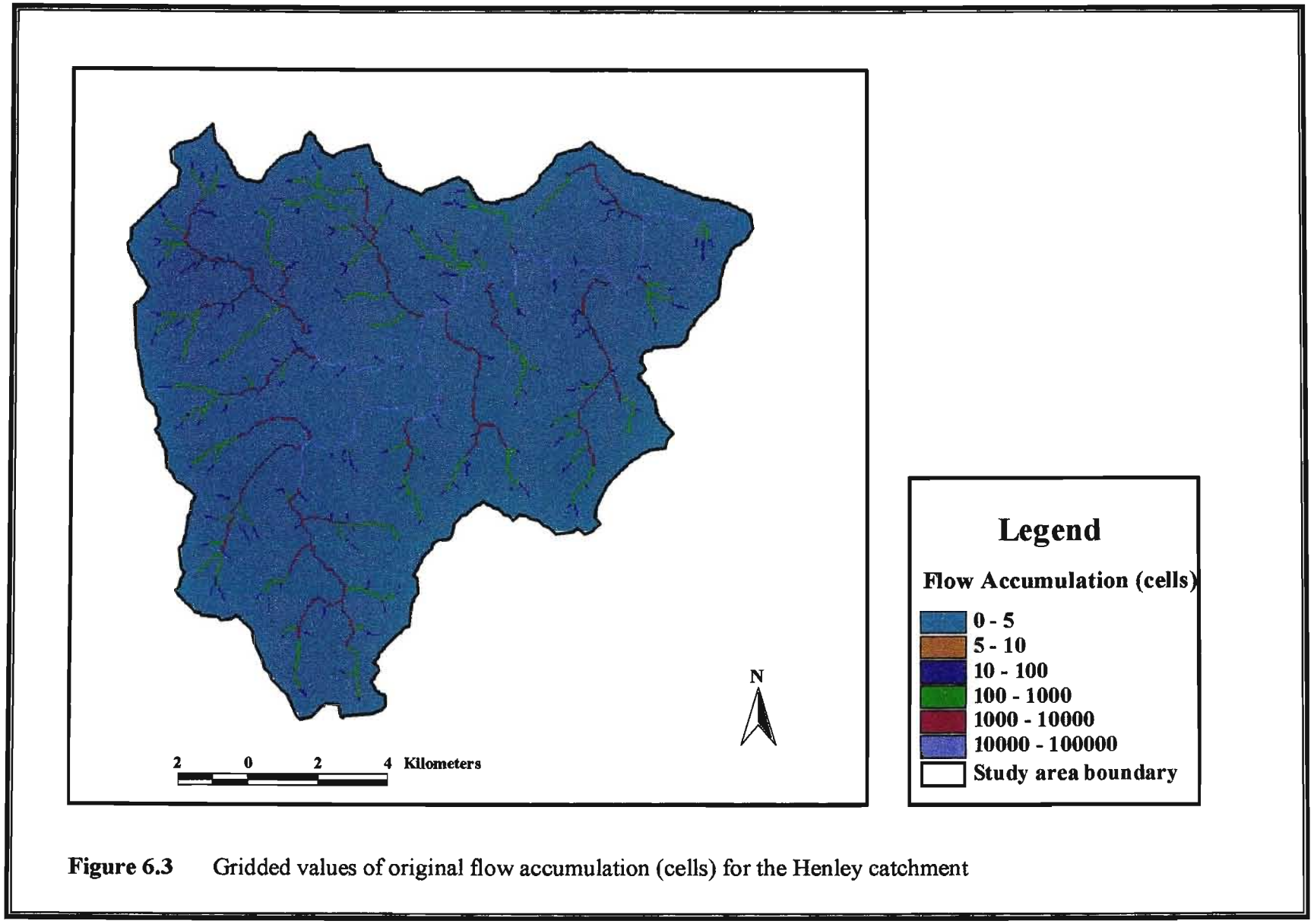


**Figure 6.3** Gridded values of original flow accumulation (cells) for the Henley catchment

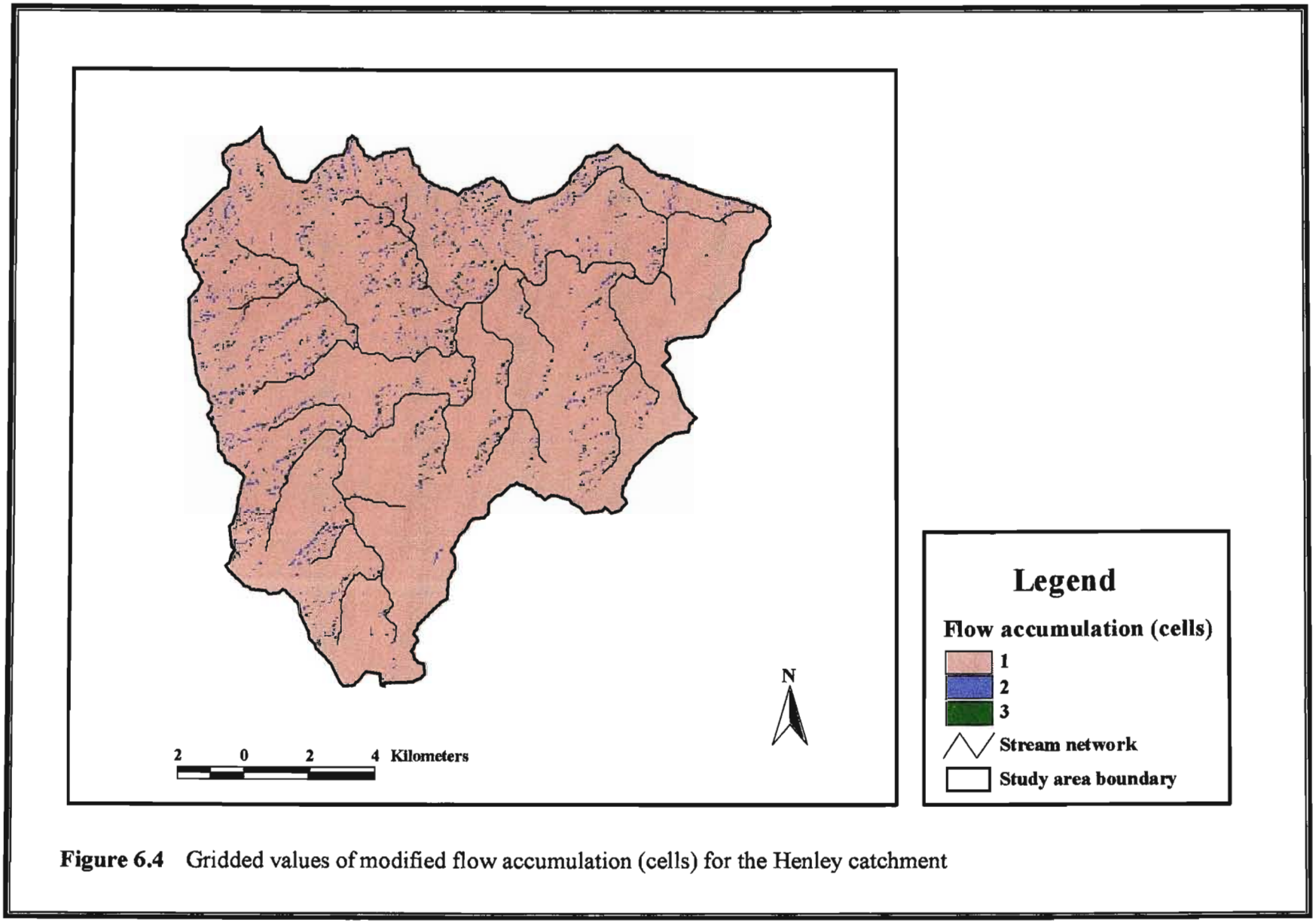


**Figure 6.4** Gridded values of modified flow accumulation (cells) for the Henley catchment

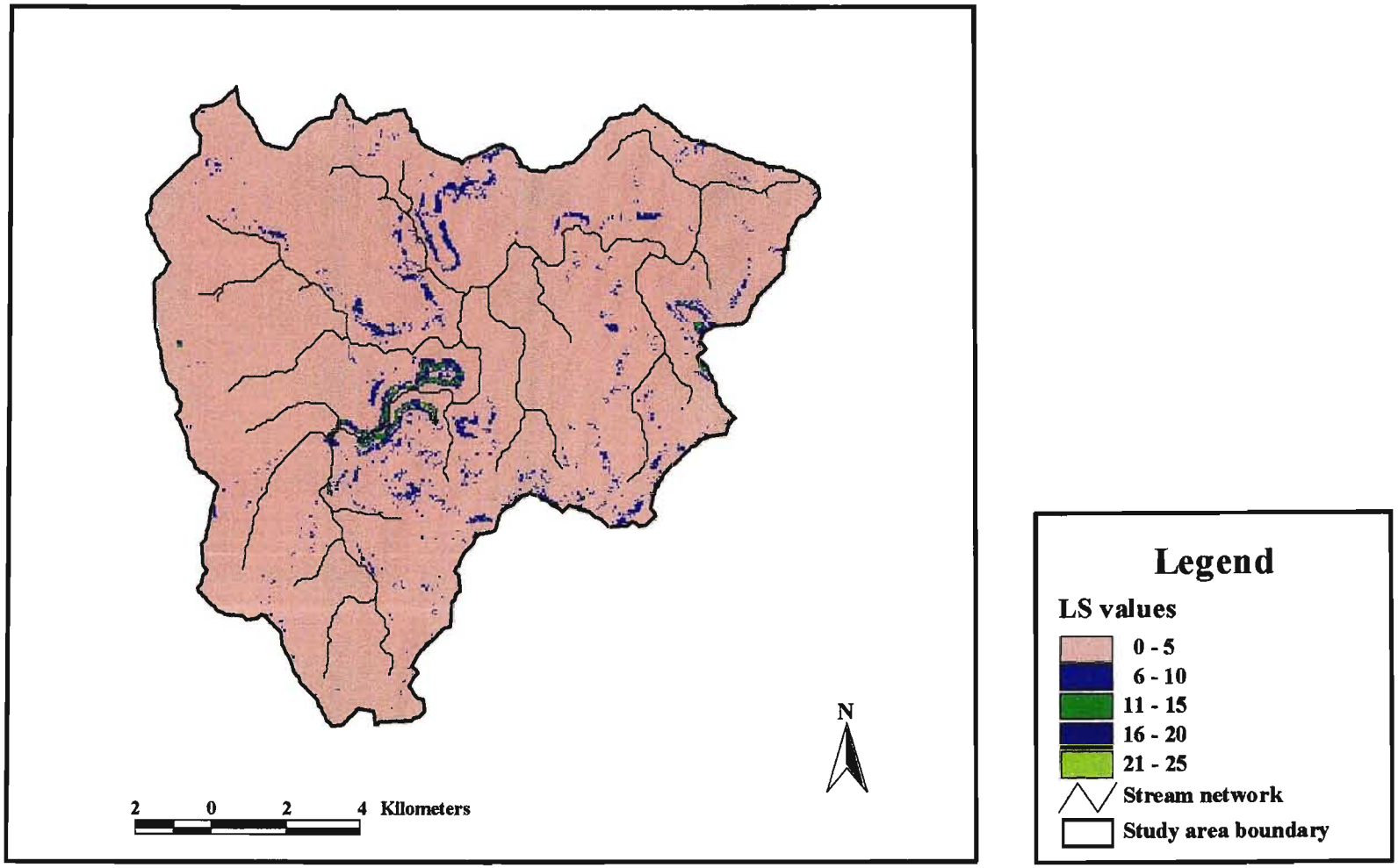


**Figure 6.5** Gridded values of slope length (*LS*) for the Henley catchment

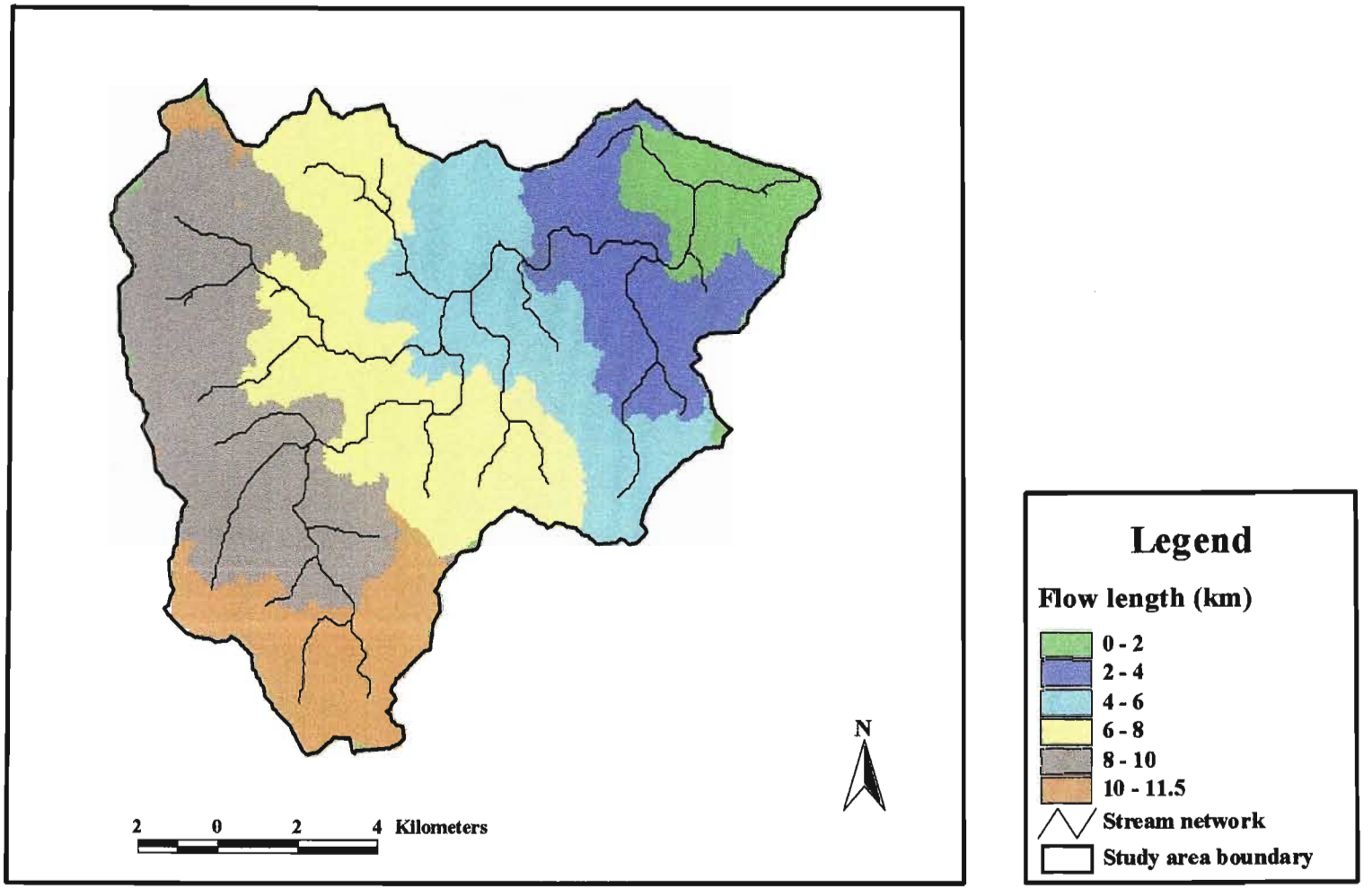


**Figure 6.6** Gridded values of flow length (km) for the Henley catchment

## 6.3 Calculation of Flow Velocity

In this research, the average flow velocity of overland flow is estimated from the relationship developed by Haan *et al.* (1994) which is based on the information in USDA-SCS-TR-55 (1975) Table 4.1. Based on this information an average flow velocity is assigned to each land use in the catchment. This is shown in Table 6.5 for each of the twelve land uses in the Henley catchment.

**Table 6.5** Values of surface roughness characteristics $a_i$ (m.s$^{-1}$) for the Henley catchment, adopted from Table 3.20 of Haan *et al.* (1994)

| Surface | *ai* (m.s $^{-1}$) | % areal coverage |
|---|---|---|
| CBD and industrial | 6.19 | 0.19 |
| High density residential | 6.19 | 0.15 |
| Medium density residential | 3.08 | 0.51 |
| Transitional housing | 1.56 | 0.61 |
| Low density residential, schools, parks | 1.56 | 21.29 |
| Woodland | 1.56 | 0.27 |
| Veld in fair condition and open spaces | 1.56 | 55.40 |
| Indigenous forest | 0.76 | 2.50 |
| Mixed crops | 2.62 | 12.58 |
| Wetland grasses | 2.13 | 2.11 |
| Eucalypt plantation | 0.76 | 2.36 |
| Pine plantation | 0.76 | 2.03 |

After assigning the average surface roughness characteristics to each grid cell in the land cover image (Figure 5.9), the final flow velocity for the overland flow is calculated from Equation 4.11 i.e. by multiplying the assigned land cover (Figure 5.9) and the square root of slope (m. m$^{-1}$) (Figure 6.1) for each grid cell. The flow velocity (Figure 6.7) has a mean value and standard deviation of 0.6 m. s$^{-1}$ and 0.25 m. s$^{-1}$ respectively.

**Table 6.6** Flow velocity classes with their areal coverage for the Henley catchment

| Flow velocity classes ($m.s^{-1}$) | Area ($km^2$) | % of areal coverage |
|---|---|---|
| 0-0.5 | 26.6 | 14.9 |
| 0.6-1.0 | 80.3 | 45.1 |
| 1.1-1.5 | 54.5 | 30.6 |
| 1.6-2.0 | 14.9 | 8.4 |
| 2.1-2.5 | 1.6 | 0.9 |
| 2.6-2.9 | 0.1 | 0.1 |

## 6.4 Calculation of Travel Time

Once the stream network (Figure 5.5) from the interpretation of GIS of 1:50 000 scale map had been defined and the flow lengths (Figure 6.6) from each cell to the outlet calculated, an average flow velocity is calculated to each cell (Figure 6.7). If both flow direction and velocity are known and the pathway from each cell to the nearest stream has been specified, then a grid can be created of the flow travel times (Figure 6.8). This uses Equation 4.10, where the value in each cell is the time taken for the water from that cell to reach the nearest stream (Maidment, 1993). The travel time (Figure 6.8) has a mean value and standard deviation of 2.5 h and 2.9 h respectively. About 67.3 % of the cells have a travel time less than the mean value.

**Table 6.7** Travel time classes with their areal coverage for the Henley catchment

| Travel time classes (h) | Area ($km^2$) | % of areal coverage |
|---|---|---|
| 0-2.5 | 81.5 | 45.8 |
| 2.6-5 | 62.5 | 35.3 |
| 5.1-7.5 | 23.5 | 13 |
| 7.6-10 | 7 | 3.9 |
| 10.1-12.5 | 3.5 | 2 |

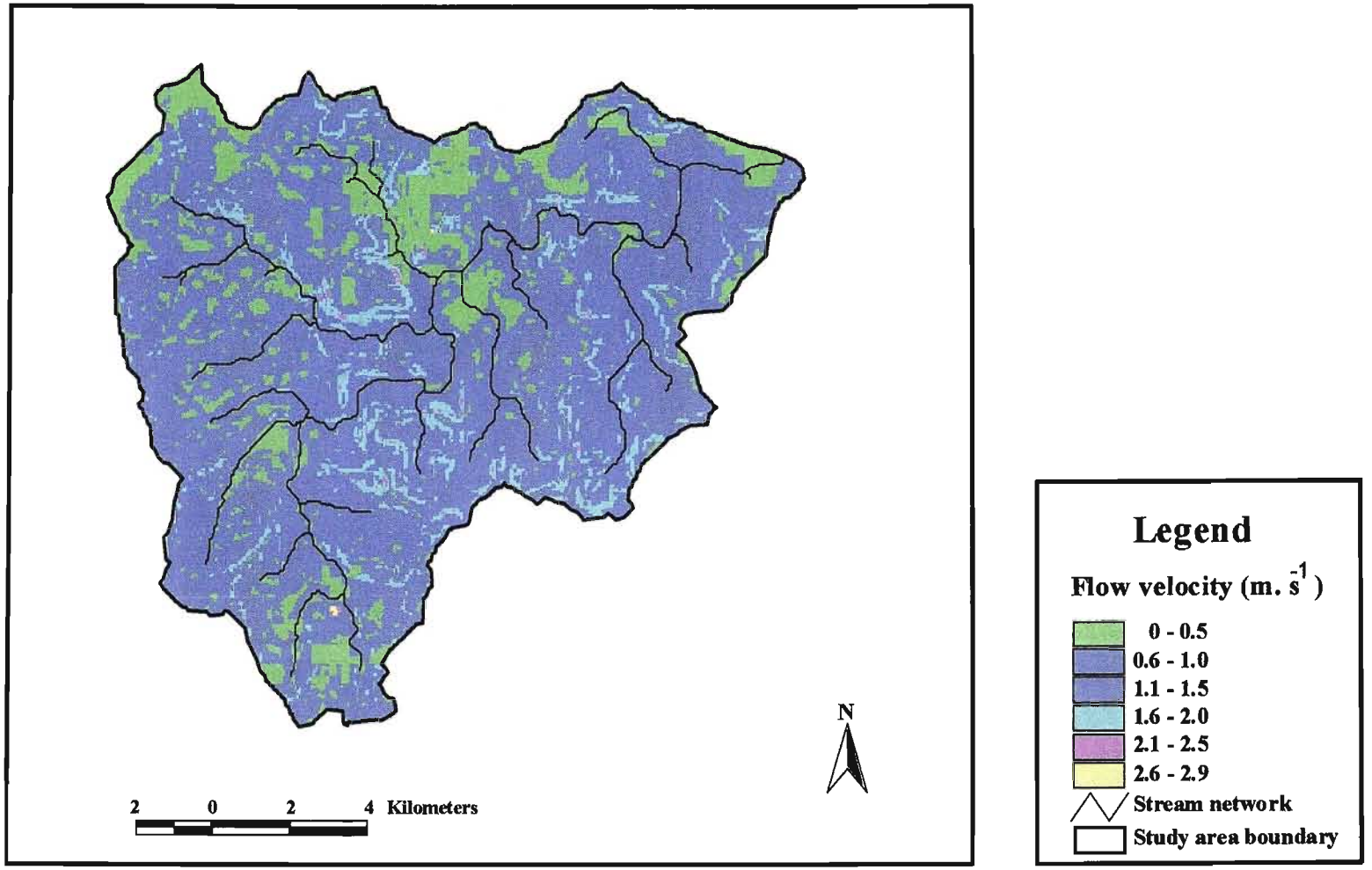


**Figure 6.7** Gridded values of flow velocity ($m.s^{-1}$) for the Henley catchment

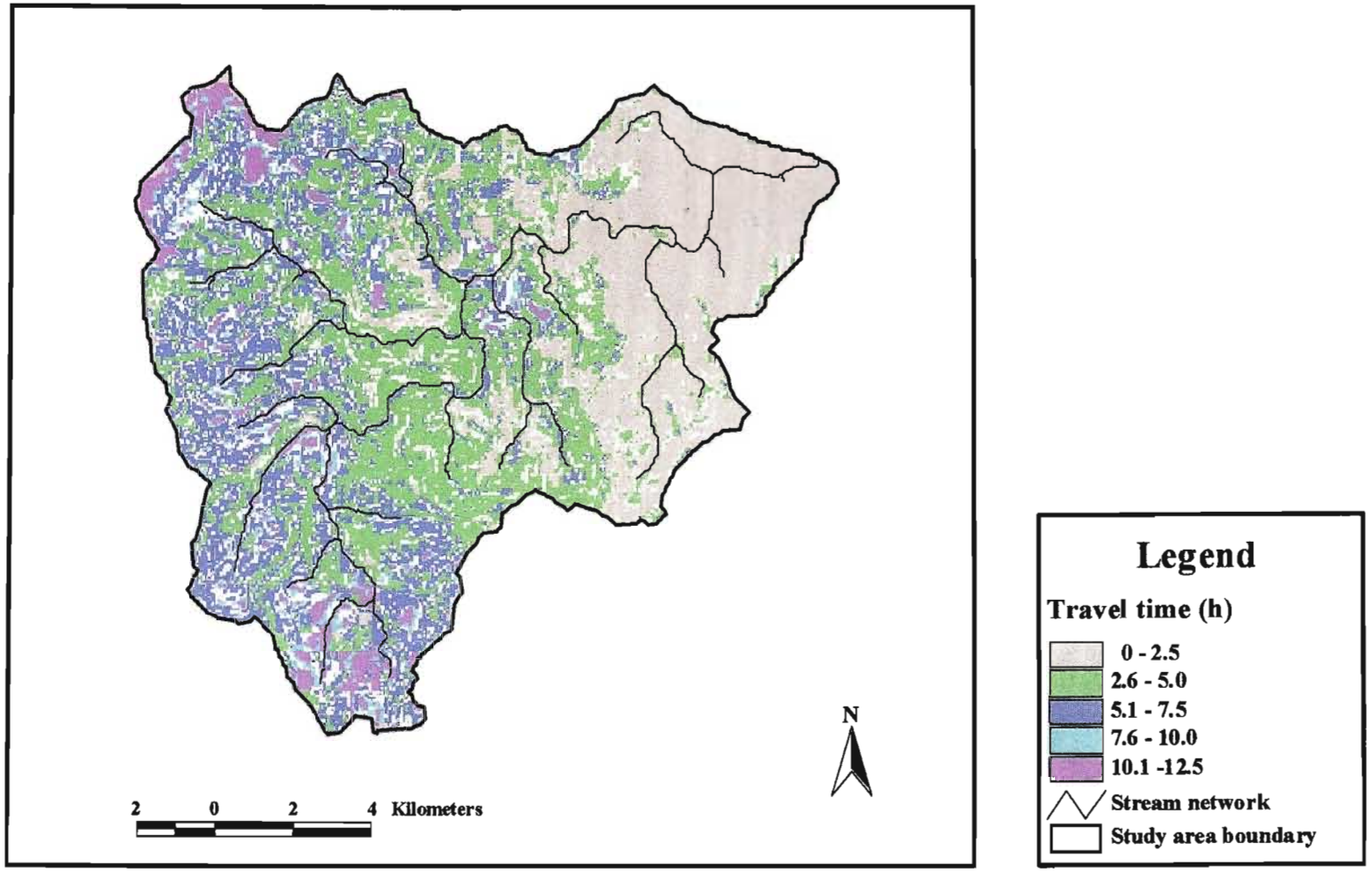


**Figure 6.8** Gridded values of travel time (h) for the Henley catchment

## 6.5 Calculation of Subcatchment Specific Parameter ($\beta$)

It should be recalled from Chapter 4 that the subcatchment specific parameter $\beta$, is a coefficient which is assumed to be constant for a given subcatchment because the relationship between, $lnF_i$, and travel time ($t_i$) is linear in a given subcatchment. Thus the subcatchment specific parameter ($\beta$) for each subcatchment can be determined by a regression that fits the relationship between $lnF_i$ and travel time ($t_i$) of all grid cells in a given subcatchment. An example is shown for subcatchment 1 in Figure 6.9.

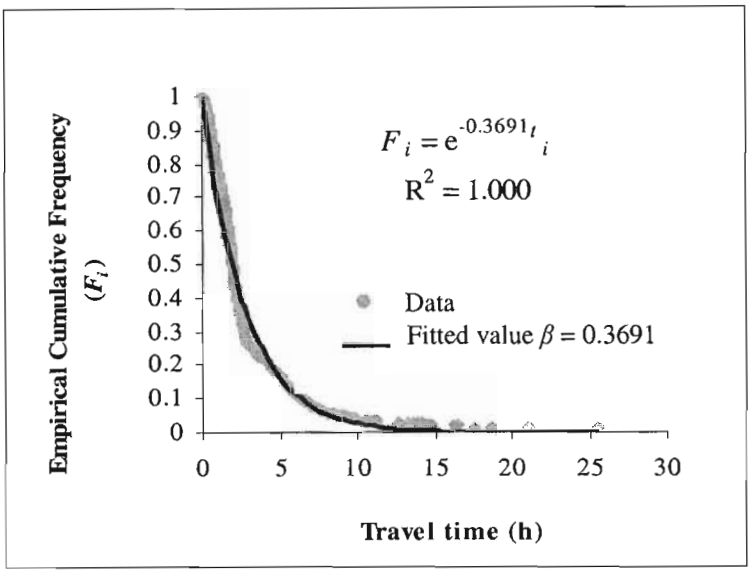


**Figure 6.9** Graph showing the Cumulative Frequency Distribution of travel times, ($F_i$) and the fitted curve (Equation 4.9) yielding the parameter, $\beta$ for subcatchment 1

From Figure 6.9 above, the fitted value for the constant defining the relationship between $lnF_i$ and travel time ($t_i$) in the form of Equation 4.9 of all the grid cells in subcatchment 1 is $\beta$ equal to 0.3691. Therefore, this value represents the subcatchment specific parameter $\beta$ for subcatchment 1. The same procedure was followed for the rest of the subcatchments (cf. Appendix D). Table 6.8 shows the fitted values of $\beta$ coefficients for each subcatchment in the Henley catchment.

**Table 6.8** The subcatchment specific parameter $\beta$ values for each subcatchment in the Henley catchment

| Subcatchment | Area ($km^2$) | $\beta$ |
|---|---|---|
| 1 | 10.01 | 0.3691 |
| 2 | 26.55 | 0.3821 |
| 3 | 27.59 | 0.6857 |
| 4 | 29.36 | 0.2898 |
| 5 | 11.69 | 0.6789 |
| 6 | 16.49 | 0.3756 |
| 7 | 19.88 | 0.3412 |
| 8 | 16.36 | 0.6901 |
| 9 | 19.14 | 0.4101 |

## 6.6 Calculation of the Sediment Delivery Ratio (*SDR*)

Table 6.9 shows the sediment delivery ratios ($SDR_i$) with their respective areal coverage in the Henley catchment. The average $SDR_i$ for all grid cells in the catchment was 0.19. About 69 % of the catchment has an $SDR_i$ value less than the average. This value is in a close agreement with the work of Kienzle *et al.* (1997) which yielded *SDR* ranging between 0.1 and 0.2, determined by comparing erosion and sediment yield data in their Mgeni study. Average sediment delivery ratio values were also calculated at the outlets for each subcatchment (cf. Table 6.13). The estimation of sediment delivery ratio in a spatially distributed (cell based) form allows the identification of critical sediment source and delivery areas as well as site specific implementation of proper management practices within a catchment. Dai and Tan (1996) note that the sediment delivery ratio values imply the integrated capability of a catchment for storing and transporting the eroded soil. An increase in sediment supply at one location in a certain period may be compensated by a decline in other places and times and *vice versa*.

**Table 6.9** Sediment Delivery Ratio (*SDR*) values for the Henley catchment

| *SDR* Classes | Area ($km^2$) | % of areal coverage |
|---|---|---|
| 0-0.10 | 29.0 | 16.3 |
| 0.11-0.20 | 94.8 | 53.3 |
| 0.21-0.30 | 18.0 | 10.0 |
| 0.31-0.40 | 11.8 | 6.6 |
| 0.41-0.50 | 8.0 | 4.5 |
| 0.51-0.60 | 6.5 | 3.7 |
| 0.61-0.70 | 4.4 | 2.5 |
| 0.71-0.80 | 3.0 | 1.7 |
| 0.81-0.90 | 1.5 | 0.8 |
| 0.91-1.00 | 1.0 | 0.6 |

Equation 4.8 states that the logarithm of $SDR_i$ is inversely proportional to travel time, which is a function of both flow length and velocity. Hence, the further away an area is from the stream the longer the travel time and the lower the $SDR_i$; the greater the flow velocity along the flow path the shorter the travel time and the higher the $SDR_i$ as reflected in the results (Figure 6.10). It should also be emphasised that any two locations that are equidistant from the nearest stream may not have the same travel time, i.e. travel time distribution does not follow concentric zones. Flow velocity in nature is controlled as in the case of this research by conditions such as surface vegetation type and roughness, slope and elevation changes over the drainage area. Randhir *et al.* (2001) found from their studies that longer travel times tends to occur in areas with rougher surfaces (vegetated areas) compared to areas with impervious and open land surfaces.

The sediment delivery ratio (*SDR*) values obtained for the Henley catchment did not exhibit a clear relation with land uses. It can be seen from Figure 6.10 that large $SDR_i$ values occur adjacent to channel areas in the catchment and smaller $SDR_i$ values are mainly found adjacent to overland regions surrounding the higher order streams. As expected this may result from the sediment delivery ratio (*SDR*) being affected more by the characteristics of the drainage system than by land use (Novotny and Chesters, 1989).

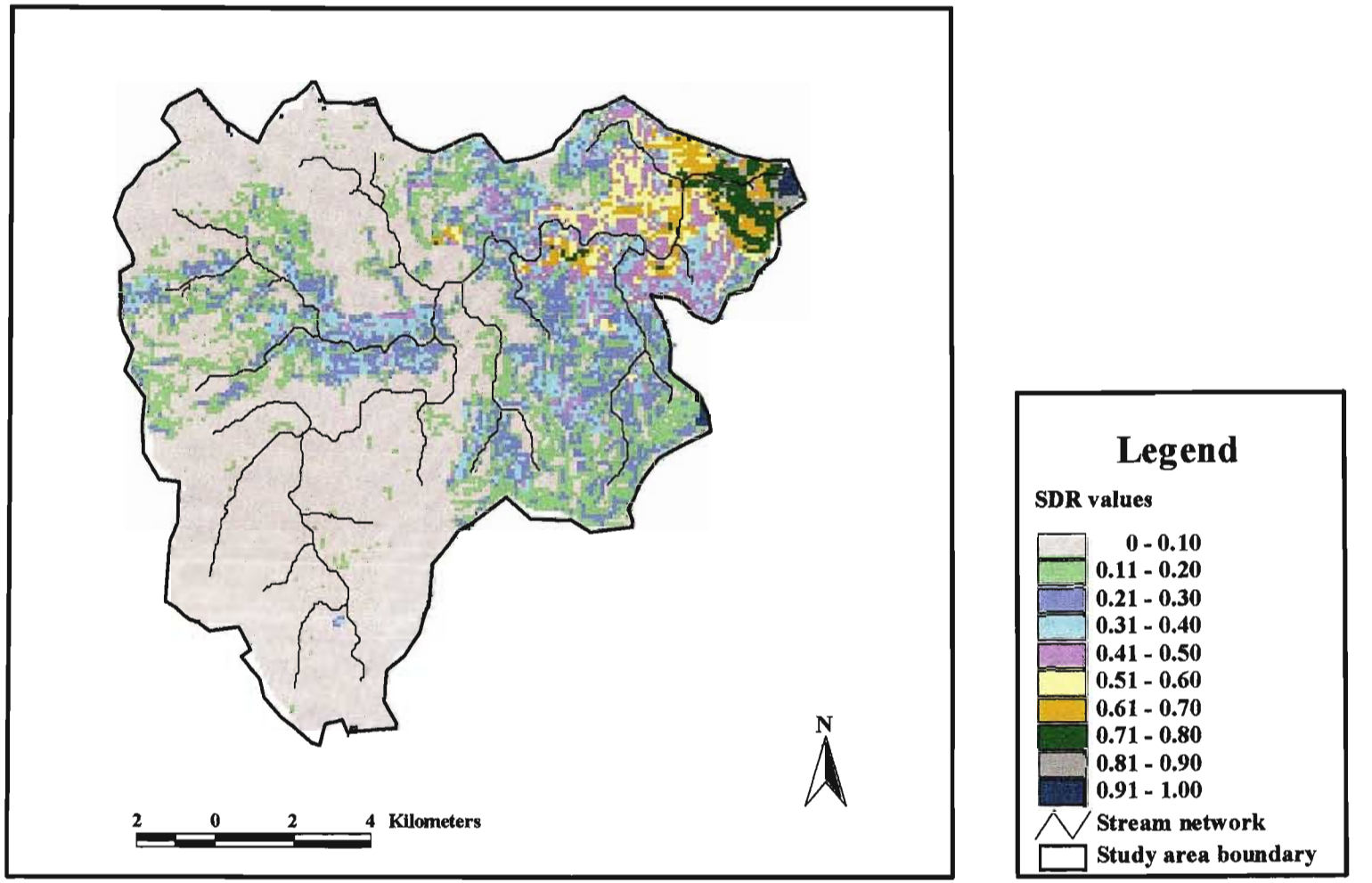


**Figure 6.10** Gridded values of Sediment Delivery Ratio (*SDR*) for the Henley catchment

## 6.7 Calculation of Potential Source Erosion

Source erosion is described as the soil eroded at a particular pixel or grid cell under study. This is opposed to transport erosion which is a term used to describe the eroded material (soil) which reaches the catchment outlet (Bradbury, 1994). In this research the source erosion estimation for each grid cell is based on the RUSLE. Multiplying the raster images of the five parameters of RUSLE Equation 4.1 results in the spatial distribution of the source erosion image (Figure 6.11) with which the amount of eroded soil within each cell can be estimated. A high value of this term indicates a high potential of soil erosion in the cell and *vice versa*. The average soil erosion in the catchment predicted by RUSLE is 26 t. $ha^{-1}.yr^{-1}$. About 64 % of the catchment has a value less than the average soil loss, (Table 6.10). The information shown in Figure 6.11 may also be used for the identification of the sediment source areas of the catchment.

In typical RUSLE applications, gullies and net depositional zones, and areas of vertical walls are eliminated from the study area because RUSLE was not developed for such conditions (Renard *et al.*, 1997). However, areas of deposition or concentrated flow often generate much higher soil loss than estimated for regular slopes by RUSLE, and therefore it may be necessary to include these areas since they reflect considerable increase in erosion (Mitasova *et al.*, 1996). In fact, these areas were included in this research because in reality a zone of deposition or concentrated flow would generally occur when slope length becomes 120 m to 150 m (McCool *et al.*, 1993). It should be recalled that, in Chapter 4 the maximum slope length that flow can be concentrated was taken as 150 m.

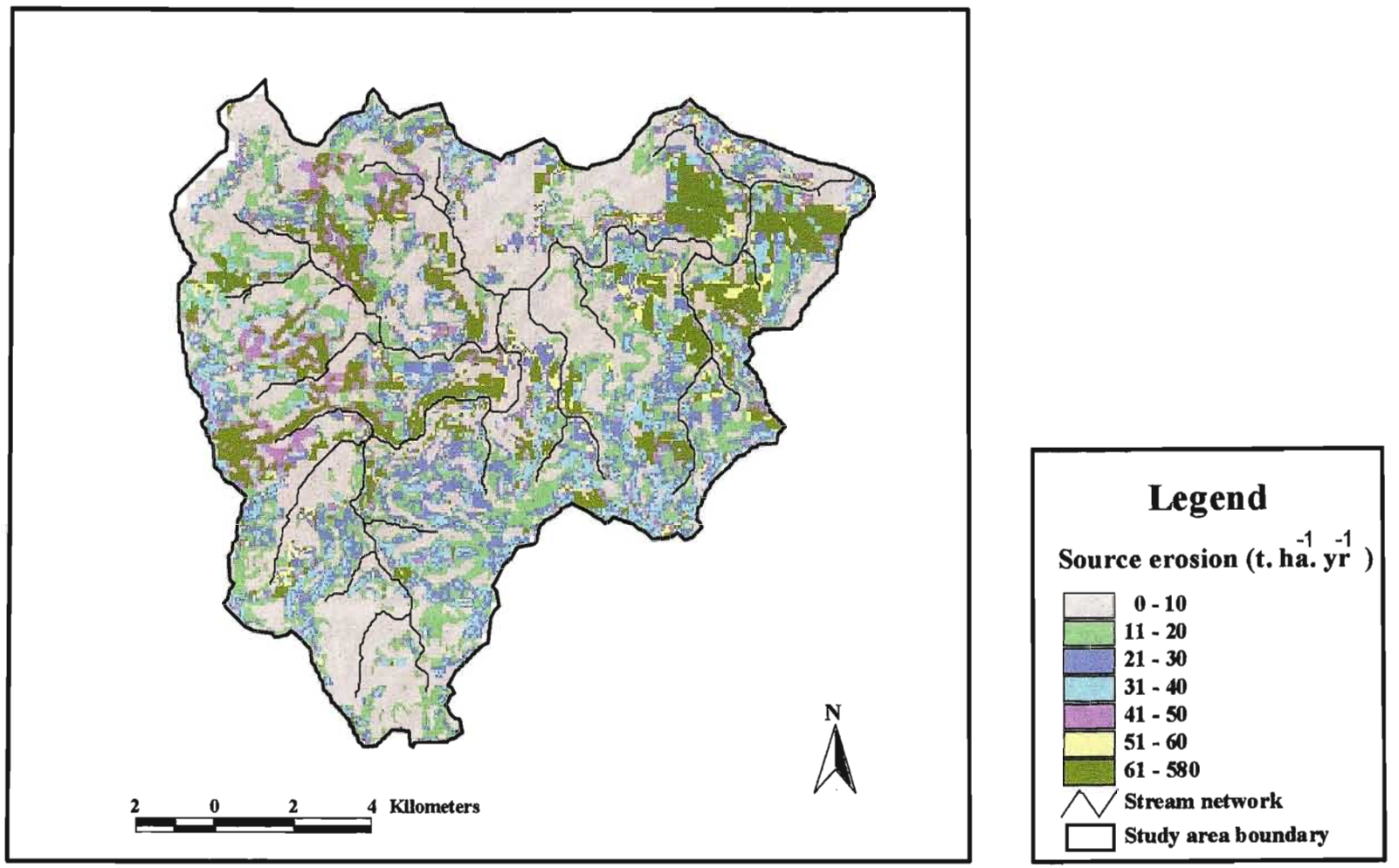


**Figure 6.11** Gridded values of potential source erosion ($t.ha^{-1}.yr^{-1}$) for the Henley catchment

**Table 6.10** The potential source erosion classes and their areal coverage for the Henley catchment

| Source erosion classes (t. $ha^{-1}$. $yr^{-1}$) | Area ($km^2$) | % of area coverage |
|---|---|---|
| 0-25 | 112.54 | 64.10 |
| 26-120 | 59.02 | 33.60 |
| 120-300 | 3.90 | 2.22 |
| 300-580 | 0.19 | 0.11 |

In determining the effect of the erosion control practice, or the *P*-factor, four hypothetical scenarios (Table 6.11) were compared to the current land use in the Henley catchment. More attention was given to residential and agricultural areas of the catchment which exhibit much higher source erosion rates (Figure 6.11) and sediment yield (Figure 6.12) than the non cultivated lands.

**Table 6.11** Results from four different hypothetical land use scenarios for erosion control practices *P* for the Henley catchment

| Type of scenario | Average sediment delivery ratio (*SDR*) | Average annual sediment yield (t. $ha.^{-1}$ $yr^{-1}$) | Change in sediment yield from the current land use (%) |
|---|---|---|---|
| Land use during the study | 0.19 | 1.60 | - |
| Cross-slope farming in agricultural areas only | 0.16 | 1.12 | 15.5 |
| Contour farming in agricultural areas only | 0.13 | 0.98 | 26.6 |
| Contour banks with grassed waterways in residential areas and contour and strip cropping in agricultural areas | 0.10 | 0.76 | 35.5 |
| Contour and strip cropping in agricultural areas only | 0.12 | 0.84 | 31.1 |

Considering the different scenarios (Table 6.11), substantial reduction in soil loss can be achieved when contour banks with grassed waterways in residential areas and contour and strip cropping in veld and mixed crops were applied. This scenario leads to an average sediment yield reduction in the catchment of 35.5 %, resulting in an average sediment yield loss of 0.84 t. $ha^{-1}.yr^{-1}$. This reveals the effectiveness and importance of conservation practices, and also suggests that practices other than the ones evaluated in this research may be incorporated by catchment managers depending on the economic feasibility in the catchment in order to further reduce erosion and sediment delivery. Conservation support practices typically affect erosion by redirecting runoff around the slope (Lorentz and Schulze, 1995; Endale *et al.*, 2000).

GIS techniques which need further investigation are the influence of grid size on slope and *LS* calculations. Comparing results from the 250 m, 100 m and the 50 m grids (Table 6.12) reveals the large influence of the grid size on slope and *LS* distribution. One of the most evident facts is that slope (steepness) calculations based on the 250 m grid are not higher than 33 %, whereas the 100 m and 50 m grid based calculations result in slopes exceeding 400 % and 134 % respectively. The evident smoothing of slopes with coarser grids has a dramatic effect on slope, slope length factor and resulting soil erosion calculations (Table 6.12). Compared to the 250 m elevation grid and keeping all other factors the same, soil erosion estimation are more than 50 % higher when using the 100 m elevation grid and about 70 % higher when using 50 m elevation grid.

**Table 6.12** Cell of slope and slope length values and simulated soil erosion for three different grid sizes for the Henley catchment

| Grid size | mean slope (%) | min slope (%) | max slope (%) | mean slope length factor | min slope length factor | max slope length factor | mean soil erosion (t. $ha^{-1}$. $yr^{-1}$) | min soil erosion (t. $ha^{-1}$. $yr^{-1}$) | max soil erosion (t. $ha^{-1}$. $yr^{-1}$) |
|---|---|---|---|---|---|---|---|---|---|
| 250 m | 8.8 | 0.2 | 33.0 | 1.77 | 0.05 | 5.06 | 33.4 | 0.0 | 174.0 |
| 100 m | 13.4 | 0.0 | 485.9 | 2.53 | 0.03 | 17.52 | 47.5 | 0.0 | 359.0 |
| 50 m | 14.8 | 0.0 | 77.3 | 2.24 | 0.0 | 23.0 | 26.0 | 0.0 | 579.0 |

Therefore soil erosion is very sensitive to slope and slope length values which are a function of grid size resolution. Hence further research is required to provide information on the optimal grid size information and the sensitivity of grid size on soil loss in different terrains.

## 6.8 Computation of Sediment Yield

The RUSLE equation was used for determining the source erosion component of the model in the Henley catchment. In most developing countries, suitable calibration data are not available for sediment yield models. A methodology has been described in Chapter 4 in which a suitable sediment delivery ratio concept could be used for modelling sediment yield in ungauged catchments without any calibration. The Henley catchment was selected to verify the model as the catchment has good data and has been modelled by different techniques for relatively long period of time. The final sediment yield within each grid cell was calculated using Equation 4.12.

The average annual sediment yield for the Henley catchment, calculated as an average of sediment yields from all the cells, was 1.6 t. $ha^{-1}.yr^{-1}$ (Table 6.13). Channel erosion was not included in this research. The spatial variation of the sediment yield across the entire catchment is shown in Figure 6.12. The higher sediment yield values evident in the residential and agricultural areas of the catchment are all representative of the higher source erosion depicted by source area coverage (Figure 6.11), which are characterised by degradation. The degradation is due to overgrazing and traditional and peri-urban settlements with mixed crops, which tends to produce higher source erosion and sediment yield.

Similar patterns of soil loss and sediment delivery could be observed from the analysis made on individual subcatchments (Table 6.13). Note that there exist high variations in the predicted sediment yield within each subcatchment. Such high variations are a result of the diverse land uses and the wide range of land slopes and distances to channels within the individual subcatchment. Those subcatchments in which forest and grass are the principal land uses tend to produce both low soil erosion and sediment yield, although some of these subcatchments have relatively high sediment delivery ratio values. For example, in subcatchment 1, a very small non

**Table 6.13** Values of RUSLE parameters, *SDR*, and predicted soil loss and sediment yield by subcatchment for the Henley catchment

| Subcatchment | Area ($km^2$) | RUSLE Parameters | | | | | Soil loss ($t.ha^{-1}.yr^{-1}$) | *SDR* | Sediment yield ($t.ha^{-1}.yr^{-1}$) |
|---|---|---|---|---|---|---|---|---|---|
| | | R | K | LS | C | P | | | |
| 1 | 10.01 | 318 | 0.41 | 1.6 | 0.10 | 0.68 | 13.3 | 0.20 | 2.4 |
| 2 | 26.55 | 329 | 0.29 | 2.0 | 0.11 | 0.68 | 15.2 | 0.17 | 2.3 |
| 3 | 27.59 | 325 | 0.29 | 2.9 | 0.16 | 0.82 | 30.8 | 0.28 | 7.9 |
| 4 | 29.36 | 321 | 0.41 | 1.9 | 0.17 | 0.78 | 30.0 | 0.11 | 3.1 |
| 5 | 11.69 | 325 | 0.29 | 2.4 | 0.16 | 0.75 | 26.0 | 0.25 | 6.2 |
| 6 | 16.49 | 318 | 0.39 | 2.0 | 0.12 | 0.75 | 20.8 | 0.18 | 3.3 |
| 7 | 19.88 | 316 | 0.32 | 2.0 | 0.13 | 0.71 | 19.5 | 0.14 | 2.5 |
| 8 | 16.36 | 325 | 0.29 | 2.8 | 0.15 | 0.81 | 33.8 | 0.30 | 9.2 |
| 9 | 19.14 | 314 | 0.40 | 2.2 | 0.15 | 0.81 | 39.7 | 0.23 | 8.2 |
| overall | 177.07 | 322 | 0.35 | 2.24 | 0.14 | 0.77 | 26.1 | 0.19 | 1.6 |

**Note:**

***SDR*** = sediment delivery ratio

cultivated subcatchment has a sediment delivery ratio as high as 0.2, and consequently 20 % of the detached material is expected to reach the stream. However, because of its low soil loss rate, this subcatchment has a sediment yield lower than that of any of the other subcatchments. Small catchments generally have less area to accommodate sediment deposition compared to large catchments. FitzHugh and Mackay (2001) distinguish between transport-limited and source-limited catchments. In the former more material can be detached than can be carried away by transport processes, while in the latter the opposite is observed. Subcatchment 1, for example, may be classified as source-limited.

There is also a great difference in sediment yield when comparing sediment yield at the outlet of each subcatchment and at the outlet of the Henley catchment (Table 6.13). This shows that there is a probability that the eroded particles will deposit somewhere along the flood plans of channel system and sediment storage sites en route to the outlet of the Henley catchment. This channel system itself is a function of branching and configuration of the stream network and total stream length. Therefore the incorporation of these properties of the river network in the calculation of the sediment delivery ratio can improve the result of sediment routing to the catchment outlet (Ferro, 1997).

Among all the factors affecting soil loss, the *R*, *K* and *P* factors have relatively uniform values across the whole catchment and their impacts are similar between the subcatchments. However, the *LS* and *C* factors vary considerably between the subcatchments and display a positive relation with soil erosion and sediment yield. The major source areas generating high erosion are subcatchments 3, 4, 8, and 9 (average 34 t. $ha^{-1}.yr^{-1}$) for which either the *LS* or *C* or both factors have high values. On the other hand, in contrast to subcatchment 1, subcatchment 4 has a high soil loss rate and a low sediment delivery ratio (0.20 vs. 0.11). Offsetting of high sediment delivery ratio with low erosion (or low sediment delivery ratio with high erosion) means that certain subcatchments produce similar amounts of sediment yield, but have markedly different erosion rates.

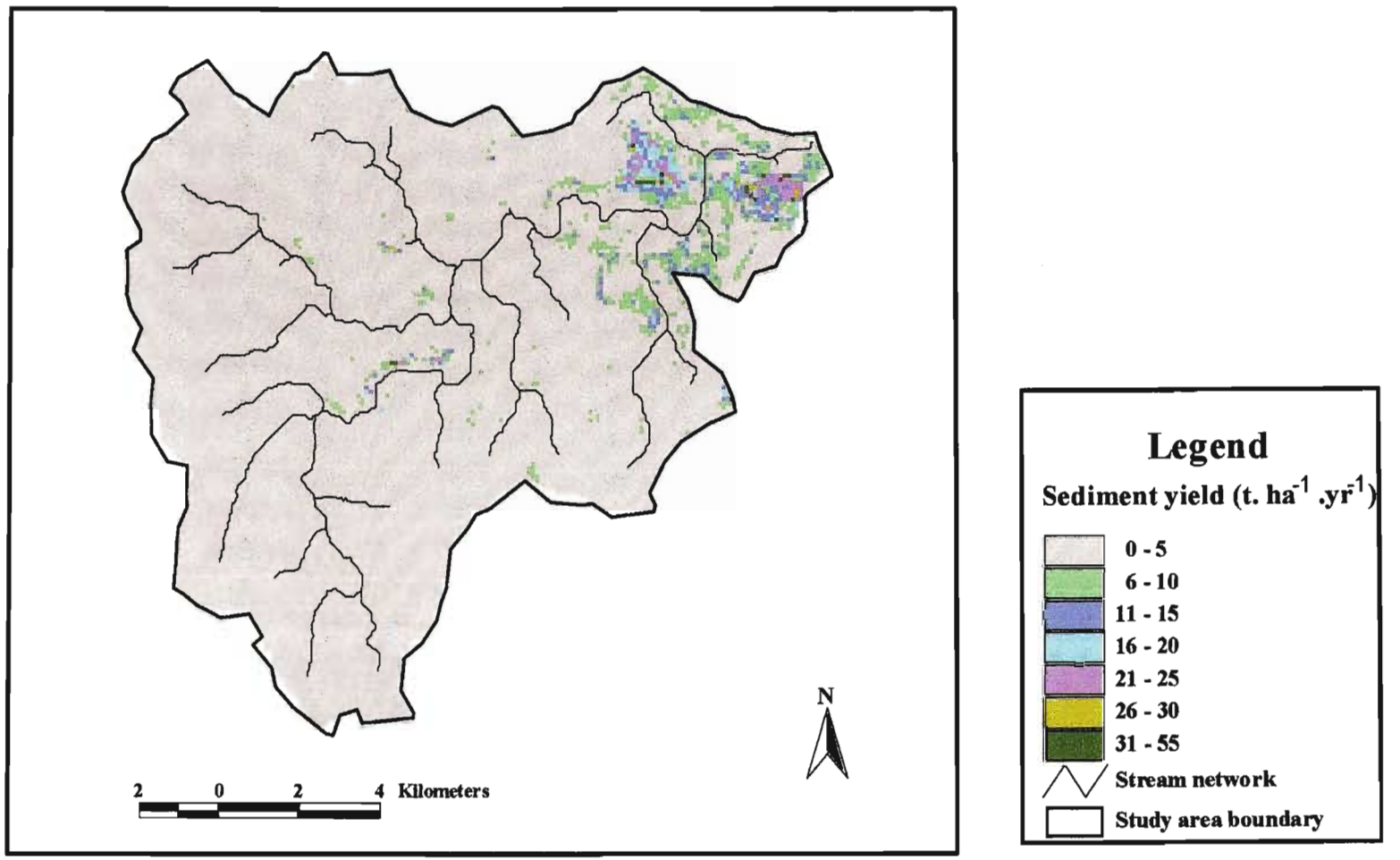


**Figure 6.12** Gridded values of sediment yield (t. ha $^{-1}$.yr$^{-1}$) for the Henley catchment

## 6.9 Identification of Sediment Source Areas

The gross soil erosion map (Figure 6.11) and sediment delivery ratio map (Figure 6.10) were overlaid in raster Arcview GIS to identify source areas for sediments reaching the outlet from within the catchment. Through such overlaying, the areas producing large sediment amounts in the catchment have been identified and are shown in Figure 6.12 for the Henley catchment. It is to be emphasised that the areas producing more sediment would need special priority for implementation of soil erosion control measures.

## 6.10 Event Basis Sediment Yield Simulation

Event based sediment yield simulation models can be used to estimate sediment yield from individual stormflow producing rainfall events at the catchment scale. In this research the gross amount of soil erosion for each grid cell during a stormflow event was generated by multiplying the terms *K*, *LS* and *P* and the *R*-factor for the respective stormflow event, given in Table 6.14 with the *C*-factor for that month. The eroded sediment was routed from each grid cell in the hillslopes to the nearest stream reach using the sediment delivery ratios developed in the previous section 4.3.

The *R*-factor is commonly represented by the $EI_{30}$. In this research, the event based $EI_{30}$ is calculated by Equation 6.2 (Renard *et al.*, 1997) from the two automatic recording raingauge stations in the Henley catchment. Rainfall measurements are commonly observed at point locations and these values are required to be converted to a raster format. The same $EI_{30}$ value was used when there was only one rainfall record from either of the two raingauges while, when there is a rainfall record from the two raingauges, the inverse distance weighting interpolation technique was used to convert point data to continuous surface over the space to be used for overlaying in a GIS. The technique is relatively accurate for rainfall data interpolation at unmeasured locations (Lynch, 1998).

$$EI_{30} = 0.29\left[1 - 0.72\, e^{(-0.05 i_m)}\right] \qquad 6.2$$

where $EI_{30}$ = rainfall kinetic energy (MJ. $ha^{-1}.mm^{-1}$) and

$i_m$ = the maximum 30 minutes rainfall intensity during the day ($mm.h^{-1}$).

The monthly *C*-factor was taken from the original work of Kienzle *et al.* (1997) on the Mgeni catchment. The factors *K*, *LS* and *P* remain constant throughout the year. The results of event based sediment yields simulated from the model are given in Table 6.14.

## 6.11 Verification Studies of Sediment Yield

In recent years, increasing application of spatially distributed models of erosion and sediment delivery in modelling soil loss and sediment yield from a catchment have been carried out. Use of a distributed approach permits both the spatial heterogeneity of catchment land use, soil properties, topography, and the spatial interaction of erosion and sediment transport processes to be represented. The advantage of this is that spatially distributed prediction of erosion and sediment yield within a catchment can be carried out. However, verification and application of such spatially distributed models can be constrained by the lack of spatially distribution sediment mobilisation and deposition data or observations within a catchment. Therefore verification and application have commonly been restricted to comparison of the predicted and measured sediment outputs from a catchment in terms of sedigraphs and sediment yields (He and Walling, 2003). Although close agreement of modelled and measured sediment yields affords some degree of verification, it can not provide conclusive confirmation of the internal functioning of the model and thus of the predicted erosion and sediment yield rates. For example, it is possible to conceive of situations where there is a close agreement between observed and predicted sediment yields from a catchment, but where both the magnitude and spatial distribution of erosion and sediment yield rates within the catchment predicted by the models may differ substantially from the actual values ( Svorin, 2003).

In South Africa there are different approaches to verifying the prediction of sediment loads that are simulated using different modelling techniques. These includes verification using reservoir survey studies and estimates, weekly grab samples and integrated sediment sampling techniques.

In this research conducted between 1994 and 1999, data were measured by an integrated sediment sampling technique was employed because it uses the continuous automatic ISCO sampler to establish a frequent representation of suspended solids and discharge data (Howe, 1999).

### 6.11.1 Verification using flow integrated sediment sampling techniques

In this research, the suspended solids and discharge data collected by the School of Bioresources Engineering and Environmental Hydrology of the University of KwaZulu-Natal at the Henley Weir were used for verification studies. The data were collected at frequent, selected intervals during the course of a number of runoff events in 1994, using an automatic ISCO sediment sampler (Howe, 1999). An ISCO automatic sampler was programmed to pump a water sample from the river at an interval related directly to incremental volumes of river discharge. This resulted in samples being taken more frequently at high flow rates than during lower flows, allowing for adequate definition of the rapidly changing concentrations during the peak flows of the event. The sediment loads resulting from these events were estimated by integrating the incremental sediment fluxes derived from the concentration of suspended solids samples and the associated streamflow. The incremental sediment fluxes could then be summed for the duration of the event to yield the total sediment yield. Sediment yield simulations for seven events were taken during 1994 because successful monitoring of catchment rainfall and sediment yield occurred during these periods.

A comparison of the simulated sediment loads by the model and a daily time step *ACRU* simulation for the period of 1960-1994 and those estimated from concentration measurements during the automatic monitoring period using an ISCO sampler at weir U2H011 during 1994 are given in Table 6.14. The loads estimated from the seven monitored events vary between 13 and 1246 tonnes per event. The proposed model is therefore tested over a wide range of sediment loadings. As can be seen, the model described herein produced estimates of sediment yield adequately. Note that the coefficient values used in various equations of the model especially the sediment delivery ratio was determined using standard procedures and without any calibration. The reason for this is that the model was developed for purposes of applying it to ungauged

catchments where there is a lack of sediment yield data, either for calibration or for designing and planning of water resource projects.

**Table 6.14** Comparison of *SDR* model simulated sediment loads with sediment loads estimated from automatic ISCO and *ACRU* simulations at Henley Weir U2H011 for seven events during 1994 (Howe, 1999)

| Event No. | Date of event | estimated sediment load from observations (t) | *ACRU* simulated sediment load (t) | *SDR* model simulated sediment load (t) |
|---|---|---|---|---|
| 1 | 08/01/94 | 581 | 1278 | 491 |
| 2 | 01/02/94 | 1246 | 1586 | 1453 |
| 3 | 29/03/94 | 140 | 10 | 129 |
| 4 | 25/07/94 | 105 | 125 | 1685 |
| 5 | 15/11/94 | 13 | 0 | 21 |
| 6 | 24/12/94 | 428 | 177 | 472 |
| 7 | 27/12/94 | 697 | 369 | 788 |

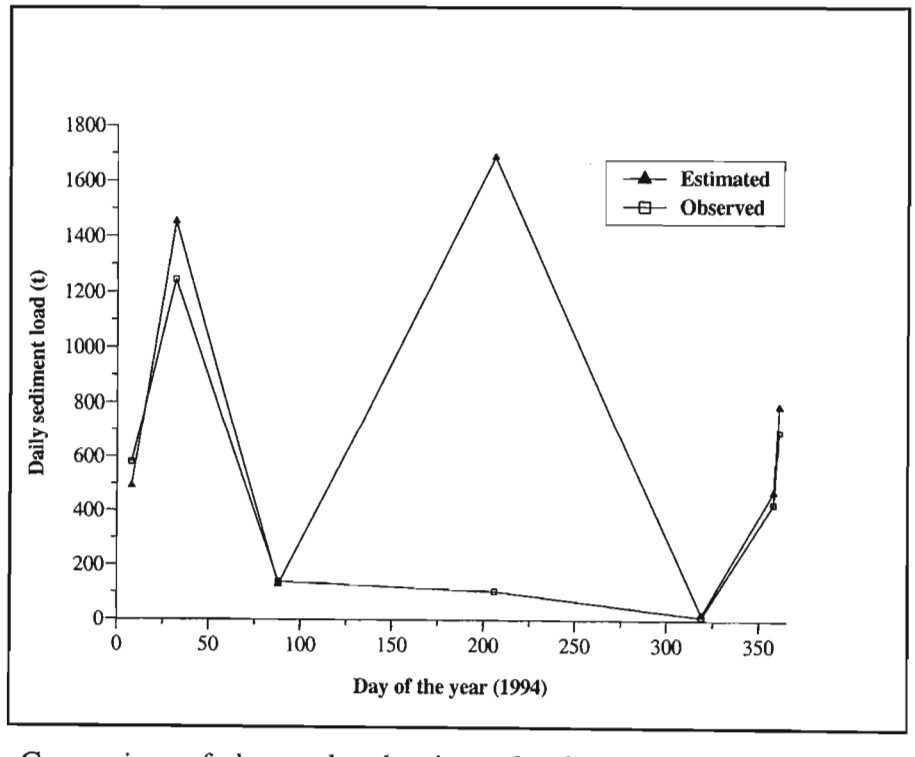


**Figure 6.13** Comparison of observed and estimated sediment loads at Henley Weir U2H011 for seven events during 1994 (Howe, 1999)

The prediction accuracy of the proposed model can be rated as satisfactory, particularly considering the fact that the prediction from some process based models show large differences between measured and computed sediment yields (Wu *et al.,* 1993). Nevertheless, poor agreement is found to exist between the observed and computed values of sediment yield for one storm event in the Henley catchment (Table, 6.14) and (Figure 6.13). An anomaly occurs in Event 4 on 25/07/94 where the simulated load is more than ten times that estimated from measurements. This could be related to the poor representation of $EI_{30}$, which in turn, is dependent on the rainfall input. The rainfall which was recorded and used in this simulation was found only from one raingauge in the catchment. Therefore this value exaggerates the calculation of source erosion and ultimately the sediment yield.

It is evident that a notable difficulty with sediment yield modelling is that adequate sediment yield simulations are dependent on representative rainfall measurements. It is hypothesised that the slightly higher values in the estimation of sediment yield in the above events are ascribed to the likely uncertainties due to the poor representativeness of the two automatic recording raingauges in the 178 $km^2$ catchment to monitor rainfall events. The application of RUSLE, a soil erosion model designed to predict the long term water erosion for event based simulations, may be considered to be another source of uncertainty. In addition, the simulated sediment loads were simply the sum of the sediment yields from all grids in the catchment i.e. no, channel sediment routing was undertaken. This is so because the hypothesised sediment delivery ratio model is applicable at the mean annual basis and therefore assumes that over a long period, a stream must essentially transport all the sediments delivered to it. Hence, the channel network sediment delivery processes have to be considered at short temporal scales (e.g. event, month).

In conclusion, results of the verification study are encouraging since the simulated sediment yields compared well with those estimated from the integrated sediment sampling technique. The ability of the model to predict the magnitude of the estimated sediment loads appears to be good for loads varying in magnitude in individual events.

### 6.11.2 Comparing results against those from other estimation approaches in South Africa

Comparing the results of the model against other sediment yield modelling techniques in South Africa helps to identify the potential use of the model as an effective catchment management tool. Thus the result from the model was compared against the Rooseboom *et al.* (1992) sediment yield map and *ACRU* sediment yield modelling.

#### *6.11.2.1 Comparison of results with Rooseboom et al. (1992) sediment yield Map*

Rooseboom *et al.* (1992) derived a regionalised regression technique which allows for the estimation of long term average sediment yield from ungauged catchments within certain confidence limits.

The approach followed was to divide the southern Africa region into nine relatively homogenous regions. Statistical analysis was then performed on each of these regions to overcome the wide variability observed in the measured sediment yield. The result of the model was standardised sediment yield values for each of the nine regions (Details in Rooseboom *et al.*, 1992). The Henley catchment falls within the sediment yield homogenous region 4. The resulting average annual sediment yield simulated from the model is 1.6 t. $ha^{-1}.yr^{-1}$, which fall within the values of 0.2 and 7.23 t. $ha^{-1}.yr^{-1}$ reported by Rooseboom *et al.* (1992), for this region.

#### *6.11.2.2 Comparison of results with the ACRU sediment modelling system in Mgeni catchment*

The Henley catchment is found in the south western portion of the Mgeni catchment. In their studies on the Mgeni catchment, Kienzle *et al.* (1997) derived the average annual subcatchment sediment yields by first simulating daily sediment loads for each subcatchment for the period 1960-1993 and then computing annual averages. The mean annual *ACRU* simulated sediment yield for the subcatchments ranges from 0.02 to 6.29 t. $ha^{-1}.yr^{-1}$. The resulting long term average annual sediment yield from the *SDR* model is 1.6 t. $ha^{-1}.yr^{-1}$ which falls within the range of values reported by these authors on the Mgeni catchment.

#### *6.11.2.3 Conclusion*

In conclusion, both estimation techniques compared with the *SDR* model prediction have their own advantages and disadvantages. The Rooseboom *et al.* (1992) method is very easy to use and may produce results very quickly for specific catchments. The technique is not good in accounting for well vegetated land cover and small regions as it considers large scale homogeneity classifications (Donald, 1997). A further problem with this technique is that although a lumped value for a subcatchment can be determined, the details, often required by catchment managers, may not be possible.

On the other hand, the *ACRU* approach is by far the most detailed approach. The ability of *ACRU* to predict sediment yields for various events is certainly an advantage. The main problem with the *ACRU* model however is that it requires detailed input parameters, especially for event based modelling, which may not always be available at the location of concern. If required data sets are not available, then the more generalised models, such as the *SDR* model applied in this research, can be used to predict the average annual sediment yields.

Comparing the mean annual sediment yield of the *SDR* model against alternative sediment yield modelling techniques in South Africa demonstrated that the results from the *SDR* model compared well with the results from these techniques. Therefore the model presented in this research can be used as a potential tool for predicting long term average annual sediment yield, especially for regions with a lack of sediment yield data.

### 6.12 Sediment Yield Sensitivity Analysis

Sensitivity analysis is the study used to ascertain how a given model output depends upon the information (input data) fed into it, upon its structure and upon the framing assumptions made to build it (Saltelli *et al.*, 2000). Sensitivity analysis is used to increase the confidence in the model and its predictions, by providing an understanding of how the model responds to changes in the input parameters. This is an important method for checking the quality of a given model, as well as a powerful tool for checking the robustness and dependability of a model on its analysis. The

topic is acknowledged as essential for good modelling practice, and is an implicit part of any modelling field (Saltelli *et al.*, 2000).

In this research, the increasing and decreasing of variables (*R*, *K*, *LS*, *C*, *P* and *SDR*) by an arbitrary percentage of their standard deviation from their mean were used as criteria to measure the sensitivity of the model prediction to a change in the variable value (Lorentz, 2004). The point values of each grid cell of the variables of the sediment yield model were extracted from their respective GIS coverages using the GeoProcessing Wizard in Arcview GIS. Thereafter these point values of the variables of the model were used as input into the *GENESTAT* statistical software. The fitted frequency distribution curve of the different variables of sediment yield and *SDR* from which the mean, standard deviation and coefficient of variation can be calculated are given in Appendix E and the output is summarised in Table 6.15.

**Table 6.15** Summary statistics of the different sediment yield model variables

| Variable | Mean | Standard deviation | Coefficient of variation |
|---|---|---|---|
| *R* | 320.7 | 5.10 | 0.016 |
| *K* | 0.354 | 0.12 | 0.332 |
| *LS* | 2.280 | 2.02 | 0.887 |
| *C* | 0.144 | 0.08 | 0.578 |
| *P* | 0.774 | 0.22 | 0.288 |
| *SDR* | 0.190 | 0.19 | 1.000 |

Figure 6.13 shows the results of the sensitivity analysis performed on the sediment yield model by increasing and decreasing of each of the variables by arbitrary percentages. For the sake of simplicity it is better to classify the sensitivity analysis into two conditions, i.e. overestimating and underestimating the variables from their respective mean by fixed percentages of their standard deviations.

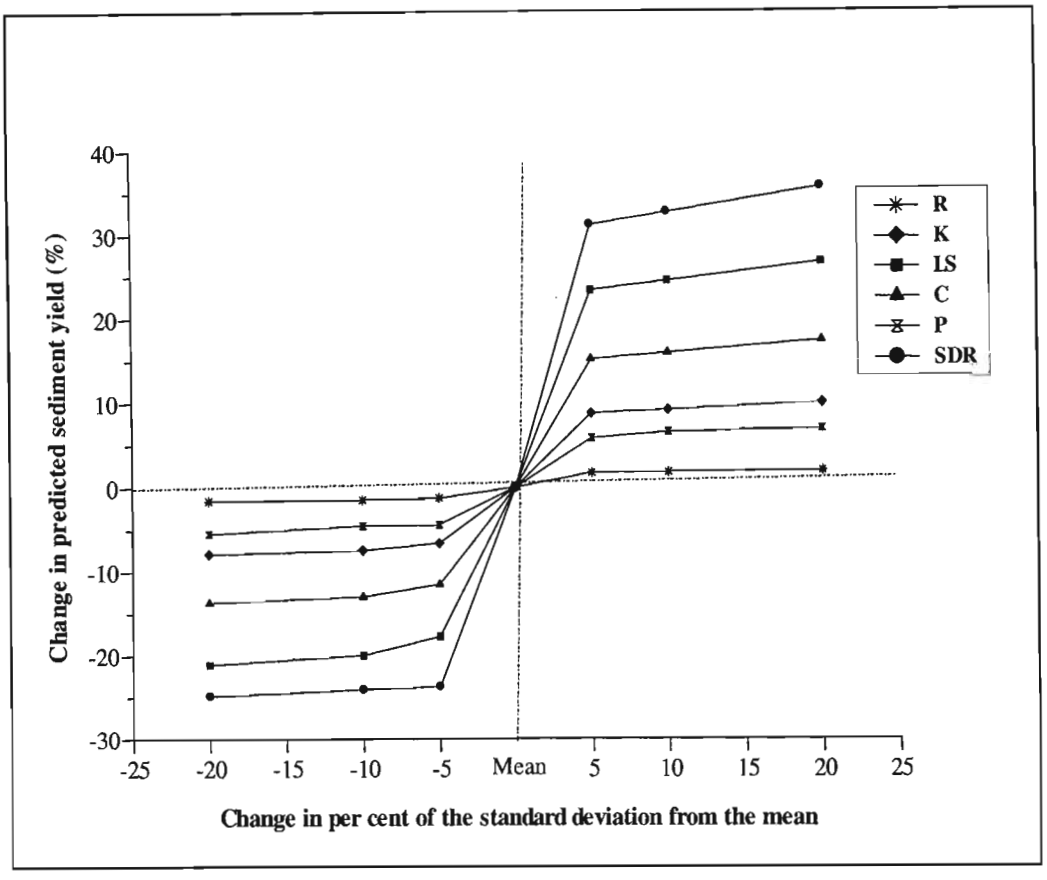


**Figure 6.14** Effects of changes in sediment yield model variables value on predicted sediment yield

### 6.12.1 Sensitivity of sediment yield to overestimation of model variables

From the results of the sensitivity analysis in Figure 6.13, model prediction of sediment yield was found to be most sensitive to change in the *SDR* variable. For example, a 20 % of standard deviation increase from the mean *SDR* value resulted in 35 % increase in the sediment yield. This implies that as the value of *SDR* increases, the amount of sediment yield that is delivered to the catchment outlet increases. Therefore, the higher the *SDR* value the higher the sediment yield and *vice versa*. The second most sensitive variable was found to be the variable *LS*, where a 20 % of standard deviation increase from the mean in the *LS* value resulted in 26.6 % increase in the sediment yield. This implies that, as the *LS* value increases, the amount of soil eroded from the land and subsequent sediment yield also increases. This might be due to the fact that an increased *LS* produces higher overland flow velocities and correspondingly higher sediment loads (Haan *et al.*, 1994). The third most sensitive variable was found to be the cover factor, *C*, where a 20 % of

standard deviation increase from the mean in the *C* value resulted in 17.3 % increase in sediment yield. This is so since a high *C* factor implies low vegetation cover in the catchment and thus there is an increased opportunity for rainfall to detach sediments, overland flow to scour and transport sediments, ultimately causing an increase in sediment production. The least sensitive variable is the *R* variable because a change in its values does not have a significant change in the sediment yield from the catchment. For example, a 20 % of standard deviation increase from the mean in the *R* value caused only a 1.9 % increase in the sediment yield. The variables *K* and *P* are not as sensitive as the variables *SDR*, *LS* and *C* as they show only slightly increased sediment yield over the wide range of percentage of standard deviation change from their mean.

### 6.12.2 Sensitivity of sediment yield to underestimation of model variables

The same pattern was also observed when underestimating the variables, i.e. the most sensitive variable in the model is the *SDR*. For example, a 20 % of standard deviation decrease from the mean of the *SDR* value resulted in 25 % decrease in predicted sediment yield. This implies that as the value of *SDR* decreases, the amount of sediment yield that is delivered to the catchment outlet also decreases. The second most sensitive variable in the model is again the *LS*. A decrease of 20 % of standard deviation in the value of *LS* from its mean causes a decrease of 21 % in the predicted sediment yield. The *R* variable is again the least sensitive variable in the prediction of sediment yield. The rest of the variables can be explained in the same manner by observing Figure 6.13.

From the results of the sensitivity analysis, it can be concluded that the predicted sediment yield is highly sensitive to *SDR*, *LS* and *C* variables in both overestimating and underestimating the variable. Comparing the two conditions the predicted sediment yield is more sensitive when overestimating the variables.

### 6.12.3 Prediction of *SDR*

In this research, sediment yield is the product of the RUSLE variables and the sediment delivery ratio of the catchment. But the sediment delivery ratio (*SDR*) in turn is a function of slope, catchment roughness coefficient and travel time of overland flow. Therefore it is expedient to analyse this variable independently. In the same way as the sediment yield model variables have

been analysed, the *SDR* variables were extracted from their respective GIS coverages using the GeoProcessing Wizard in Arcview GIS. Then these point values of the *SDR* variable were used as input into the *GENESTAT* statistical software from which the mean, standard deviation and coefficient of variation of the *SDR* variables can be calculated as shown in Table 6.16.

**Table 6.16** Summary statistics of the different sediment delivery ratio (*SDR*) variables

| Variable | Mean | Standard deviation | Coefficient of variation |
|---|---|---|---|
| Roughness coefficient (*RC*) | 1.70 | 0.48 | 0.28 |
| Slope (*S*) | 0.15 | 0.10 | 0.67 |
| Time (*t*) | 2.50 | 2.90 | 1.16 |

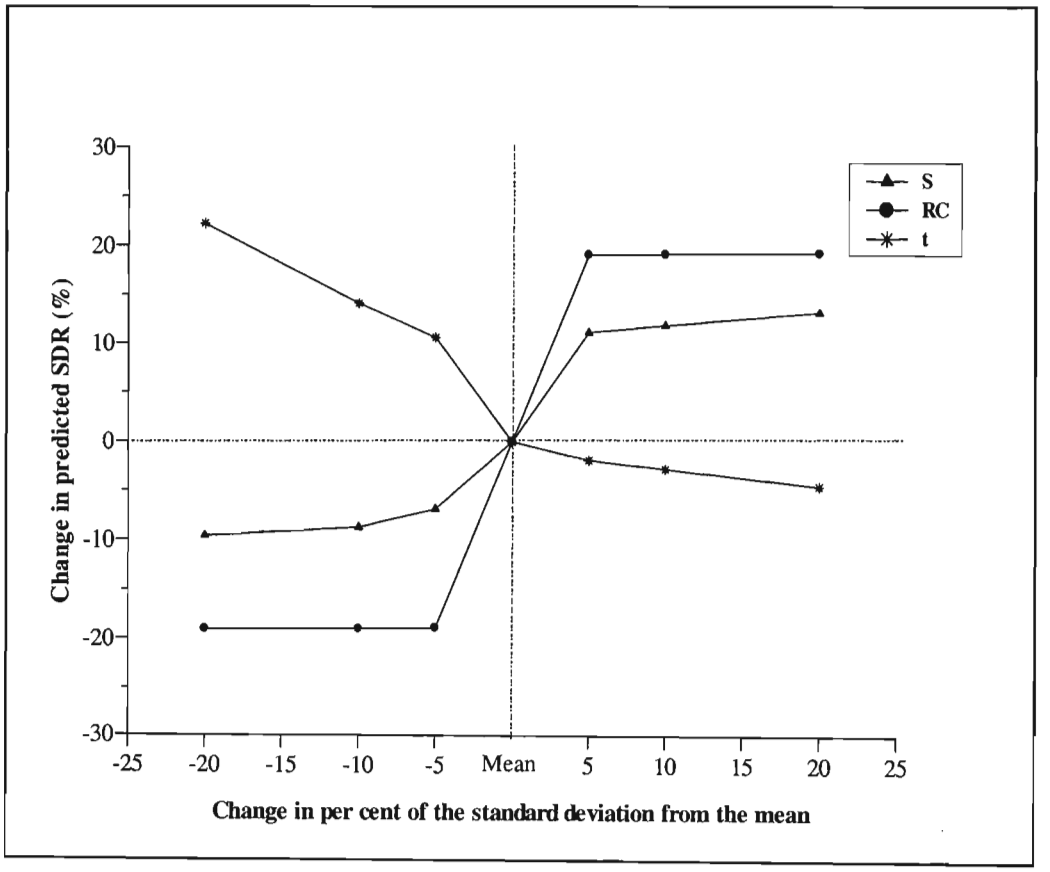


**Figure 6.15** Effects of changes in sediment delivery ratio variables value on predicted sediment delivery ratio

From the results of the sensitivity analysis, shown in Figure 6.14, overestimation of the variables contributing to the *SDR* was found most sensitive to change in the roughness coefficient (*RC*). For example, a 20 % of standard deviation increase from the mean in the *RC* value resulted in 19 % increase in the *SDR* of the catchment. This can be explained by noting that the lack of any physical features like depressions and conservation practices there would result in increased sediment transport by runoff. The second most sensitive variable for *SDR* is slope ($m.m^{-1}$). Here, a 20 % of standard deviation increase from the mean in the *S* value resulted in 13 % increase in the *SDR* of the catchment. This can be justified since an increased slope steepness produces higher overland flow velocities and correspondingly increased sediment delivery (Haan *et al.*, 1994).

When underestimating the contributing variables, *SDR* was found to be most sensitive to travel time, *t*. For example, a 20 % of standard deviation decrease from the mean in the *t* value resulted in 22 % increase in the *SDR* of the catchment. This implies that *SDR* and *t* are inversely related in this specific catchment and condition sensitivity analysis. This can be explained since, as the travel time decreases, there is less opportunity for sediment deposition along the travel path. As a result a large amount of sediment is delivered to the nearest stream reach.

### 6.12.4 Conclusion

In conclusion, when overestimating the variables, *SDR* was found highly sensitive to *RC* and *S* and when underestimating the variables, *SDR* was found most to be sensitive to travel time.

Generally, from this catchment and condition specific sensitivity analysis, it is shown that the sediment yield and *SDR* are highly sensitive to the topography and land use of the catchment and hence the model should be used for estimating of sediment yield in other such ungauged catchments with great care given to the accuracy of parameters derived from topography and land use conditions.

This chapter has presented and discussed the results from the proposed model, verification results for event based sediment yield modelling, comparison against other sediment yield modelling techniques in South Africa and the sensitivity of the model. These results allow for the identification of primary sediment source areas, the spatially varying sediment transport capacity

and ultimately, the sediment yield from each area. The model's verification against measured data and comparison against other modelling techniques in South Africa has demonstrated its potential for predicting the spatial and temporal variability of sediment yield. The sensitivity analysis of the model shows that the model is highly sensitive to topography and land use conditions of the catchment. The following chapter presents concluding remarks on this research.

# 7. CONCLUSIONS AND RECOMMENDATIONS

Soil erosion and sediment delivery are subject to highly complex processes that are sometimes not fully understood by catchment modellers. These processes and their interactions with each other are often major factors affecting soil loss and sediment yield. Owing to the importance of these processes a number of models that use these processes to simulate catchment soil loss and sediment yield have been developed over the years. An attempt was made to group these different soil loss and sediment yield models according to the approaches they used in modelling the catchment.

Many published soil loss and sediment yield modelling approaches, operating over a range of scales were first reviewed to understand the specific motivation behind their development and processes implied in their techniques. Relative merits and shortcomings of these modelling approaches were discussed. It was concluded that there is no universally acceptable method or approach to modelling a catchment's soil erosion and sediment yield. Based on this review it was decided to combine RUSLE, GIS and a distributed sediment delivery ratio concept to simulate the magnitude and variability of soil erosion and sediment yield in a catchment. This was done because the equations and concepts used in the model are simple and its components have been researched extensively worldwide, particularly the calculation of source erosion component in the RUSLE. It was concluded that, the RUSLE was particularly suitable in developing regions where there is limited or sometimes no sediment yield data either for model calibration or for designing and planning of water resource projects.

A motivation was presented for the combined use of RUSLE, GIS and a distributed, grid based sediment delivery ratio concept to estimating the magnitude and describing the spatial variability of soil erosion and sediment yield through out the catchment. More importantly, it allows easy definition of spatial subunits or grids of relatively uniform properties. Hence with the aid of GIS, soil loss and sediment yield modelling can be performed on the individual subunits or grids. The identification of the spatially distributed erosion source areas within the modelled catchment makes possible the implementation of focused conservation efforts in these source areas.

The combined use of RUSLE, GIS and distributed sediment delivery ratio concept was modelled in an Arcview GIS grid analyst to determine which grid cells in a catchment contribute erosion and possibly sediment to the nearest stream channel and ultimately to the catchment outlet. The proposed model was designed with the objective of identifying the primary source erosion areas and finally the spatially varying sediment yield contribution from each grid cell. The source erosion generated on any grid cell is routed to the nearest stream reach as a function of travel time. As opposed to the traditional "black-box" sediment delivery ratio (*SDR*) for an entire catchment (cf. Table 3.1), the distributed sediment delivery ratio ($SDR_i$) values, based on the travel time from individual cells and a catchment specific coefficient which is a function of topography and land use characteristics, permits identification of those critical areas with high potential for soil erosion and sediment yield. The integrated approach also facilitates fast and efficient assessment of different management alternatives, and thus can serve as a useful tool in natural resource management and planning.

The evaluation of the combined use of RUSLE, GIS and the distributed sediment delivery ratio concept for estimating and identifying source areas and sediment yield was tested on the Henley catchment, South Africa. The event based simulations from this model were compared with observed sediment yields and proved to be suitably accurate. No sediment yield model is likely to yield absolute results and hence the results achieved by the model which compare well with the measured sediment yields for the Henley catchment, suggest that the model may be used with confidence as a catchment management tool. However, careful evaluation of topography (slope) and land use conditions are required since the model is highly sensitive to these parameters. Therefore it is concluded that the model's results for this relatively simple analysis are successful enough to warrant further time and effort on its testing and verification.

Comparing the results of the model prediction against *ACRU* sediment yield modelling and the Rooseboom *et al.* (1992) sediment yield map in South Africa, demonstrated the usefulness of the model as an effective catchment management tool. The use of raster GIS technology was an advantage over the Rooseboom *et al.* (1992) sediment yield map which does not use a grid based analysis to identify areas contributing elevated sediment loads. Implementing the model on a GIS

raster modelling system also allows for suitable identification of primary source areas for sediments and hence for implementation of focused conservation techniques for these areas.

In the case study of Henley catchment the residential and agricultural areas of the catchment which are characterised by degradation due to overgrazing and traditional and peri-urban settlements with mixed crops, exhibit much higher source erosion rates and sediment yield than the non cultivated lands. A reduction in sediment yield of up to 35.5 % can be expected when contour banks with grassed waterways in residential areas and contour and strip cropping in the veld and mixed cropping land use are implemented. This clearly reveals the effectiveness and importance of conservation practices and also suggests that practices other than those evaluated in the research may further reduce erosion and sediment delivery. However, care must be taken when considering the economic effectiveness of the specific conservation practice proposed.

The combined use of RUSLE, GIS and a distributed sediment delivery ratio concept to modelling source erosion and sediment yield in a catchment requires further testing and development of its components. Further research with the model should focus on the distributed sediment delivery ratio concept used in the model. However, there are also opportunities to improve on its use of GIS techniques, as the model depends solely on these. Based on the results obtained from verification of event based simulations and comparisons against other modelling techniques in South Africa, the following paragraphs outline some recommendations for future work with the model.

- Subcatchment estimation of sediment yield/load is necessary to improve the application of the distributed sediment delivery ratio concept. These data should also be used to test the various processes affecting sediment delivery like the branching and configuration of stream network and stream length. Therefore, further work with the model should test the advantage of incorporation of the stream network parameters in routing of sediment from the hillslopes to the catchment outlet. Such a technique would enhance the distributed sediment delivery ratio concept already used in the model.
- Two forms of erosion and sediment yield processes, namely gully erosion and stream bank erosion, are currently not modelled by RUSLE because RUSLE is developed only

for interrill and rill erosion (Renard *et al.*, 1997). Gully erosion refers to the process responsible for the removal of soil from a rill large enough that it cannot be removed by normal tillage practices. It incorporates the processes of waterfall erosion at the gully head, channel erosion caused by water flowing through the gully, raindrop splash on unprotected soil, alternate freezing and thawing of the exposed soil banks, and slides or mass movement of the soil in the gully. Stream bank erosion includes the processes of soil removal from stream banks or soil movement in the channel or stream banks eroded either by runoff flowing over the side of the stream bank or by scouring and undercutting below the water surface. It is recommended that equations which are capable of describing the processes of gully and stream bank erosion be incorporated in the respective soil loss and sediment yield models. The methodology presented in this research facilitates the simulation of these processes due to its grid based capabilities which already model flow path, flow accumulation and velocities as a function of topography and land use.

- The GIS techniques which require further investigation are the influence of grid size. The selection of a grid size is a scale issue and is a function of the size of the catchment being modelled. For example, coarsening grid size results in missing of some physical features of the catchment (such as slope) which will affect the calculation of the slope length and gradient of RUSLE and ultimately the delivery ratio component of the model. Currently the Arcview GIS used in this research has only a single flow direction algorithm which routes flow in the steepest downslope direction from any point. Multiple flow direction algorithms have been developed to proportion flow to more than just one downslope grid cell as a function of slope (Tarboton, 1997). Therefore it may be better to incorporate such algorithms to represent the process as it occurs naturally in the field. However, their application is more complex. Selection of different algorithms for calculations of flow direction and slope will affect the calculation of the sediment delivery ratio and therefore the sediment yield through the catchment to the catchment outlet.

- It is known that all methods of raster DEM processing for watershed segmentation and parameterisation ultimately rely on some form of overland flow simulation to define drainage courses and catchment area (Martz and Garbrecht, 1998). These methods have

difficulty dealing with closed depressions and flat areas which are normally corrected or removed prior to drainage analysis on digital models of the land surface. However, closed depressions and flat areas are real landscape features which are particularly important to sediment deposition and should be handled in a hydrologically meaningful way during drainage analysis. In this research, consideration of depression and flat areas may have improved the precision of the sediment yield analysis as the catchment has about 5.8 $km^2$ of these areas.

To conclude, it is commonly recognised that simple but valid lumped models have historically been shown to give as good, if not better soil erosion and sediment yield predictions than some of the more complex distributed models (Howe, 1999). However, the more complex distributed models provide additional information on the different processes occurring in a catchment and enhance our understanding or more often than not, highlight our lack of understanding the different soil erosion and sediment delivery processes.

Finally, the objective of this research was to estimate the magnitude and spatial distribution of soil erosion and sediment yield by combining RUSLE, GIS and a sediment delivery ratio concept. Thus a convenient catchment management tool has been developed which may be used to identify variable source areas and determine quick, yet reasonably accurate, source erosion and sediment yield for developing countries where there is limited information on sediment yield data for designing and planning of water resource projects. The methodology has demonstrated that it can be applied to other regions by focusing on the accuracy of topography and land use conditions derived parameters.

# 8. REFERENCES


**Alonso, CV, Neibling, WH and Foster, GR.** 1981. Estimating sediment transport capacity in watershed modelling. *Transactions of the ASAE*, 24(2): 1211-1220.

**Atkinson, E.** 1995. Methods for assessing sediment delivery in river system. *Hydrological Sciences Journal*, 40(2): 273-279.

**Bao, J, Maidment, D and Olivera, F.** 1997. Using GIS for hydrologic data processing and modelling in Texas. CRWR online report 97-4. Center for Research in Water Resources. University of Texas, Austin, Texas, USA.

**Beasley, DB, Huggins, LF and Monke, EJ.** 1980. ANSWERS: A model for watershed planning. *Transactions of the ASAE*, 23(2): 938-944.

**Beuselinck, L, Govers, G, Hairsine, PB, Sander, GC and Breynaert, M.** 2002. The influence of rainfall on sediment transport by overland flow over areas of net deposition. *Journal of Hydrology*, 257: 145-163.

**Beven, KJ.** 1989. Changing ideas in hydrology: The use of physically based models. *Journal of Hydrology*, 105: 157-172.

**Bingner, RL.** 1990. Comparison of the components used in several sediment yield models. *Transactions of the ASAE* 33, (4): 1229-1238.

**Boardman, J and Favis-Mortlock, D.** 1998. *Modelling Soil Erosion by Water.* Springer-Verlag, Heidelberg, Berlin, Germany.

**Boardman, J, Foster, IDL, and Dearing, JA.** 1990. *Soil Erosion on Agricultural Land.* J Wiley and Sons, Chichestere, UK.

**Borah, DK.** 1989. Sediment discharge model for small watersheds. *Transactions of the ASAE*, 32(3): 874-880.

**Borah, DK and Ashraf, MS.** 1990. Modelling storm runoff and sediment with seasonal variations. *Transactions of the ASAE*, 33(1): 105-110.

**Boyce, RC.** 1975. Sediment routing with sediment delivery ratios. In: *Present and Prospective Technology for Predicting Sediment Yield and Sources.* US Dept. Agric. Publ. ARS-S40, 61-65. USDA, USA.

**Bradbury, PA, Lea, NJ, Bolton, P.** 1993. Estimating catchment sediment yield: development of the GIS-based CALSITE model. Report No. OD 125, HR Wallingford, UK.

**Bradbury, PA.** 1994. CALSITE: A catchment planning tool for simulating soil erosion and sediment yield. In: ed. Kirby and White, *Integrated River Basin Development.* J Wiley and Sons, Chichester, UK.

**Bradbury, PA.** 1995. CALSITE VERSION 3.1, calibrated simulation of transported erosion, user manual. Overseas Development Unit, HR Wallingford, UK.

**Bromley, KA.** 1989. Land cover classes in the Mgeni river catchment. Supplement to CSIR Report AAL 21, Institute of Natural Resources, University of Natal, Pietermaritzburg, South Africa.

**Cochrane, TA and Flanagan, DC.** 1996. Detachment in a simulated rill. *Transactions of the ASAE*, 40(1): 111-119.

**Crosby, CT, McPhee, PJ and Smithen, AA.** 1983. Introduction of the universal soil loss equation in the Republic of South Africa. Paper No. 83-2072, Presentation to the Society of Agricultural Engineers, Pretoria, South Africa.

**Dai, D and Tan, Y.** 1996. Soil erosion and sediment yield in the Upper Yangtze River Basin. In: *Proceedings of the Exeter Symposium Erosion and Sediment Yield: Global and Regional Perspectives.* IAHS Pub. No. 236. pp 191-203, Wallingford, Oxfordshire, UK.

**De Roo, APJ and Affermans, RJE.** 1995. LISEM: A physically-based hydrological and soil erosion model for basin-scale water and sediment management. In: ed. Chen, Z and Huang, GH, *Modelling and Management of Sustainable Basin-Scale Water Resources Systems.* IAHS publ. No. 225. pp 339-407, Wallinford, Oxfordshire, UK.

**Desmet, PJJ and Govers, G.** 1996. A GIS procedure for automatically calculating the USLE LS factor on topographically complex landscape units. *Journal of Soil and Water Conservation*, 51(5): 427-433.

**Dickinson, A and Collins, R.** 1998. Predicting soil erosion and sediment yield at the catchment scale. In: ed. Penning de Vries, FWT, Angus, H and Kerr, J, *Soil Erosion at Multiple Scales, Principles and Methods for Assessing Causes and Impacts.* pp 317-342, Oxon, New York, USA. (From Fernandez *et al.*, 2003).

**Dietrich, CR, Timothy, R, Green, R and Jakeman, AJ.** 1999. An analytical model for stream sediment transport: application to Murray and Murrumbidgee River reaches, Australia. *Hydrological Processes*, 13: 763-776.

**Donald, PD.** 1997. GIS modelling of erosion and sediment yield in a semi-arid environment. Unpublished MSc Eng thesis. Faculty of Engineering, University of Witwatersrand, Johannesburg, South Africa.

**Eck, HV, Gore, C and Stewaet, BA.** 1995. Manure. In: ed. Rechigl, JE, *Soil Amendment and Environmental Quality*. CRS press, Inc., USA.

**Elliot, WJ and Laflen, JM.** 1993. A process-based rill erosion model. *Transactions of the ASAE*, 36(1): 65-72.

**Endale, DM, Schomberg, HH and Steiner, JL.** 2000. Long term sediment yield and mitigation in a small southern Piedmont watershed. *International Journal of Sediment Research*, 14(1): 60-68.

**Engel, B.** 2003. Estimating soil erosion using RUSLE (Revised Universal Soil Loss Equation) Using Arcview. [Internet] Available from: < http://pasture.ecn.purdue.edu/~engelb/agen526/gisrusle/gisrusle.html > [Accessed 15 April 2004].

**Environmental System Research Institute (ESRI).** 1994. Cell based modelling with GRID. Environmental Systems Research Institute Inc., Redlands, California, USA.

**Environmental System Research Institute (ESRI).** 1996. Cell based modelling with GRID. Environmental System Research Institute Inc., Redlands, California, USA.

**Fernandez, C, Wu, JQ, McCool, DK and Stöckle, CO.** 2003. Estimating water erosion and sediment yield with GIS, RUSLE, and SEDD. *Journal of Soil and Water Conservation*, 58(3): 128-136.

**Ferro, V and Minacapilla, M.** 1995. Sediment delivery processes at basin scale. *Hydrological Sciences*, 40(6): 703-717.

**Ferro, V and Porto, P.** 2000. Sediment Delivery Distributed (SEDD) model. *Journal of Hydrologic Engineering*, 5(4): 411-422.

**Ferro, V, Porto, P and Tusa, G.** 1998. Testing a distributed approach for modelling sediment delivery. *Hydrological Sciences*, 43(3): 425-442.

**Ferro, V.** 1997. Further remarks on a distributed approach to sediment delivery. *Hydrological Sciences*, 42(5): 633-647.

**FitzHugh, T and Mackay, DS.** 2001. Impact of subwatershed partitioning on modelled source and transport-limited sediment yields in an agricultural nonpoint source pollution model. *Journal of Soil and Water Conservation*, 56(2): 137-143.

**Foster, GR and Wischmeier, JR.** 1974. Evaluating irregular slopes for soil loss prediction. *Transactions of* the *ASAE*, 17(2): 305-309.

**Foster, GR, Lane, LJ, Nowlin, JD, Laflen, JM and Young, RA.** 1981. Estimating erosion and sediment yield on field-sized areas. *Transactions of the ASAE*, 24: 1253-1262.

**Foster, GR.** 1982. Special problems in the application of the USLE to rangelands: C and P factors. In: *Proceedings of the Workshop on Estimating Erosion and Sediment Yield on Rangelands.* US department of agriculture, agricultural research service and agricultural reviews and manuals, Tucson, Arizona, USA.

**Francis, PB and Cruse, RM.** 1983. Soil water matrix potential effects on aggregate stability. *Soil Science Society American Journal*, 47: 578-581.

**Gerits, JJP, Delima, JLMP and Van Den Broek, TMW.** 1990. Overland flow and erosion. In: ed. Anderson, MG and Burt, TP, *Process Studies in Hillslope Hydrology.* pp 173-214, John Wiley and Sons Ltd, UK.

**Ghadiri, H and Payne, D.** 1988. The formation and characteristics of splash following raindrop impact on soil. *Journal of Soil Science*, 39: 563-575.

**Gibson, CE and Ford, D.** 1998. The dynamics of phosphorus in fresh water and Marin environment. In: ed. Tunney, H, Carton, OT, Brookes, PC and Johnston, AE, *Phosphorus loss from soil to water.* Biddles Ltd, Guildford and King's Lynn, UK.

**Goldman, SJ, Jackson, K, Bursztynsky, PE.** 1986. Erosion and Sedimentation Control Handbook. McGraw-Hill Book Company, USA.

**Grayson, RB, Bloschl, G, Barling, RD and Moore, ID.** 1993. Process, scale and constraints to hydrological modelling in GIS. In *HydroGIS 93: Application of Geographic Information Systems in Hydrology and Water Resources.* IAHS Publ. No. 211. pp 83-92, Wallinford, Oxfordshire, UK.

**Haan, CT, Barfield, BJ and Hayes, JC.** 1994. *Design Hydrology and Sedimentology for Small Catchments.* Academic Press, New York, USA. (From Fernandez *et al.*, 2003).

**Hadley, RF and Mizuyama, T.** 1993. Sediment problems: Strategies for monitoring, prediction and control. IAHS publ. No. 217. pp 231-240, Wallingford, Oxfordshire, UK.

**Hairsine, PB and Rose, CW.** 1991. Rainfall detachment and deposition: Sediment transport in the absence of flow-driven processes. *Soil Science Society of American Journal*, 55: 320-324.

**Hairsine, PB and Rose, CW.** 1992. Modelling water erosion due to overland flow using physical principles: 1. Sheet flow. *Water Resources Research*, 28(1): 237-243.

**He, Q and Walling, DE.** 2003. Testing distributed soil erosion and sediment delivery models using 137Cs measurements. *Hydrological Processes*, 17: 901-916.

**Hession, WC and Shanholtz, VO.** 1988. A Geographic Information System for targeting nonpoint-source agricultural pollution. *Journal of Soil and Water Conservation*, 43: 264-266.

**Hickey, R, Smith, A and Jankowski, P.** 1994. Slope length calculations from a DEM within ARC/INFO GRID. *Computers, Environment and Urban Systems*, 18(5): 365-385.

**Hirschi, MC and Barfield, BJ.** 1988. KYERMO – A physically based research erosion model. Part I: Model development. *Transactions of the ASAE*, 31(3): 804-813.

**Hornberger, GM, Beven, KJ, Cosby, BJ and Sappington, DE.** 1985. Shenandoah watershed study: Calibration of a topography-based, variable contributing area hydrological model to a small forested catchment. *Water Resources Research*, 21(12): 1841-1850.

**Howe, BJ.** 1999. Development of new techniques for variable source area sediment yield modelling. Unpublished MSc Eng dissertation. School of Bioresources Engineering and Environmental Hydrology, University of Natal, Pietermaritzburg, South Africa.

**Hudson, N.** 1995. *Soil Conservation*. Redwood Books, Trowbridge, UK.

**ISCW** 1993. Land type series. In: *Memoirs on the Agricultural Natural Resources of South Africa.* Institute for Soil Climate and Water, Department of Agriculture and Water Supply, Pretoria, South Africa.

**Jain, MK and Kothyari, UC.** 2000. Estimation of soil erosion and sediment yield using GIS. *Hydrological Sciences*, 45(5): 771-786.

**Jones, DS, Kowalski, DG and Shaw, RB.** 1996. Calculating RUSLE estimates on department of defence lands: A review of RUSLE factors and U.S. army land condition-trend analysis (LCTA) data gaps. Centre for Ecological Management of Military Lands, Department of Forest Science, Colorado State University, Fort Collins, Colorado, USA.

**Jonson, S and Domingue, J.** 1988. Extracting Topographic Factor from Digital Elevation Data for Geographic Information System Analysis. *Photogrammetric Engineering and Remote Sensing*, 54(10): 1593-1600.

**Julien, PY and Simons, DB.** 1985. Sediment transport capacity of overland flow. *Transactions of the ASAE*, 28(3): 755-762.

**Karvonen, T, Koivusalo, H, Jauhiainen, M, Palko, J and Weppling, K.** 1999. A hydrological model for predicting runoff from different land use areas. *Journal of Hydrology*, 217: 253-265.

**Kemper, WDT, Trout, TJ, Brown, MJ and Rosenau, RC.** 1985. Furrow erosion and water and soil management. *Transactions of the ASAE*, 28(5): 1564-1572.

**Khanbilvardi, RM, Rogowski, AS and Miller, AC.** 1983. Modelling upland erosion. *Water Resources Research*, 19(1): 29-35.

**Kienzle, SW and Lorentz, SA.** 1993. Production of a sediment source area map and simulation of sediment yield in the Henley dam catchment, Natal. In: *Proceeding of the Sixth South Africa National Hydrological Symposium.* University of Natal, Department of Agricultural Engineering, 1: 565-573, Pietermaritzburg, South Africa.

**Kienzle, SW, Lorentz, SA and Schulze, RE.** 1997. Hydrology and water quality of the Mgeni catchment. Report TT87/97.pp 5-6, Water Research Commission, Pretoria, South Africa.

**Kinnell, PIA.** 1993. Runoff as a factor influencing experimentally determined interrill erodibilities. *Australian Journal of Soil Research*, 31(3): 333-342.

**Kothyari, UC and Jain, SK.** 1997. Sediment yield estimation using GIS. *Hydrological Sciences*, 42(6): 833-843.

**Lal, R.** 1994. Soil erosion by wind and water: Problems and prospects. In: ed. Lal, R, *Soil Erosion: Research Methods.* pp 1-9, Soil and Water Conservation Society, St. Lucie Press, Florida, USA.

**Lane, LJ, Kidwell, MR and Weltz, MA.** 2000. Watershed sediment yield and rangeland health. *International Journal of Sediment Research,* 15(1): 51-59 (From Fernandez *et al.*, 2003).

**Lorentz, SA.** 2004. Personal Communication. University of KwaZulu-Natal, Pietermaritzburg, South Africa, 24 November 2004.

**Lorentz, SA. and Howe, BJ.** 1995. Modelling sediment yield at the basin scale. *Agricultural Engineering in South Africa*, 27:57-70.

**Lorentz, SA and Schulze, RE.** 1995. Sediment yield. In: ed. Schulze, RE, *Hydrology and Agrohydrology: A Text to Accompany the ACRU 3.00 Agrohydrological Modelling System.* Department of Agricultural Engineering, University of Natal, Pietermaritzburg, South Africa.

**Lynch, SD.** 1998. Converting point estimates of daily rainfall fall into a rectangular grid. Department of Agricultural Engineering, University of Natal, Pietermaritzburg, South Africa. [Internet] Available from: < http://www.geocomputation.org/1998/93/gc_93.htm> [Accessed 20 April 2004].

**MacVicar, CN, Scotney, DM, Skinner, TE, Niehaus, HS and Loubser, JH.** 1974. A classification of land (climate, terrain form, soil) primarily for rain fed agriculture. *South African Journal of Agricultural Extension*, 3:21-24.

**Maidment, DR.**1993. Developing a Spatially Distributed Unit Hydrograph by Using GIS [Internet]. Available from < http://www.ce.utexas.edu/prof/olivera/disstn/frontpgs/referenc.htm> [Accessed 9 April 2004].

**Maidment, DR.** 1994. Digital delineation of watersheds and stream networks in the Allegheny basin. Prepared for Hydrologic Engineering Centre, Davis, California, USA.

**Mandaville, SM.** 1997. A Brief Treatise on Eutrophication of Lakes. Soil and Water Conservation Society of Metro Halifax, Dartmouth NS, Canada [Internet]. Available from: <http://lakes.chebucto.org/eutro.html > [Accessed 20 April 2003].

**Maner, SB.** 1958. Factors affecting sediment delivery ratio in the red hill physiographic area. *Transactions of the AGU*, 39(4): 669-675 (From Howe, 1999).

**Mankin, KR, DeAusen, RD and Barnes, PL.** 2002. Assessment of a GIS-AGNPS interface model. *Transactions of the ASAE*, 45(5): 1375-1383.

**Martz, LW and Garbrecht, J.** 1998. The treatment of flat areas and depressions in automated drainage analysis of raster digital elevation models. *Hydrological Processes*, 12: 843-855.

**McCool, DK, Brown, GR, Foster, CK, Mutchler, and Meyer, LD.** 1993. Revised slope steepness factor for the Universal Soil Loss Equation. *Transactions of the ASAE*, 30(5): 1387-1396.

**McPhee, PJ and Smithen, AA.** 1984. Application of the USLE in republic of South Africa. *Agricultural Engineers South Africa*, 18(1): 352-367.

**McPhee, PJ, Smithen, AA, Venter, CJ, Hartmann, MO and Crosby, CT.** 1983. The South African rainfall simulator programme for assessing soil loss and runoff. Proceedings of the South African National Hydrological Symposium. Report No. TR119. pp 352-367, Water Research Commission, Pretoria, South Africa.

**Miller, RW and Gardiner, DT.** 1998. *Soil in Our Environment*. New Jersey, Prentice, Hall, USA.

**Mitasova, H.** 2004. Personal Communication. University of Illinois at Urbana-Champaign, USA, 25 March 2004.

**Mitasova, H. and Mitas, L.** 1999. Modelling soil detachment with RUSLE 3d using GIS. Geographic modelling system laboratory University of Illinois at Urbana-Champaign [Internet]. Available from: < http://skagit.meas.ncsu.edu/~helena/gmslab/erosion/usle.html > [Accessed 20 September 2003].

**Mitasova, H, Hofierka, J, Zlocha, M and Iverson, LR.** 1996. Modelling topographic potential for erosion and deposition using GIS. *International Journal of Geographic Information Science*, 10(5): 629-641.

**Moglen, GE.** 2004. Determining Flow Lengths or Travel Distances in GIS. (Personal Communication). Department of Civil and Environmental Engineering, University of Maryland, College Park, USA, 08 April 2004.

**Moore, ID and Wilson, JP.** 1992. Length-Slope factor for the Revised Universal Soil Loss Equation: Simplified method of estimation. *Journal of Soil and Water Conservation*, 47(5): 423-428.

**Moore, ID, Burch, GJ and Mackenzie, DH.** 1988. Topographic effects on the distribution of surface soil water and the location of ephemeral gullies. *Transactions of* the *ASAE*, *38*(4): 1099-1110.

**Moore, RJ and Clarke, RT.** 1983. A distribution function approach to modelling basin sediment yield. *Journal of Hydrology*, 65: 239-257.

**Morgan, RPC, and Davidson DA.** 1986. *Soil Erosion and Conservation*. Longman Group Limited, Longman House, Burnt Mill, Harlow, ESSEX CM20 2JE, UK.

**Morgan, RPC, Quinton, JN and Rickson, RJ.** 1992. EUROSEM documentation manual. Version 1. Silsoe College, Silsoe, UK.

**Morgan, RPC.** 1980. *Soil Erosion*. Longman Group Limited, Longman House, Butnt Mill, Harlow, ESSEX CM20 2JE, UK.

**Morgan, RPC.** 1995. *Soil Erosion and Conservation.* Longman Group Limited, Longman House, Burnt Mill, Harlow, ESSEX CM20 2JE, UK.

**Mou, J and Meng, Q.** 1980. Sediment delivery ratio as used in the computation of the watershed sediment yield. Chinese Society of Hydraulic Engineering, Beijing, China.

**Mutchler, CK and Bowie, AJ.** 1976. Effect of land use on sediment delivery ratios. In: *Proceedings of the Third Federal Inter-Agency Sedimentation Conference.* pp 11-12. Water Resources Council, Washington, D.C., USA.

**Muzik, I.** 1996. Lumped modelling and GIS in flood prediction: In: ed. Singh VP, and Fiorentino, M, *Geographic Information System in Hydrology.* Kluwer Academic Publishers Dordrecht, Bosten, UK.

**Nathalie, EMA.** 1999. Suspended sediment dynamics in a large drainage basin: The River Rhine. *Hydrological Processes*, 13: 1437-1450.

**Nearing, MA, Foster, GR, Lane, LJ and Finkner, SC.** 1989. A process-based soil erosion model for USDA-water erosion prediction project technology. *Transactions of the ASAE*, 32(5): 1587-1593.

**Nearing, MA, Lane, LJ and Lopes, VL.** 1994. Modelling soil erosion. In: ed. Lal. R, *Soil Erosion Research Methods.* pp 127-156, Soil and Water Conservation Society, St. Lucie Press, USA.

**Nearing, MA, Lane, LJ, Alberts, EE and Laflen, JM.** 1990. Prediction technology for soil erosion by water: Status and research needs. *Soil Science Society of American Journal*, 54: 1702-1711.

**Novotny, V and Chesters, G.** 1989. Delivery of sediment and pollutants from nonpoint sources: A water quality perspective. *Journal of Soil and Water Conservation*, 44(6): 568-576.

**Novotny, V and Olem, H.** 1994. *Water Quality: Prevention, Identification, and Management of Diffuse Pollution.* Van Nostrand, New York, USA.

**Novotny, V.** 1980. Delivery of suspended sediment and pollutant from nonpoint sources during overland flow. *Water Resources Bulletin*, 16 (6): 1057-1065.

**O'Callaghan, JF and Mark, DM.** 1984. The extraction of drainage network from digital elevation data: Computer Vision. *Graphics and Image Processing*, 28: 323-344 (From Howe, 1999).

**Onstad, CA.** 1984. Sediment Yield Modelling: In: ed. Hadley and Walling, *Erosion and Sediment Yield: Some Methods of Measurement and Modelling.* University Press, Cambridge, UK.

**Ouyang, D and Bartholic, J.** 1997. Predicting Sediment Delivery Ratio In: Saginaw Bay Watershed. Institute of Water Research, Michigan State University, East Lansing, MI [Internet]. Available from: <http://www.iwr.msu.edu/~ouyangda/sdr/sag-sdr.htm> [Accessed 23 February 2003].

**Owoputi, OL and Stolte, WJ.** 1995. Soil detachment in the physically based soil erosion process: A review. *Transactions of the ASAE*, 38(4): 1099-1109.

**Picouet, C, Hingray, B and Olivry, JC.** 2001. Empirical and conceptual modelling of the suspended sediment dynamics in a large tropical Africa River: the Upper Niger River Basin. *Journal of Hydrology*, 250: 19-39.

**Poesen, J, Vandaele, K and Wesemael, B.** 1998. Gully erosion: Importance and modelling implications. In: ed. Boardman, J and Favis-Mortlock, D, *Modelling Soil Erosion by Water.* pp 285-312, Springer-Verlag, Heidelberg, Berlin, Germany.

**Quimpo, RG.** 1993. Distributed models of the watershed. In: ed. Wang, SSY, *Advances in Hydro-Science and Engineering.* 1(B): 548-555, Washington DC, USA.

**Randhir, TO, O'Connor, RO, Penner, PR and Goodwin, DW.** 2001. A watershed-based land prioritisation model for water supply protection. *Forest Ecology and Management*, 143(1-3): 47-56 (From Fernandez *et al.*, 2003).

**Refsgaard, JC and Knudsen, J.** 1996. Operational validation and intercomparison of different types of hydrological models. *Water Resources Research*, 32(7): 2189-2202.

**Rekolainen, S, Eklom, P, Ulen, B and Gustafson, A.** 1998. Phosphorus losses from agriculture to surface waters in the Nordic countries. In: ed. Tunney, H, Carton, OT, Brookes, PC and Johnston, AE, *Phosphorus loss from soil to water.* Biddles Ltd, Guildford and King's Lynn, UK.

**Renard, KG, Foster, GR, Weesies, GA and Porter, JP.** 1991. RUSLE, Revised Universal Soil Loss Equation. *Journal of Soil and Water Conservation*, 46(1): 30-33.

**Renard, KG, Foster, GR, Weesies, GA and McCool, DK.** 1992. Predicting soil erosion by water –a guide to conservation planning with the revised universal soil loss equation (RUSLE). Draft 6/92.US, Agricultural Research Service, Department of Agriculture, USA.

**Renard, KG, Laflen, JM, Foster, GR and McCool, DK.** 1994. The Revised Universal Soil Loss Equation. In: ed. Lal, R., *Soil Erosion Research Methods*. Soil and Water Conservation Society, St. Lucie Press, USA.

**Renard, KG, Foster, GR, Lane, LJ and Laflen, JM.** 1996. Soil Loss Estimation. In: ed. Agassi, M, *Soil Erosion, Conservation and Rehabilitation*. pp 169-202 New York, Marcel Dekker, Inc., USA.

**Renard, KG, Foster, GR, Weesies, GA, McCool, DK and Yoder, DC.** 1997. Predicting soil erosion by water: A guide to conservation planning with the Revised Universal Soil Loss Equation (RUSLE). Handbook No. 703, US Department of Agriculture-Agriculture, USA.

**Richards, K.** 1993. Sediment delivery and drainage network. In: ed. Beven, K and Kirkby, MJ, *Channel Network Hydrology*. pp 221-254, John Wiley, Chichester, UK.

**Roehl, JW.** 1962. Sediment source area, delivery ratios and influencing morphological factors. In: *Symposium of Bari* (1-8 October, 1962). IAHS publ. No. 59. pp 202-213, Wallingford, Oxfordshire, UK (From Howe, 1999).

**Rooseboom, A, Verster, E, Zietsman, HL and Lotriet, HH.** 1992. The development of the new sediment yield map of southern Africa. Report No. 297/2/92, Water Research Commission, Pretoria, South Africa.

**Rose, CW.** 1985. Developments in soil erosion and deposition models. In: ed. Stewart, BA, *Advances in Soil Science*. pp 1-63, Springer-Verlag, New York, USA.

**Rose, CW, Dickinson, WT, Ghadiri, H and Jorgensen, SE.** 1990. Agricultural nonpoint –source runoff and sediment yield water quality (NPSWQ) models: Modeller's perspective. In: ed. DeCoursey, DG, *Proceedings of the International Symposium on Water Quality Modelling of Agricultural nonpoint –Sources*. pp 145-169, Agriculture Research Service, US Department of Agriculture, USA.

**Rose, CW, Williams, JR, Sander, GC and Barry, DA.** 1983. A mathematical model of soil erosion and deposition processes: Theory for a plane land element. *Soil Science Society of American Journal*, 47: 991-995.

**Saltelli, A, Chan, K and Scott, EM.** 2000. Sensitivity Analysis. [Internet] Available from: < http://www.wiley.com/WileyCDA/WileyTitle/productCd-0471998923.html > [Accessed 27 June 2004].

**Schultz, GA.**1994. Meso-scale modelling of runoff and water balances using remote sensing and other GIS data. *Hydrological Sciences*, 39 (2): 121-142.

**Schulze, RE.** 1995. Hydrology and Agrohydrology: A Text to Accompany the *ACRU 3.00* Agrohydrological Modelling System. Report No. TT69/95, Water Research Commission, Pretoria, South Africa.

**Schwab, GO, Fangmeier, DD and Elliot, WJ.** 1995. *Soil and Water Management Systems*. John Wiley and Sons. Inc. USA.

**Schwab, GO, Frevert, RK, Edminster, TW and Barnes, KK.** 1981. *Soil and Water Conservation Engineering*. John Wiley and Sons. Inc. USA.

**Scotney, DM and McPhee, PJ.** 1992. Soil erosion and conservation. In: ed. Van Oudtshoorn, FP, *Guide to Grasses of South Africa.* pp 11-34, Briza Publikasies, South Africa.

**SIRI: Memoirs No. 12.** 1989. Land Types of the Maps 2330 Tzaneen and 2430 Pilgrims Rest. Department of Agriculture and Water Supply, Pretoria, South Africa (From Howe, 1999).

**Smithen, AA and Schulze, RE.** 1982. The spatial distribution in southern Africa of rainfall erosivity for use in the Universal Soil Loss Equation. *Water South Africa,* 8(2): 74-78.

**Smithers, J and Schulze, RE.** 1995. *ACRU* Agrohydrological Modelling System: User Manual Version 3. Report No. TT70/95, Water Research Commission, Pretoria, South Africa.

**Svorin, J.** 2003. A test of three soil erosion models incorporated into a geographic information system. *Hydrological Processes*, 17: 967-977.

**Tarboton, DA.** 1997. A new method for the determination of flow directions and upslope areas in grid digital elevation models. *Water Resources Research*, 33(2): 309-319.

**Tim, US, Mostaghimi, S and Shanholtz, VO.** 1992. Identification of critical non point pollution source areas using Geographic Information Systems and water quality modelling. *Water Resources Bulletin*, 28(5): 877-887.

**Troeh, FR, Hobbs, JA, and Donahue, RL.** 1980. *Soil and Water Conservation for Productivity and Environmental Protection*. Prentice-Hall, Inc., Englewood Cliffs, New Jersey, USA.

**USDA-SCS.** 1975. Urban hydrology for small watersheds. Technical Release No. 55. USDA-SCS, Washington, DC., USA (From Fernandez *et al.,* 2003).

**USDA-SCS.** 1983. Sedimentation. National Engineering Handbook. USDA-SCS. Washington, D.C., USA (From Fernandez *et al.,* 2003).

**Vijay, P, Singh, VP and Fiorentino, M.** 1996. *Geographic Information System in Hydrology.* Kluwer Academic Publishers, Dordrecht, Boston, UK.

**Walling, DE.** 1983. The sediment delivery problem. *Journal of Hydrology,* 65: 209-237.

**Walling, DE and Hadley, RF.** 1980. *Erosion and Sediment Yield: Some Methods of Measurement and Modelling.* Cambridge, University Press, UK.

**Walling, DE and Webb, BW.** 1996. Erosion and sediment yield: Global and regional perspectives. IAHS publ. No.236, Wallinford, Oxfordshire, UK.

**Wicks, JM and Bathurst, JC.** 1996. SHESED: A physically based, distributed erosion and sediment yield component for the SHE hydrological modelling system. *Journal of Hydrology*, 175: 213-238.

**Wild, A.** 1993. *Soil and the Environment: An Introduction.* Cambridge University Press, UK.

**Williams, JR.** 1975. Sediment routing for agricultural watersheds. *Water Resources Bulletin*, 11(5): 965-974.

**Williams, JR.** 1977. Sediment delivery ratios determined with sediment and runoff models. In: *Erosion and Solid Matter Transport in Inland Waters.* IAHS publ. No. 122, Wallingford, Oxfordshire, UK.

**Williams, JR and Berndt, HD.** 1972. Sediment yield computed with the Universal Soil Loss Equation. *Journal of American Society Civil Engineers*, 98(2): 2087-2098.

**Wischmeier, WH and Smith, DD.** 1978. Predicting Rainfall Erosion Losses - a Guide to Conservation Planning. USDA Agricultural Handbook. pp 537, Agricultural Research Service, USDA Washington DC, USA.

**Wu, TH, Hall, JA and Bonta, JV.** 1993. Evaluation of runoff and erosion models. *Journal of Irrigation and Drainage Engineering*, 119(4): 364-382.

**Yalin, YS.** 1963. An expression for bed-load transportation. *Journal of Hydraulic Division*, 89 (HY3): 221-250 (From Alonso *et al.*, 1981).

**Young, A.** 1994. Modelling changes in soil properties. In: ed. Greenland, DJ, and Szabolcs, I, *Soil Resilience and Sustainable Land Use.* pp. 423-447, CAB international, UK.

**Young, RA, Onstad, CA, Bosch, DD and Anderson, WP.** 1987. AGNPS: An agricultural non-point source pollution model. Conservation Research Report 35, US Department of Agricultural Research Service, Washington DC, USA.

**Zhang, GH, Liu, BY, Nearing, MA, Huang, CH and Zhang, KL.** 2002. Soil detachment by shallow flow. *Transactions of the ASAE*, *45*(2): 351-357.

**Zhang, GH, Haan, CT, and Nofzinger DL.** 1990. Hydrologic modelling with GIS: An overview. *Transactions of the ASAE*, *6*(4): 453-45.

# APPENDIX A

**Calculation of flow length**

In this study the flow length or distance to the nearest channel, is calculated using a syntax algorithm written in Arcview avenue script (Moglen, 2004) in which accumulated flow length downstream to each cell is calculated as follows:

Overhead operations: Getting the view and grids

*theView = av.FindDoc("View1")*

*theshed = theView.FindTheme("A Watershed").GetGrid*

*flowdir = theView.FindTheme("Flow Direction").GetGrid*

Calculate the flow lengths within the grid in the downstream direction (stored in "downgrid")

***downgrid = flowdir.FlowLength* (NIL, FALSE)**

Mask out only the flow lengths within the watershed

*downgrid = downgrid * theshed/theshed*

Get flow length statistics. The first item in the length_stat list is the minimum distance, corresponding to the distance to the catchment outlet. We subtract this off the flow length distance.

*length_stat = downgrid.GetStatistics*

*length_at_outlet = length_stat.Get(0)*

*downgrid = downgrid - length_at_outlet .AsGrid*

Finally, we generate and add the new flow length theme to the view.

*theGTheme = GTheme.Make(downgrid)*

*theGTheme.SetName("Flow Lengths")*

*theView.AddTheme(theGTheme)*

# APPENDIX B

## Neighbourhood method for calculating slope angle

Slope maps are often used as layers within a GIS and can exhibit major differences depending on the algorithms used in their derivation. In this study the neighbourhood method was chosen for calculation of the slope steepness. This is because the neighbourhood method calculates the average across the centre cell using at least four of the surrounding eight cells.

This method uses a moving three by three mask over a DEM to predict slope for the centre cell from its eight neighbours. For example the equation for slope (rise/run ratio) of the centre cell (#9) (per cent slope) is:

| | | |
|---|---|---|
| 1 | 2 | 3 |
| 4 | 9 | 5 |
| 6 | 7 | 8 |

$$S = (\sqrt{S_{e-w}^2 + S_{n-s}^2}) * 100 \qquad 1$$

East-West slope is given by:

$$S_{e-w} = \left( \frac{(Z_3 + 2Z_4 + Z_5) - (Z_1 + 2Z_8 + Z_7}{4 * 2 * d} \right) \qquad 2$$

North-South slope is given by:

$$S_{n-s} = \left( \frac{(Z_1 + 2Z_2 + Z_3) - (Z_7 + 2Z_6 + Z_5)}{4 * 2 * d} \right) \qquad 3$$

where:

| | | |
|---|---|---|
| $S$ | = | slope ratio in per cent |
| $Z_1$ *to* $Z_9$ | = | elevation of cells 1 to 9 (m) |
| $d$ | = | cell resolution (m) |

# APPENDIX C

## Calculation of modified flow accumulation

It should be recalled from Chapter 4 that Equation 4.5 was used for calculating the RUSLE *LS*-factor that was proposed by Mitasova *et al.* (1996). They derived the equation based on flow accumulation and slope steepness. The GIS executable form of this equation is given as follows:

$$LS = \left[ FlowAccomulation * \frac{Cell\ resolution}{22.1} \right]^{0.6} \left[ \frac{\sin slope}{0.01745} \right]^{1.3} * 1.6 \qquad 1$$

where: ***Flow Accumulation*** is a grid theme of flow accumulation expressed as number of grid cells (readily derived from hydrologic processing steps in Arcview).

***Cell resolution*** is the length of a cell side (i.e. 50 m).

***Slope*** (degree) is derived from DEM using the drive slope option in Arcview.

Since RUSLE is only suitable for estimating erosion due to interrill and rill processes, it is necessary to have an upper bound on the slope length that should be used. It is know that the flow accumulation uses a flow direction theme for its derivation and is given as the number of all cells that drain into an output cell (ESRI, 1996). Since this output is a network of cells over which water flows, the number of cells that flow into this channel is high. This value should, therefore, be modified to comply with the RUSLE threshold values. For example, in this study the upper bound was taken 150 m due to the undulating nature of the landscape of the catchment. Since the grid cell width is 50 m, this translates to an accumulation of a maximum of 3 grid cells and a minimum of 1 grid cell where flow will be initiated. The following steps demonstrate how to modify the flow accumulation theme in Arcview.

Step one: Create a theme using the map calculator in Arcview that contains 0 if the flow accumulation is less than or equal to 3 and a 1 if flow accumulation is greater than 3. Then specify this theme as Map Calculator 1.

Step two: Multiply Map Calculator 1 by 3. This will give a new theme with a 3 in all grid cells that have a flow accumulation greater than 3.

Step three: Create a theme using map calculator in Arcview that contains a 1 in areas in which the flow accumulation is less than or equal to 3. Then using the map calculator, multiply this theme by the original flow accumulation theme. Then specify this theme as Map Calculator 2.

Step four: Grid cells with a flow accumulation value of 0 (these are where flow initiates) should be set to 1 so that the slope length for these cells is not 0. Use the same procedure to that above to identify these cells and create a map with a value of 1 for these areas. Then specify this theme as Map Calculator 3.

Now add the three themes that contain flow accumulation (i.e. steps one, three and four). This results a new theme (flow accumulation) that has a maximum flow accumulation value of 3 (cf. Figure 6.4). Use this new flow accumulation theme in Equation 1 above for computing the RUSLE *LS*-factor (cf. Figure 6.5). Note that the slope must be converted to radians from the degrees by multiplying the slope by 3.14, ($\pi$), and divide it by 180°.

# APPENDIX D

Graphs showing the Cumulative Frequency Distribution of the travel times, ($F_i$) and the fitted curve (Equation 4.9) yielding the parameter, $\beta$ for the 9 subcatchments in the Henley catchment:

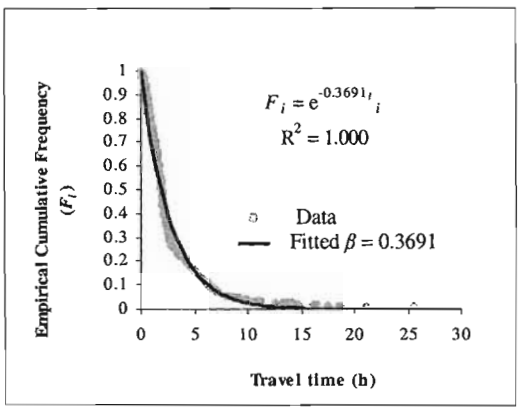


1

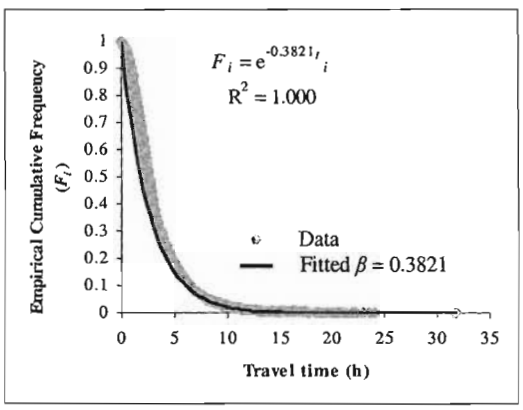


2

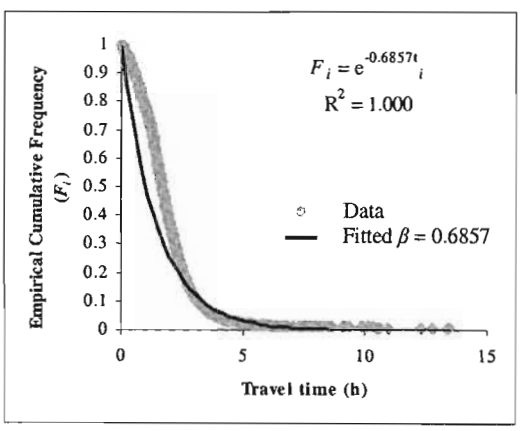


3

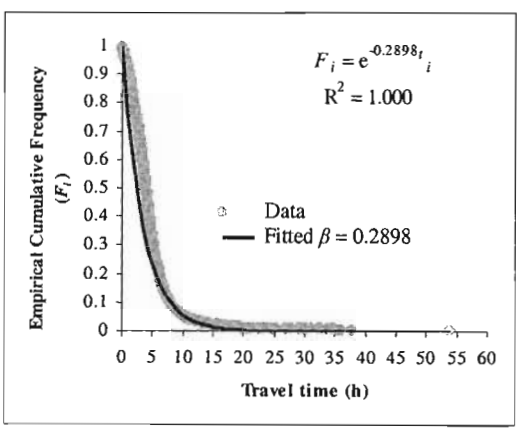


4

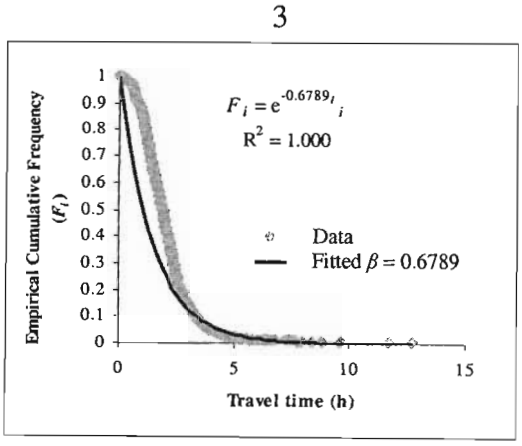


5

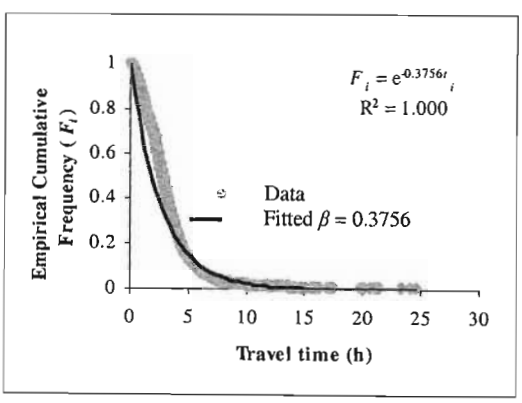


6

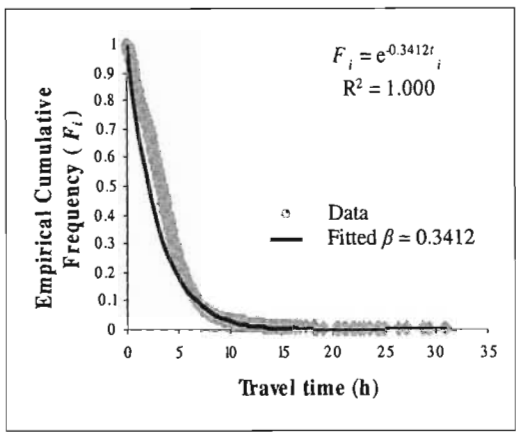
$F_i = e^{-0.3412t_i}$
$R^2 = 1.000$
Data
Fitted $\beta = 0.3412$
Empirical Cumulative Frequency ( $F_i$ )
Travel time (h)

7

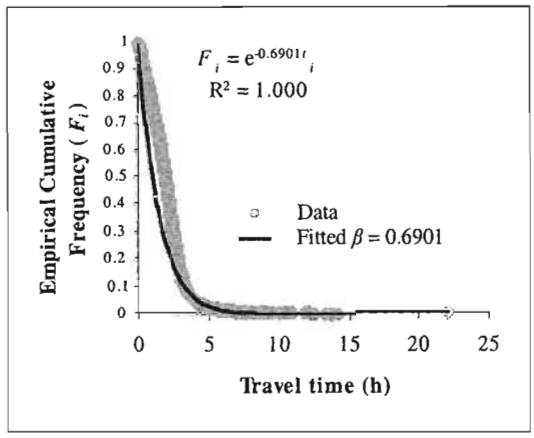
$F_i = e^{-0.6901t_i}$
$R^2 = 1.000$
Data
Fitted $\beta = 0.6901$
Empirical Cumulative Frequency ( $F_i$ )
Travel time (h)

8

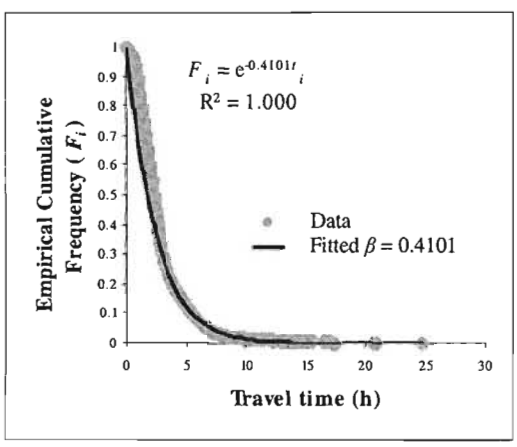
$F_i = e^{-0.4101t_i}$
$R^2 = 1.000$
Data
Fitted $\beta = 0.4101$
Empirical Cumulative Frequency ( $F_i$ )
Travel time (h)

9

# APPENDIX E

Graphs showing the fitted frequency distribution of the different sediment yield and sediment delivery ratio variables

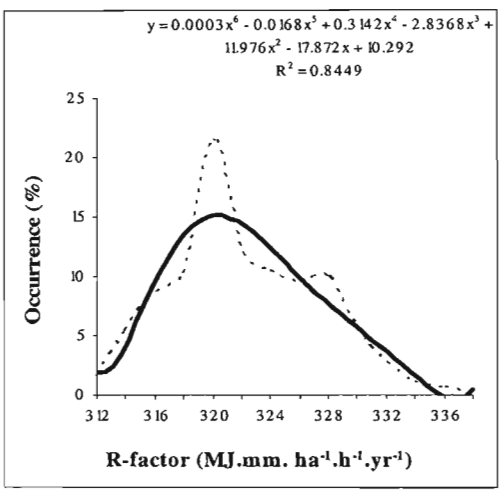


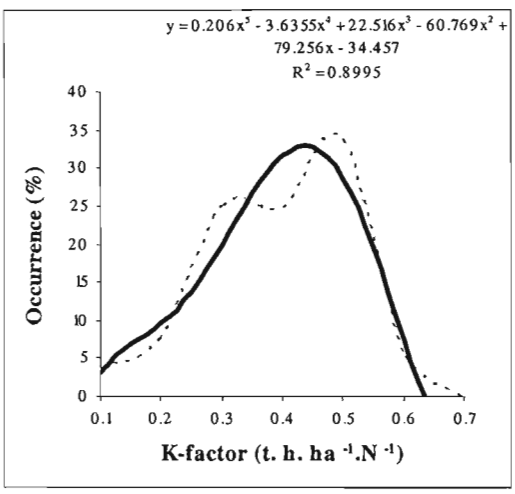


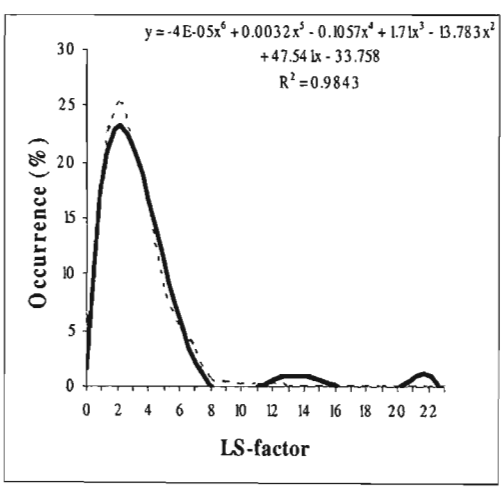


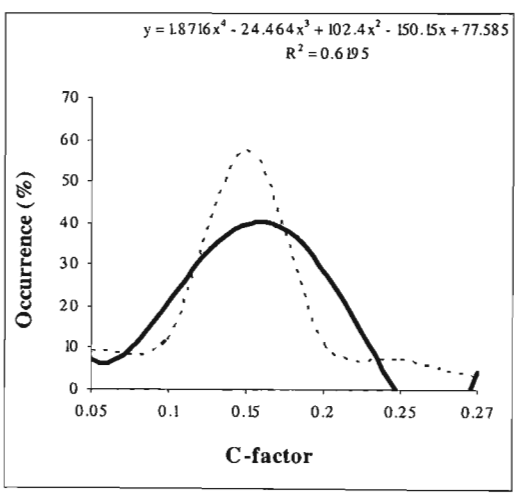

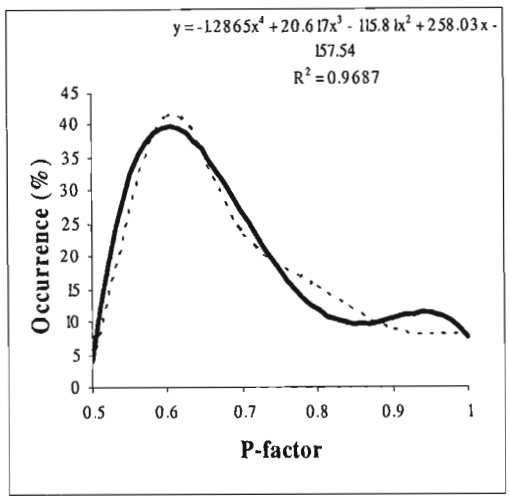
y = -1.2865x⁴ + 20.617x³ - 115.81x² + 258.03x - 157.54
R² = 0.9687
Occurrence (%)
P-factor

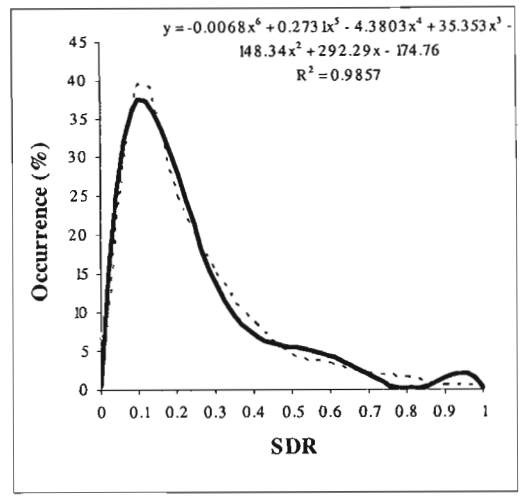
y = -0.0068x⁶ + 0.2731x⁵ - 4.3803x⁴ + 35.353x³ - 148.34x² + 292.29x - 174.76
R² = 0.9857
Occurrence (%)
SDR

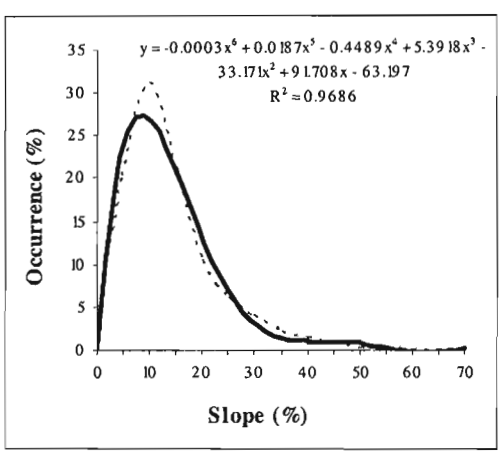
y = -0.0003x⁶ + 0.0187x⁵ - 0.4489x⁴ + 5.3918x³ - 33.171x² + 91.708x - 63.197
R² = 0.9686
Occurrence (%)
Slope (%)

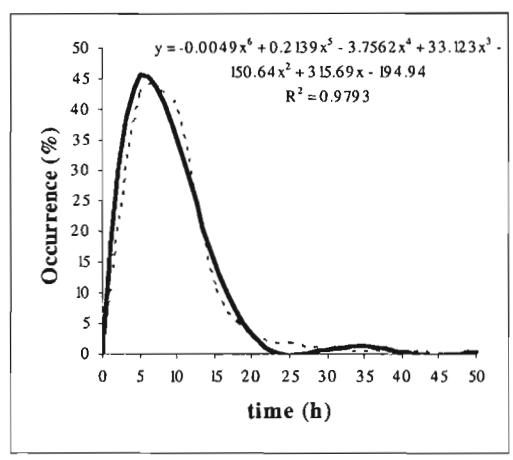
y = -0.0049x⁶ + 0.2139x⁵ - 3.7562x⁴ + 33.123x³ - 150.64x² + 315.69x - 194.94
R² = 0.9793
Occurrence (%)
time (h)

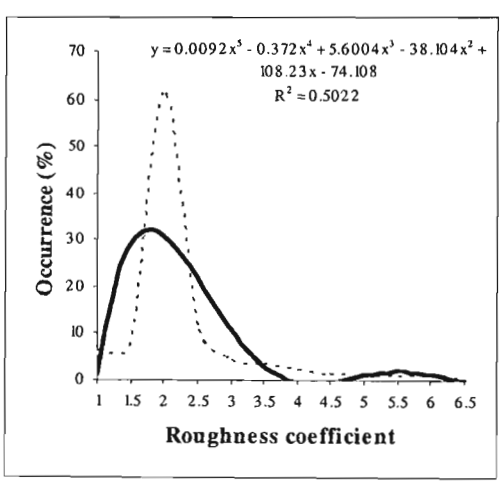
y = 0.0092x⁵ - 0.372x⁴ + 5.6004x³ - 38.104x² + 108.23x - 74.108
R² = 0.5022
Occurrence (%)
Roughness coefficient